CONSTELLATION RECONFIGURATION:

TOOLS AND ANALYSIS

A Dissertation

by

JEREMY JOHN DAVIS

Submitted to the Office of Graduate Studies of
Texas A&M University
in partial fulfillment of the requirements for the degree of

DOCTOR OF PHILOSOPHY

August 2010

Major Subject: Aerospace Engineering

CONSTELLATION RECONFIGURATION:

TOOLS AND ANALYSIS

A Dissertation

by

JEREMY JOHN DAVIS

Submitted to the Office of Graduate Studies of
Texas A&M University
in partial fulfillment of the requirements for the degree of

DOCTOR OF PHILOSOPHY

Approved by:

Co-Chairs of Committee,	John L. Junkins
	Daniele Mortari
Committee Members,	John E. Hurtado
	J. Maurice Rojas
Head of Department,	Dimitris Lagoudas

August 2010

Major Subject: Aerospace Engineering

ABSTRACT

Constellation Reconfiguration:

Tools and Analysis. (August 2010)

Jeremy John Davis, B.S., Virginia Tech

Co–Chairs of Advisory Committee: Dr. John L. Junkins
Dr. Daniele Mortari

Constellation reconfiguration consists of transforming an initial constellation of satellites into some final constellation of satellites to maintain system optimality. Constellations with phased deployment, changing mission requirements, or satellite failures would all benefit from reconfiguration capability. The constellation reconfiguration problem can be broken into two broad sub-problems: *constellation design* and *constellation transfer*. Both are complicated and combinatorial in nature and require new, more efficient methods. Having reviewed existing constellation design frameworks, a new framework, the *Elliptical Flower Constellations* (EFCs), has been developed that offers improved performance over traditional methods. To assist in rapidly analyzing constellation designs, a new method for orbit propagation based on a sequential solution of Kepler's equation is presented. The constellation transfer problem requires an optimal assignment of satellites in the initial orbit to slots in the final orbit based on optimal orbit transfers between them. A new method for approximately solving the optimal two-impulse orbit transfer with fixed end-points, the so-called minimum Δv Lambert's problem, is developed that requires the solution of a 4^{th} order polynomial, as opposed to the 6^{th} or higher order polynomials or iterative techniques of existing methods. The recently developed Learning Approach to sampling optimization is applied to the particular problem of general orbit transfer

between two generic orbits, with several enhancements specific to this problem that improve its performance. The constellation transfer problem is then posed as a Linear Assignment Problem and solved using the auction algorithm once the orbit transfers have been computed. Constellations designed for global navigation satellite systems and for global communications demonstrate significant improvements through the use of the EFC framework over existing methods. An end-to-end example of constellation reconfiguration for a constellation with changing regional coverage requirements shows the effectiveness of the constellation transfer methods.

Learn from yesterday, live for today, hope for tomorrow.
The important thing is not to stop questioning.
Albert Einstein

ACKNOWLEDGMENTS

No effort as significant as a graduate degree can be achieved without the loving support of friends and family. I would like to thank my parents, Glen and Terri, my sister, Karen, and my brother, Chris, for being being a constant source of love and encouragement on which I could always rely.

Since I arrived at Texas A&M, Lesley Weitz has provided me invaluable guidance in navigating graduate school and life in general. From late night philosophical discussions to weekly poker nights to a couple of drinks at the end of a long day, the friendship of Lasse Maeland and Jeff Cheek throughout my time here has kept me sane. And I could not have asked for a better friend or collaborator than James Doebbler, whom I have worked with for the past four years on a daily basis. Beyond the technical insights that these individuals have imparted over countless conversations, these friends have, quite simply, made graduate school fun.

I would be remiss not to acknowledge the people that have gotten me to this point. I am greatly indebted to Mr. Harold Houghton, whose enthusiastic high school physics lessons inspired me to become an engineer and still influence how I solve problems to this day. The further inspiration and tutelage provided by Dr. Hanspeter Schaub during my time at Virginia Tech gave me the motivation and confidence to pursue graduate studies.

Having Dr. John L. Junkins as an advisor has been fantastic. He trusted me with the freedom to pursue whatever research sparked my interest and gave me all of the resources I needed to succeed, all the while imparting his sage wisdom. I was blessed with a second great advisor, Dr. Daniele Mortari, whose constant enthusiasm and stream of new ideas kept me excited about my research. Dr. John Hurtado has been an invaluable resource in all things dynamics since I arrived, and I appreciate the efforts

of Dr. Maurice Rojas on my committee. The development of the constellation design theory would have been impossible without the assistance of Dr. Martìn Avendaño. I thank all of these teachers and mentors who have led me to this point.

Of course, none of this would be possible without the continual assistance of Lisa Willingham, who keeps all of us in line, and the help of all of the other professors and administrators of the Aerospace Engineering Department that provide such a great experience here at Texas A&M.

TABLE OF CONTENTS

CHAPTER Page

I INTRODUCTION 1
A. Motivation 1
B. Literature Review 2
C. Statement of Purpose 6

II CONSTELLATION DESIGN 10
A. Walker Constellations 12
1. Standard Methodology 13
2. Repeating Ground-Tracks 14
B. Flower Constellations 15
1. Original Formulation 16
2. Lattice Flower Constellations 18
3. Equivalence to Walker Constellations 19
C. Elliptical Flower Constellations 21
1. Conceptual Design 21
2. Mathematical Formulation 23
3. Properties 26
4. Generalizations 35
5. Other Design Considerations 37
D. Fast Orbit Propagation 43
1. Review of Existing Methods 44
2. Sequential Orbit Propagation 47
3. Expansion of the Difference Form of KE 51
4. Numerical Analysis 53
E. Conclusions 67

III CONSTELLATION TRANSFERS 70
A. Assignment Problems 71
1. Linear Assignment Problem 71
2. Auction Algorithm 72
3. Alternative Formulations 73
B. Minimum Δv^2 Lambert's Problem 74
1. Problem Definition 75

CHAPTER Page

2. Approach . . . 76
3. Multiple Solutions and Error Analysis . . . 79
4. Singularity . . . 83
5. Pork-chop Example . . . 88
C. Optimal Two-Impulse Transfers . . . 91
1. Learning Approach to Sampling Optimization . . . 91
2. Refinements . . . 92
3. Application to Two-Impulse Transfers . . . 96
D. Conclusions . . . 110

IV CASE STUDIES . . . 112

A. Global Navigation Satellite System . . . 112
1. Cost Function . . . 113
2. Design Study: 27 Satellites . . . 114
3. Design Study: 25 Satellites . . . 119
B. Iridium Design . . . 121
C. Surveillance Reconfiguration . . . 123
1. Constellation Design . . . 123
2. Constellation Transfer . . . 126
D. Conclusions . . . 127

V CONCLUSION . . . 129

A. Summary . . . 129
1. Constellation Design . . . 129
2. Constellation Transfer . . . 131
B. Future Work . . . 132
1. Constellation Design . . . 133
2. Constellation Transfer . . . 134
C. Conclusion . . . 135

REFERENCES . . . 136

VITA . . . 146

LIST OF TABLES

TABLE		Page
I	Broucke's method parameters	46
II	Algorithmic complexity of existing methods	54
III	Algorithmic complexity of sequential methods	54
IV	Error in position propagation as percent of semi-major axis of existing methods	55
V	Error in position propagation as percent of semi-major axis of sequential methods	58
VI	Error in position propagation as percent of semi-major axis for small to moderate eccentricities	66
VII	Orbit parameters for four solution case	80
VIII	Orbit parameters range	82
IX	Orbit parameters for pork-chop plots	90
X	Values of semi-major axis used for GNSS optimization	117
XI	Elliptical Flower Constellation parameters for 25 satellite GNSS	120
XII	GA generated LFC designs for coverage of Baghdad and Kabul	125
XIII	View time per day of each site by each constellation in minutes	126
XIV	Required Δv to transfer from one slot in Constellation B (B_i) to another slot in Constellation K (K_i) in km/s. Optimal assignment in bold.	126

LIST OF FIGURES

FIGURE		Page
1	Elliptical Flower Constellation concept.	22
2	Minimum encounter distance in the 27/3/1 Walker constellation as a function of inclination.	39
3	Error in position propagation as percent of semi-major axis of existing methods.	56
4	Error in position propagation as percent of semi-major axis of method M_1.	59
5	Error in position propagation as percent of semi-major axis of method M_2.	60
6	Error in position propagation as percent of semi-major axis of method M_3.	61
7	Error in position propagation as percent of semi-major axis of method M_4.	62
8	Error in position propagation as percent of semi-major axis of method M_5.	63
9	Error in position propagation as percent of semi-major axis of method M_6.	64
10	Error in position propagation as percent of semi-major axis of method M_7.	65
11	Special transfer case with four real roots.	81
12	Histogram of percent error in $\|\Delta\boldsymbol{v}_1\|+\|\Delta\boldsymbol{v}_2\|$ using the $J = \|\Delta\boldsymbol{v}_1\|^2+ \|\Delta\boldsymbol{v}_2\|^2$ cost function over one million random transfers.	83

FIGURE Page

13 Contour plots showing $|\Delta \boldsymbol{v}_1| + |\Delta \boldsymbol{v}_2|$ cost using the Δv_{tot} optimality (left) and Δv_{tot}^2 optimality (right) over the ranges of true anomaly for initial and final orbit. 89

14 Percent error in $|\Delta \boldsymbol{v}_1| + |\Delta \boldsymbol{v}_2|$ using the Δv_{tot}^2 optimality. 90

15 Initial distribution of 10 points for both the LA sampling algorithm and a purely random sampling algorithm. The LA algorithm accepts the first 10 points regardless of accept-reject criterion. 99

16 Accepted points for the LA sampling algorithm. 101

17 Accepted points for the random sampling algorithm. 103

18 Percent error of the minimum Δv value using the Δv_{tot}^2 cost function. 106

19 Error in degrees of the location of the global minimum using the Δv_{tot}^2 cost function. 107

20 Percent error of the minimum ΔV value using the Δv_{tot} cost function. 108

21 Error in degrees of the location of the global minimum using the Δv_{tot} cost function. 109

22 Demonstrating the lower Δv requirements for elliptic orbits vs. circular orbits of the same semi-major axis 116

CHAPTER I

INTRODUCTION

A. Motivation

Constellations of satellites working collectively for a common purpose have been utilized in space systems since the 1970s with the launch of the GPS constellation. Satellite constellations have the advantage of providing regional or global coverage from low Earth orbit (LEO), allowing for less demanding requirements on sensing and communications systems and lower launch costs compared to satellites in geosynchronous orbit (GEO).

Recent constellations include global communications constellations such as GlobalStar and Iridium, both launched in the mid to late 90s. Both Iridium and GlobalStar quickly went bankrupt following the successful deployment of those constellations due to demand severely depressed from that expected when the constellations were designed. The experience of these two companies has led researchers to propose phased deployment of constellations where the capacity of the system is increased as merited by increased demand [1, 2].

Other researchers have considered constellations optimized for regional or zonal coverage, either for communications or reconnaissance [3, 4, 5]. Because these satellites sit in LEO orbits, they generally observe significant portions of the Earth beyond the desired region. As such, slight orbit modification can be used to redirect the focus of the coverage if mission requirements change.

The effectiveness of all constellations is affected by the failures of individual satellites, whether in the form of reduced capability or coverage holes. Typically

---

The journal model is *AIAA Journal of Guidance, Control, and Dynamics.*

some combination of on-orbit spares and launch-on-demand capability is built into the system to handle failures [6]. An alternate solution may be to design excess capacity into the system, allowing for a slight change in the constellation to compensate for a lost satellite.

These three scenarios, phased deployment, modified regional coverage, and coverage robustness, all encompass the idea of *constellation reconfiguration*, which we broadly define as the on-orbit transfer of satellites in a given distribution among multiple orbital planes to a new distribution consisting of more, fewer, or the same number of satellites, different orbital planes, different orbit size and shape, or some combination of these. Little attention in existing literature has been paid to the problem of constellation reconfiguration, and methods for optimal reconfiguration are the focus of this research.

B. Literature Review

Constellation reconfiguration itself has seen little research as a whole, the notable exceptions being de Weck's group at MIT [1, 2, 7, 8] and the work of Ferringer et al. at the Aerospace Corporation and Penn State [9, 10]. The work of both groups is reviewed briefly here.

De Weck and his graduate students at MIT began publishing research on constellation reconfiguration in 2003. They have focused exclusively on staged deployment of global communications constellations, citing the failures of Iridium and GlobalStar as key drivers, noting that quickly deploying a small constellation to meet the limited demand at the time with the capability to add capacity later may have saved both companies. The first step de Weck's group took was to quantify the financial benefit made possible by staged deployment [7]. In this paper they neglected the cost

of reconfiguration and computed the expected savings in life cycle cost (LCC) given uncertainty in future demand. Due to lower initial costs for the smaller constellation, a discount appreciated by pushing further deployment to later dates, and the flexibility to respond to real market pressures, they found a savings of more than 20% in LCC for a case study modeled after Iridium. Rather than optimize each successive constellation (as capacity increases) independently, they found the optimal set of consecutive constellations that minimized cost.

With this result, de Weck's group then developed a framework for finding an optimal pair of constellations where the staged deployment strategy consisted of maintaining the initial constellation and simply augmenting it with additional satellites in additional planes or additional satellites per plane [2]. Using the Simulated Annealing optimization method, they found optimal pairs of constellations where the initial constellation was rarely optimal on its own. This paper included satellite costs based on the requirements demanded from the selected constellation and the launch costs of launching all satellites in both constellations. So whereas in the first paper, they neglected reconfiguration costs, here all costs are included (though no orbit transfers occur). Though they presented a case study, they made no attempt to compare the LCC of the staged deployment-system and a standard system.

Simultaneously with this work, Scialom, a Master's student of de Weck, was researching the optimization of constellation reconfiguration, which was published in his thesis and subsequently in a journal article [1, 8]. He considered the following problem: given constellations A and B, minimize the cost of reconfiguration. The framework he developed consisted of the following parts:

- Constellation Module: Computed the optimal streets-of-coverage or Walker constellation for global coverage given an altitude and minimum elevation angle for

the sensor.

- Astrodynamics Module: Computed Δv for both low-thrust and impulsive maneuvers. The specific position of a satellite on a given plane was neglected, so Δv calculations only considered changes in orbital plane, and only circular orbits were considered.

- Assignment Module: The assignment problem, mapping satellites in the initial constellation to satellites in the final constellation, was solved using an auction algorithm. See Ref. [11] for a detailed description of the auction algorithm. The assignment module had to be run iteratively in conjunction with the Launch Module due to constraints on the number of satellites per launch (such that the assignment problem is no longer a linear assignment problem).

- Launch Module: Computed launch costs and a launch schedule.

- Transfer Schedule: Used one of 4 schedules: initiate transfers of all satellites at once, terminate transfers of all satellites simultaneously, transfer satellites individually, and transfer satellites in two groups. Since the specific positions of each satellite were neglected, the schedule was very loosely defined.

- Coverage Module: The coverage model simply assumed that the percent of global coverage was equal to the percent of satellites not in transfer at a given time. This method fails for multiple global coverage, regional coverage, and when satellites can maintain some coverage during transfer. It further fails because having two partial constellations with none in transfer does not guarantee complete global coverage.

- Cost Module: This included the launch costs, transfer costs (fuel costs), satellite costs, and lost revenue due to reduced coverage.

The comprehensive framework is a significant contribution, but as Scialom notes, a higher fidelity model is needed in several modules.

In contrast to the work of de Weck et al., the group of Ferringer et al. has focused exclusively on satellite failures, particularly the loss of a single satellite or plane of satellites in the Global Positioning System (GPS) constellation. The recent Chinese anti-satellite test that generated more than four-thousand pieces of debris reminded everyone of the dangers space debris poses to satellites, and the importance of being able to accommodate satellite failure.

For the global navigation problem, at least four satellites must be visible to a user to provide a solution. In addition to this coverage specification, Ferringer defined a number of cost functions related to the reconfiguration cost that he sought to maximize or minimize:

- Maximize four-fold average daily visibility time
- Maximize four-fold worst-case-point daily visibility time
- Minimize total flight time
- Minimize maximum Δv of a single satellite
- Minimize sum of Δv variance
- Minimize number of maneuvered satellites

Every satellite in the constellation was permitted to be rephased within the plane by being placed in a phasing orbit requiring K revolutions to achieve the desired phasing. The design space consisted of the mean anomaly's of each remaining satellite (after failure of one or of a plane) and a single value of K applied to all maneuvers.

One of the major contributions of Ferringer's group was the application of parallel computation and the use of a Pareto-optimization technique [12] to find the optimal reconfigurations given the various cost functions provided above. Even restricting the reconfiguration to simple rephasings, it took well over 500 hours on a 250 core computing cluster to solve three different scenarios. These results reinforce the challenge that constellation reconfiguration represents: the combinatorial nature makes it difficult for even the most advanced computers.

These two groups have the only direct reference to constellation reconfiguration currently in the literature, though others, such as Scott and Spencer at Penn State [13, 14], have considered reconfiguration of satellites flying in formation. Typically these involve significant assumptions about the small separation between spacecraft orbits and are not generally applicable to constellation reconfiguration.

C. Statement of Purpose

The purpose of this dissertation is to investigate various aspects of the constellation reconfiguration problem. We break these down broadly into two components - *constellation design* and *constellation transfer*.

At the heart of any constellation reconfiguration problem is the constellation design on either end. Chapter II starts by reviewing existing design methodologies, with a particular look at Walker constellations [15] in Section A, a popular constellation design method that produces uniformly distributed constellations. The Flower Constellations (FCs) of Mortari [16], introduced in 2004, can generate asymmetrical constellations for regional coverage requirements, but demonstrate a similar uniformity as special cases. Section B recaps the original formulation and then provides the development of the Lattice Flower Constellations (LFCs). The LFC framework

produces uniform (Harmonic) Flower Constellations with fewer parameters and with a much deeper mathematical understanding. Walker constellations are then shown to be the subset of LFCs that have an eccentricity of zero. The LFC framework distributes satellites uniformly in mean anomaly and right ascension of the ascending node (RAAN) using a simple 2×2 matrix of integer coefficients. Section C expands on this concept by introducing the Elliptical Flower Constellations (EFCs) that utilize a 3×3 matrix of integer coefficients to distribute satellites uniformly in mean anomaly, RAAN, and argument of perigee. Though LFCs permit elliptic orbits, allowing satellites to have varying arguments of perigee in EFCs permits the use of eccentric orbits at non-critical inclinations while preserving the uniformity of the constellation. Several important properties of EFCs are derived, including the fact that EFCs include Walker constellations, LFCs, and two other uniform distribution methodologies as subsets. Finally, optimization studies of constellation design typically require hundreds, if not thousands, of constellations to be evaluated (each with tens of satellites). To speed this process, a new technique for solving Kepler's equation is developed in Section D that significantly reduces time spent on orbit propagation, a vital aspect of any constellation design study. The topics presented in Chapter II allow for more efficient, more effective constellation design than any known methods and are a critical component of any constellation reconfiguration study.

Once initial and final constellations have been designed, the satellites in the initial constellation must execute orbit transfers to the satellite slots in the final constellation, a process we call *constellation transfer* and the focus of Chapter III. This is generally a "traveling salesman" problem that is not analytically solvable, though iterative solution techniques exist. Given a cost function value (eg. fuel cost) for each combination of initial satellite and final satellite slot where the goal is to minimize the sum total of those costs, the optimal mapping can be formulated as

the much simpler linear assignment problem (LAP). This formulation, along with an explanation of the auction algorithm (one of the most efficient methods for solving LAPs) is presented in Section A. The efficient yet accurate computation of the cost function is critical to computing an optimal constellation transfer since the cost function must be evaluated for n^2 transfers, where n is the number of satellites. Minimizing the Δv required by a satellite is roughly equivalent to minimizing the fuel cost. Section B discusses the nonlinear problem of transferring a satellite from a given initial position and velocity to a given final position and velocity while minimizing Δv using a two impulse maneuver. A new method for approximately minimizing Δv (exact solution, approximately optimal) is developed that requires only the solution of a single quartic equation, as compared to the 6^{th}-order equation or multiple iterations required by alternate methods. A related problem is solving for the locations in the initial and final orbits that give rise to a minimum Δv transfer between the two elliptic, non-coplanar orbits. This is solved using a recently developed Learning Approach to sampling optimization (LA) method [17, 18, 19]. The LA method, along with some modifications to improve its efficiency, is presented in Section C. Using an exhaustive grid search to find the true global optimum with high confidence, we show that the modified LA algorithm efficiently and reliably finds the global minimum and does so more effectively than all competing search methods tested. Each of the methods presented in Chapter III improve the ability of the analyst to efficiently solve the constellation transfer problem.

Numerical studies and examples are presented throughout Chapters II and III to verify and validate the algorithms developed. Chapter IV brings many of these methods together through three case studies. The first study considers the problem of designing global navigation satellite systems (GNSS). The EFC framework is employed to find constellation designs that provide improved performance over that

provided by the current GPS or Galileo designs. The second study considers the Iridium constellation, a constellation of 66 communications satellites in low Earth orbit used for satellite phones. An EFC is designed to provide improved coverage over that available from a Walker constellation. The third study looks at the entire constellation reconfiguration problem. Two six-satellite LFCs are designed, each optimized to provide maximum coverage of different points on Earth. The constellation transfer problem is then solved to optimally reconfigure between these two optimal constellations.

The newly developed methods for constellation design and constellation transfer allow for more efficient constellation reconfiguration analysis. The developments are summarized in Chapter V, which also provides a discussion on possible future directions of research. The incorporation of the elements presented here into a comprehensive framework is of particular interest for future efforts.

CHAPTER II

CONSTELLATION DESIGN

As James Wertz observed, "One of the most important results of decades of constellation studies has been that no absolute rules exist for constellation design." [6] Despite this prognosis, this chapter will attempt to shed some light on some powerful methods of constellation design available to the design engineer, including several new insights. Though it remains more an art than a science, these methods give hope to more rigorous studies of constellation design.

Wertz provides an overview of the current state of constellation design [6], and a brief review is presented here. Satellites in a constellation each have six independent orbital parameters defining their path through space. In designing a constellation of n satellites, where $n > 20$ is common, choosing $6n$ independent, continuous parameters is prohibitive, even with recent advances in parallel computing. To combat this curse of dimensionality, constellation designers typically hold some orbital parameters constant across the constellation, or distribute their values in some prescribed pattern such that the actual number of design parameters for a constellation is closer to 5-10, regardless of the number of satellites. See Refs. [20] and [21] for a thorough survey of constellation design methods as they have evolved over time.

Two main methods are currently practiced today - streets-of-coverage and Walker constellations. Streets-of-coverage constellations typically involve placing satellites in polar orbits that have been spaced such that the path covered by a satellite touches or overlaps the path from the satellite in the next plane over. This type of design has advantages in its simplicity of assessing coverage, but because it focuses redundant, overlapping coverage in the unpopulated polar regions, it is rarely as efficient as more uniform design strategies. The Walker constellations were developed by J.G. Walker

in the 1970s and are the most commonly used constellations today [15, 22, 23]. In a Walker constellation, the inclination of all satellites is identical, all orbits are circular, and there are just 3 integer parameters that define the distribution of all satellites in the constellation. Walker's results will be presented more extensively later in Section A.

A relative newcomer to constellation design methodology has been the Flower Constellations (FCs), initially proposed by Mortari in 2004 [16]. The Flower Constellations utilize several integer parameters, permit elliptical orbits, and enable the most general known means to enforce a single repeating ground-track (or space-track) followed by all satellites in an infinite family of constellations. Flower Constellations also allow for non-uniform distributions of satellites to maximize regional coverage capabilities. Using recent developments in reformulating the original Flower Constellation theory, presented in Section B, it is possible to show that the uniform subset of Flower Constellations are equivalent to Walker constellations, though they were developed quite independently. Put another way, the Flower Constellations generalize Walker constellations in several ways, most notably to encompass elliptical orbits. This dissertation will elucidate the general theory of FCs in a way that places these constellation design tools into a unified and generalized framework.

Using elliptical orbits poses additional challenges. The individual satellite systems, particularly sensors and antennas, must be designed to operate over a continuously varying altitude. From a constellation design perspective, elliptical orbits present unique problems due to the effects of Earth's oblateness which causes the orbits of the satellites to drift over time, thus typically destroying the symmetry or coverage capabilities of the constellation that was so carefully designed. A new approach for designing a constellation with elliptic orbits that addresses this latter problem are given in Section C.

Even with the reduced parameter set offered by such design strategies, the design space is still large enough to make full combinatorial analysis challenging if not impossible. One complication is that the metrics by which a constellation are evaluated must be computed over time. Given the complex, dynamic nature of the problem, this is typically done through brute force propagation of all satellites through some time of interest to compute the metric of interest. Since every candidate constellation must be evaluated this way, speeding up the orbit propagation phase has major implications for the speed, breadth, and effectiveness of such constellation optimization design iterations. A new, extremely efficient, method for satellite propagation, specifically focused on constellation design, is presented in Section D.

A. Walker Constellations

Throughout the 1970s, Walker studied the design of constellations for whole-earth coverage [15, 22, 23]. He was interested in emerging applications of communications, navigation, and surveillance and so considered cases of continuous multiple coverage, where $n \geq 1$ satellites are required to be in view of all locations on Earth at every instant [15]. To achieve such coverage with the minimum number of satellites, Walker hypothesized that optimal constellations would be symmetrical and uniform in their distributions of satellites and involve only circular orbits of all the same orbital period. Though the work of Draim later proved that elliptical constellations can offer improved performance [24, 25], Walker constellations have been used for virtually everything, from the Iridium communications constellation to the Galileo global navigation system, due to their simplicity and well documented tests and analyses. It is believed that the popularity of Walker constellations rests on (i) the ability to provide good sub-optimal configurations with a conceptually easy-access design

approach, and (ii) the absence of a convenient design methodology for more general constellation configurations.

1. Standard Methodology

Walker constellations, also known as Walker delta patterns, are defined by three integer parameters, $T/P/F$:

- T is the total number of satellites in the constellation
- P is the number of orbital planes
- F is a phasing parameter

All satellites in the constellation have the same inclination (i), the same semi-major axis (a), and zero eccentricity (e). The right ascensions of the ascending node (RAANs) (Ω) of the P orbital planes are distributed equally about the equator. The satellites that lie within a given plane are all evenly spaced in mean anomaly around the circular orbit. To understand the phasing parameter, F, it is important to introduce what Walker termed the pattern unit (PU), where $1\text{PU} = 360^\circ/T$. When a satellite on a given plane passes through the ascending node, the satellite on the next adjacent plane to the east has advanced F PUs past its ascending node. Requiring F to be an integer results in a repeating pattern as one moves around the equator. The values of F are limited to the range $[0, P-1]$ because that range encompasses all possible patterns (the pattern with $F = P$ is the same as the pattern with $F = 0$). To complete the notation, Walker also defined the parameter S, the number of satellites per plane ($S = T/P$).

2. Repeating Ground-Tracks

Most discussions of Walker constellation theory stop after that brief review, but Walker also developed additional theory that addresses constellations with repeating ground-tracks [15]. He defined the integers M and L to be the number of revolutions of the Earth and the number of revolutions of the satellite, respectively, before the ground-track repeats. In terms of the orbital period of the satellite, T_p, and the rotational period of the Earth, T_d, this relationship is expressed by the compatibility equation

$$MT_d = LT_p \tag{2.1}$$

Using integer values of M and L results in each individual satellite following a repeating ground-track (or more generally a repeating relative trajectory), but does not force all of the satellites to be on the *same* repeating ground-track. Walker derived the following equation for the number of unique ground-tracks, $E_{L,M}$, in a Walker constellation:

$$E_{L,M} = \frac{T}{K} \tag{2.2}$$

where $K = \gcd(SL+FM, PJ)$ and $J = \gcd(S, M)$. Clearly, K represents the number of satellites following each ground-track.

This theory is not complete without a method to design constellations where all satellites lie on the same repeating ground-track (ie. $E_{L,M} = 1$). Walker showed that given the orbit size in terms of M and L and the total number of satellites, that a single repeating ground-track could be achieved by setting

$$S = \gcd(M, T) \tag{2.3}$$

and

$$F = \left(\frac{S}{M}\right)(kP - L) \tag{2.4}$$

where k is an integer such that F falls within the allowable range $[0, P-1]$. Though this contribution is rarely referenced, it offers important insights into Flower Constellations as will be seen in the following sections.

B. Flower Constellations

The ground-track of a satellite is the Earth-fixed path generated by the radius vector piercing point on the surface of the Earth as both the Earth and the satellite move. One method for designing the orbit of a satellite for a specific mission would be to look at the ground-track and evaluate how well it covers the region of interest, provides for communications, etc. Moreover, a "ribbon" centered on the ground-track can be generated to show the cross-track coverage swath of a satellite sensor, accounting for field-of-view or elevation constraints. But, generally, ground-tracks shift in longitude from orbit to orbit, so let's consider only repeating ground-tracks - those that are specially phased to perfectly repeat after a certain number of orbits. Now imagine that an optimal ground-track has been found to maximize some coverage metric of interest. Wouldn't it be useful to have an entire constellation of satellites spaced out along that exact same ground-track to maintain persistent coverage? This is the conceptual framework in which Flower Constellations were originally developed by Mortari, starting in 2004 [16].

As will be seen through the rest of this section, there are several equations that can be solved to enforce all satellites of a constellation to move on the same repeating ground-track. They allow for an arbitrary number of satellites, for an arbitrary number of planes, and for elliptical orbits. First we describe the original formulation of Flower Constellations and some of their unique properties, followed by a discussion of the recent Lattice Flower Constellation (LFC) extension of FC

theory [26]. Finally, the LFCs are compared to the Walker constellations.

1. Original Formulation

The original Flower Constellation formulation [27] required all satellites to follow the same repeating ground-track, or equivalently, the same repeating space-track relative to the rotating frame of the Earth. The orbits were allowed to be eccentric, but all satellites had the same semi-major axis, eccentricity, inclination, and argument of perigee. In order for each individual satellite to follow a repeating ground-track, the compatibility condition was enforced:

$$N_p T_p = N_d T_d \tag{2.5}$$

where T_p is the orbital period, T_d is the period of one Earth revolution, N_p is the integer number of orbital periods before repetition, and N_d is the integer number of days before repetition. The effects of J_2 perturbation (the dominant effect of Earth's oblateness) can be accounted for in the values of T_d and T_p to maintain repeating ground-tracks. The value of T_p (computed from the specified values of N_p and N_d) directly specifies the semi-major axis of every satellite in the constellation.

In addition to the number of satellites (N_s) and the values of N_p and N_d, three other integer phasing parameters must be chosen in the original FC framework: F_n, F_d, and F_h. These six integer parameters were then used to recursively solve for the position of every satellite in (Ω, M)-space using the equations

$$\Omega_{k+1} = \Omega_k + 2\pi \frac{F_n}{F_d} \tag{2.6}$$

$$M_{k+1} = M_k - 2\pi \frac{N_p F_n + F_d F_h(k)}{F_d N_d} \tag{2.7}$$

Note that $F_h(k)$ could be specified as any sequence formed from the set $[0, N_d - 1]$,

though it was typically chosen to be constant. By choosing the six integer parameters $(N_s, N_p, N_d, F_n, F_d, F_h)$ and three continuous parameters (e, i, ω), the entire constellation is specified. This is the method used in the FC simulation and visualization software FCVAT [28].

The original FCs exhibited a complex relationship between the allowable values of the phasing parameters and the number of satellites. Avendaño, in Ref. [29], arrived at the conclusion that the number of satellites in a Flower Constellation could not exceed $N_d F_d / G$ satellites, where $G = \gcd(N_d, N_p F_n + F_d F_h)$. Constellations with this maximum number of satellites were termed Harmonic Flower Constellations (HFCs) due to the uniform distribution that they display [29].

The constraint on the number of satellites in an HFC allowed them to be reformulated to eliminate one of the integer parameters and redefine others to have a more intuitive, physical meaning. The value of F_d is actually the number of inertial orbits or orbital planes, whereas the number of satellites per orbit could be defined as $N_{so} = N_d / G$ based on the constraint on number of satellites. A new configuration number was defined $N_c \in [0, F_d - 1]$ as

$$N_c = E_n \frac{N_p F_n + F_d F_h}{G} \bmod F_d \tag{2.8}$$

where E_n and E_d are integers such that $E_n F_n + E_d F_d = 1$. These three parameters, F_d, N_{so}, and N_c are required to be coprime to be consistent with the HFC framework. The satellite positions in (Ω, M)-space for an HFC were still computed using Eq. (2.6) after solving for the requisite phasing parameters and after specifying the values (F_d, N_{so}, N_c).

2. Lattice Flower Constellations

The Harmonic Flower Constellations provide a uniform distribution, but we find they utilize a non-minimal description in their formulation, which leads to questions of uniqueness and equivalency. Lattice Flower Constellations were developed, motivated by the need to answer these questions, and can be described by five integer parameters and three continuous parameters. The integer parameters can be broken into two sets, the first describing the phasing of the satellites and the second describing the size of the orbits. The first set is (N_o, N_{so}, N_c) where N_o is the number of orbital planes, N_{so} is the number of satellites per orbit, and N_c is a phasing parameter. The second set is (N_p, N_d) which satisfies the compatibility equation of Eq. (2.5).

The phasing parameters define the RAAN (Ω) and initial mean anomaly (M) as

$$\begin{aligned} \Omega_{ij} &= \frac{2\pi i}{N_o} \\ M_{ij} &= \frac{2\pi j}{N_{so}} - \frac{N_c \Omega_{ij}}{N_{so}} \end{aligned} \tag{2.9}$$

These equations can be rewritten in matrix notation as

$$\begin{bmatrix} N_o & 0 \\ N_c & N_{so} \end{bmatrix} \begin{bmatrix} \Omega_{ij} \\ M_{ij} \end{bmatrix} = 2\pi \begin{bmatrix} i \\ j \end{bmatrix} \tag{2.10}$$

where $i = 0, \ldots, N_o - 1$, $j = 0, \ldots, N_{so} - 1$ and $N_c \in [0, N_o - 1]$. Satellite (i, j) is the j^{th} satellite on the i^{th} orbital plane. As proven in Ref. [26, Thm B.1], the LFC framework includes all of the HFCs. Note that unlike the HFC formulation, the LFCs separate the satellite phasing from the orbit size, so non-repeating ground-tracks can be used without affecting the uniformity of the satellite distribution in (Ω, M)-space. Additionally, there is no longer a requirement that (N_o, N_{so}, N_c) be coprime.

If repeating ground-tracks are used, the number of unique repeating ground-

tracks followed by the satellites in the constellation is given by

$$N_{rt} = N_s/N_{rs} \tag{2.11}$$

where $N_{rs} = \gcd(N_s, N_o N_d, N_d N_c - N_{so} N_p)$. The condition for all satellites to have the same repeating ground track requires that two integers μ and λ exist such that

$$N_d = \lambda N_{so} \tag{2.12}$$

$$N_p = \mu N_o + \lambda N_c \tag{2.13}$$

and (N_p, N_d) are coprime.

As in HFCs, the remaining parameters required to define the constellation are continuous parameters that are the same for all orbits in the constellation: the inclination angle, the eccentricity, and the argument of periapsis. It is felt that this five parameter description of the LFCs $\{N_o, N_{so}, N_c, e, i, \omega\}$ is canonical and permits important intuitive, as well as theoretical, insight to be obtained into the space of feasible constellations.

3. Equivalence to Walker Constellations

The development of the LFC framework permitted a direct comparison to the Walker constellations. First, a brief recap of notation for Walker and LFCs:

- Total of number of satellites, T, N_s
- Number of orbital planes, P, N_o
- Number of satellites per orbit, S, N_{so}
- Phasing parameter, F, N_c
- Number of orbital periods for compatibility, L, N_p

- Number of Earth revolutions for compatibility, M, N_d
- Number of repeating ground-tracks, $E_{L,M}$, N_{rt}
- Number of satellites on each ground-track, K, N_{rs}

Since both constellations require that orbital planes are uniformly distributed, the values of RAAN are the same for both constellations for a given number of orbital planes. Similarly, the satellites within a plane are uniformly distributed in mean anomaly in both cases, so in the case of an LFC restricted to circular orbits and the same number of satellites per plane, they will be identical.

To show the relationship between the two phasing parameters, F and N_c, we must investigate the physical meaning of N_c. Consider an LFC with argument of perigee occurring at the ascending node ($\omega = 0$). In that case, the first satellite on the $\Omega = 0$ plane is located at the ascending node ($M = 0$). The next plane to the east is located at $\Omega = 2\pi/N_o$, which places the first satellite on that plane at the location $M = -2\pi N_c/N_s$. Note that this is equivalent to $-N_c$ PUs as defined by Walker, or $F = -N_c$. Since the limitations on the value of F are purely to avoid repeating the same pattern, it is clear that the negative sign has no effect on the constellations achievable by each methodology.

Finally, consider the equations for the number of repeating ground tracks and the number of satellites on each of those repeating ground-tracks (Eqs. 2.2 and 2.11):

$$E_{L,M} = T/K, \quad K = \gcd(T, PM, SL + FM)$$
$$N_{rt} = N_s/N_{sr}, \quad N_{sr} = \gcd(N_s, N_o N_d, N_d N_c - N_{so} N_p)$$

Clearly, given the variable definitions above and the fact that $F = -N_c$, these equations are identical.

Despite vastly differing approaches initially, both Mortari and Walker have converged on essentially the same framework. The major difference remains that the LFCs allow elliptical orbits, while Walker constellations are restricted to circular orbits.

C. Elliptical Flower Constellations

The oblateness of the Earth is typically disregarded for initial constellation design because its effects are slow and generally not significant for circular orbits. The dominant term arising from the Earth's oblateness is known as the J_2 effect, which captures the second spherical harmonic describing the shape of the Earth's gravitational field. Though J_2 affects all of the orbital parameters instantaneously, it causes only RAAN, argument of perigee, and mean orbital rate to vary secularly. Identical semi-major axis and inclination leads to identical J_2-induced orbit precession in (Ω, M)-space, thus preserving the relative motion of the configuration in that space (so circular orbit constellations are unaffected). For Flower Constellations, slight changes to the compatibility equation (Eq. (2.5)) can compensate for the J_2 effect on RAAN and mean orbital rate. Dealing with the rotation of the argument of perigee is more difficult.

1. Conceptual Design

The rotation of the argument of perigee is obviously only meaningful in elliptic orbits. Though orbits that are critically inclined at 63.4° experience no rotation of the argument of perigee, this inclination requirement eliminates one of the design variables at the disposal of the constellation designer. To remove this critical inclination constraint, we propose that satellites within a given orbital plane be placed in mul-

tiple orbits with arguments of perigee distributed evenly from 0-360°. Given that all orbits have the same inclination, eccentricity, and semi-major axis, their rate of perigee rotation will be equal. Thus, as they each rotate, the relative perigee spacing remains constant, and periodically the constellation resumes its original structure. The concept is illustrated in Fig. 1. This approach is particularly well-suited for any mission requiring global coverage.

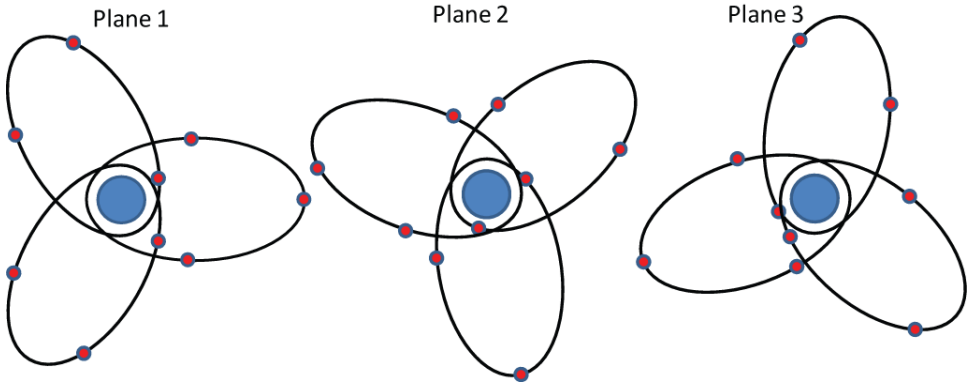

Fig. 1. Elliptical Flower Constellation concept.

Lattice Flower Constellations are particularly elegant for global coverage due to their uniformity of satellite distribution. How does one distribute satellites with multiple arguments of perigee and still maintain some level of uniformity? Many issues must be considered. First, as the arguments of perigee rotate around the orbit normal (relative to the line of nodes) due to J_2, occasionally the apogee (or perigee) of an orbit on a given plane will align with the line of nodes where it intersects with another plane. It would certainly not be uniform if an orbit on that second plane also had apogee (or perigee) along that line of nodes simultaneously, as then two satellites would be at apogee above the same point on Earth. Second, standard LFC design defines the distribution within the plane by equally spacing satellites in mean anomaly space. With satellites in different orbits within the same plane, does that

mean anomaly space lose all meaning from a uniformity standpoint? Lastly, LFC design constrains the interaction of satellites between planes, and this too must be preserved. We will use the LFC framework wherever possible to provide uniform satellite distributions as we develop the *Elliptical Flower Constellations* (EFCs).

2. Mathematical Formulation

To define the Elliptical Flower Constellations, we use N_o to represent the number of orbital planes, N_ω to represent the number of unique orbits (with different arguments of perigee) on each plane, and N'_{so} to represent the number of satellites on each of those orbits. Thus, the total number of satellites is represented by $N_s = N_o N_\omega N'_{so}$. We derive the EFCs using an "orthogonal" approach, where we hold a particular element constant and design a LFC for the remaining two parameters.

We begin with the original LFC equations, using phasing parameter N_c^1. In this step, we assume the argument of perigee is held constant, but allow the mean anomaly distribution to be affected by some unknown function, $h(\omega)$, of the argument of perigee:

$$\begin{aligned} N_o \Omega_{ijk} &= 2\pi i \\ N'_{so} M_{ijk} + N_c^1 \Omega_{ijk} &= 2\pi j + h(\omega) \end{aligned} \tag{2.14}$$

We assume here that h is a function of ω only, and not dependent on the orbital plane, which helps ensure that we recover the original LFC equations if satellites have the same argument of perigee.

Next, we address the distribution of the arguments of perigee by holding mean anomaly constant. Again we use the LFC framework with phasing parameter N_c^3, this time replacing mean anomaly with argument of perigee - thus treating each perigee

as a "satellite" to provide a uniform distribution:

$$\begin{aligned} N_o\Omega_{ijk} &= 2\pi i \\ N_\omega\omega_{ijk} + N_c^3\Omega_{ijk} &= 2\pi k \end{aligned} \tag{2.15}$$

Lastly, we consider the multiple orbits within the same plane as a planar LFC with phasing parameter N_c^2, thus treating ω as if it were Ω and distributing M by the equations

$$\begin{aligned} N_\omega\omega_{ijk} &= 2\pi k + f(\Omega) \\ N'_{so}M_{ijk} + N_c^2\omega_{ijk} &= 2\pi j + g(\Omega) \end{aligned} \tag{2.16}$$

Again, we allow these equations to be affected by functions of RAAN, since for constant orbital plane, all satellites will still maintain an LFC within the plane.

Using the LFC framework, we have addressed maintaining the satellites in LFCs when they have the same argument of perigee, phasing satellites within the plane uniformly, and distributing the arguments of perigee uniformly throughout the constellation. Comparing Eqs. (2.15) and (2.16), it is clear that $f(\Omega) = -N_c^3\Omega$. Differencing Eqs. (2.14) and (2.16), one arrives at the equation

$$N_c^2\omega + h(\omega) = N_c^1\Omega + g(\Omega) \tag{2.17}$$

Since this equation must hold for all values of Ω and ω, the only solution is that $g(\Omega) = -N_c^1\Omega$ and $h(\omega) = -N_c^2\omega$. To be mathematically rigorous, both g and h could also include an arbitrary added constant, but this constant is ignored because it does not affect the relative satellite spacing.

Equations (2.14)-(2.16) can now be reformulated into matrix notation, similar to

Eq. (2.10), to define Elliptical Flower Constellations mathematically as

$$\begin{bmatrix} N_o & 0 & 0 \\ N_c^3 & N_\omega & 0 \\ N_c^1 & N_c^2 & N'_{so} \end{bmatrix} \begin{bmatrix} \Omega_{ijk} \\ \omega_{ijk} \\ M_{ijk} \end{bmatrix} = 2\pi \begin{bmatrix} i \\ k \\ j \end{bmatrix} \tag{2.18}$$

where

$$\begin{aligned} i &= 0, \ldots, N_o - 1 & N_c^1 &\in [0, N_o - 1] \\ j &= 0, \ldots, N'_{so} - 1 & N_c^2 &\in [0, N_\omega - 1] \\ k &= 0, \ldots, N_\omega - 1 & N_c^3 &\in [0, N_o - 1] \end{aligned}$$

Note that the limits on these parameters result from the repetitious nature of the constellation. Values outside of those ranges are perfectly valid, but they describe satellites (or configurations) equivalent to ones defined within the specified ranges. The specific values of (Ω, ω, M) for all satellites in an EFC can be calculated using Algorithm 1.

Algorithm 1 Finds the location in (Ω, ω, M)-space of all satellites in an EFC

```
for i = 0, ..., N_o − 1 do
    Ω ← 2πi/N_o
    for k = 0, ..., N_ω − 1 do
        ω ← (2πk − N_c^3 Ω)/N_ω
        for j = 0, ..., N'_so − 1 do
            M ← (2πj − N_c^1 Ω − N_c^2 ω)/N'_so
            print Ω, ω, M
        end for
    end for
end for
```

3. Properties

Elliptical Flower Constellations can be considered a generalization of the Lattice Flower Constellations. Many of the properties of LFCs identified in Ref. [26] can be applied to EFCs as well, as shown in this section.

First, we generalize the EFC concept to include any matrix $E \in \mathbb{Z}^{3\times3}$ with $\det(E) \neq 0$ in the form

$$E \begin{bmatrix} \Omega_{ijk} \\ \omega_{ijk} \\ M_{ijk} \end{bmatrix} = 2\pi \begin{bmatrix} i \\ k \\ j \end{bmatrix} \tag{2.19}$$

This matrix represents a 3-D torus, where the intersections of the three lines defined by the three rows of E define the locations of the satellites. Any matrix E with the above properties can be reduced by integer row operations to a unique lower triangular form presented in Eq. (2.18), known as the *Hermite Normal Form* [30] of E, which we call E_H. We define the three integer row operations that can be performed on a matrix:

- Reflection: multiply a row by -1
- Permutation: switch two rows
- Shear: add a multiple of one row to another

We can further define four unique matrices required to carry out these operations on a 3×3 matrix:

- Multiply first row by -1

$$U_{N1} = \begin{bmatrix} -1 & 0 & 0 \\ 0 & 1 & 0 \\ 0 & 0 & 1 \end{bmatrix} \tag{2.20}$$

- Switch rows 1 and 2

$$U_{S12} = \begin{bmatrix} 0 & 1 & 0 \\ 1 & 0 & 0 \\ 0 & 0 & 1 \end{bmatrix} \tag{2.21}$$

- Switch rows 1 and 3

$$U_{S13} = \begin{bmatrix} 0 & 0 & 1 \\ 0 & 1 & 0 \\ 1 & 0 & 0 \end{bmatrix} \tag{2.22}$$

- Add row 1 to row 2

$$U_{A12} = \begin{bmatrix} 1 & 0 & 0 \\ 1 & 1 & 0 \\ 0 & 0 & 1 \end{bmatrix} \tag{2.23}$$

Note that these elementary row operations can all be performed on the EFC matrix without changing the solution space. These four transformation matrices can also be used to form all of the other row operations by switching rows:

- Negate row 2: $U_{N2} = U_{S12}U_{N1}U_{S12}$
- Negate row 3: $U_{N3} = U_{S13}U_{N1}U_{S13}$
- Switch rows 2 and 3: $U_{S23} = U_{S13}U_{S12}U_{S13}$
- Add row 2 to row 1: $U_{A21} = U_{S12}U_{A12}U_{S12}$
- Add row 1 to row 3: $U_{A13} = U_{S23}U_{A12}U_{S23}$
- Add row 3 to row 1: $U_{A31} = U_{S13}U_{A13}U_{S13}$
- Add row 2 to row 3: $U_{A23} = U_{S12}U_{A13}U_{S12}$
- Add row 3 to row 2: $U_{A32} = U_{S13}U_{A12}U_{S13}$

Note that the transformation matrices have a determinant of ± 1 and integer coefficients, and the product of these matrices can produce any integer matrix with determinant ± 1.

Theorem C.1. *Two EFCs described by E and E' are equivalent in (Ω, ω, M)-space if and only if $E'E^{-1}$ is a matrix with integer coefficients and determinant of ± 1. In other words, they are equivalent if and only if it is possible to achieve E' from E via a sequence of integer row operations.*

Proof. First, assume $E'E^{-1} = U \in \mathbb{Z}^{3\times 3}$ and $\det(U) = \pm 1$. Therefore, $E' = UE$. All values of U can be constructed from U_{N1}, U_{S12}, U_{S13}, and U_{A12}. Since these transformations have no effect on the solution space of E, it is clear that E and E' are equivalent if $E'E^{-1} = U \in \mathbb{Z}^{3\times 3}$ and $\det(U) = \pm 1$.

Second, we must also prove that if E and E' are equivalent then U exists such that $U \in \mathbb{Z}^{3\times 3}$ with $\det(U) = \pm 1$. Assume E and E' are equivalent and consider three satellites that exist in both:

$$\begin{bmatrix} \Omega_1 \\ \omega_1 \\ M_1 \end{bmatrix} = 2\pi E^{-1} \begin{bmatrix} i_1 \\ k_1 \\ j_1 \end{bmatrix} = 2\pi E'^{-1} \begin{bmatrix} i'_1 \\ k'_1 \\ j'_1 \end{bmatrix}$$

$$\begin{bmatrix} \Omega_2 \\ \omega_2 \\ M_2 \end{bmatrix} = 2\pi E^{-1} \begin{bmatrix} i_2 \\ k_2 \\ j_2 \end{bmatrix} = 2\pi E'^{-1} \begin{bmatrix} i'_2 \\ k'_2 \\ j'_2 \end{bmatrix}$$

$$\begin{bmatrix} \Omega_3 \\ \omega_3 \\ M_3 \end{bmatrix} = 2\pi E^{-1} \begin{bmatrix} i_3 \\ k_3 \\ j_3 \end{bmatrix} = 2\pi E'^{-1} \begin{bmatrix} i'_3 \\ k'_3 \\ j'_3 \end{bmatrix}$$

Premultiply these equations by E' to get

$$E'E^{-1}\begin{bmatrix} i_1 \\ k_1 \\ j_1 \end{bmatrix} = \begin{bmatrix} i'_1 \\ k'_1 \\ j'_1 \end{bmatrix}, \quad E'E^{-1}\begin{bmatrix} i_2 \\ k_2 \\ j_2 \end{bmatrix} = \begin{bmatrix} i'_2 \\ k'_2 \\ j'_2 \end{bmatrix}, \quad E'E^{-1}\begin{bmatrix} i_3 \\ k_3 \\ j_3 \end{bmatrix} = \begin{bmatrix} i'_3 \\ k'_3 \\ j'_3 \end{bmatrix}$$

Or equivalently,

$$E'E^{-1}\begin{bmatrix} i_1 & i_2 & i_3 \\ k_1 & k_2 & k_3 \\ j_1 & j_2 & j_3 \end{bmatrix} = \begin{bmatrix} i'_1 & i'_2 & i'_3 \\ k'_1 & k'_2 & k'_3 \\ j'_1 & j'_2 & j'_3 \end{bmatrix}$$

$$E'E^{-1}C = C'$$

Similarly, by premultiplying by E, one arrives at $EE'^{-1}C' = C$. At this point C and C' can be arbitrarily chosen as any three satellites. By choosing $C = I$, it is clear that $E'E^{-1} = C' = U \in \mathbb{Z}^{3\times3}$. Similarly, choosing $C' = I$ yields $EE'^{-1} = C = V \in \mathbb{Z}^{3\times3}$. Clearly, $UV = VU = I$ and $\det(UV) = \det(U)\det(V) = \det(I) = 1$. Since U and V are integer matrices, this relationship of determinants requires that $\det(U) = \det(V) = \pm1$. Therefore, if $E \equiv E'$, then U exists such that $U \in \mathbb{Z}^{3\times3}$ with $\det(U) = \pm1$. □

Whereas EFCs can be represented by any 3×3 integer matrix, this is a non-minimal representation, so in practice the lower Hermite Normal Form, with six intuitively understood parameters, is the best representation for design optimization work. Note that Thm C.1 can be used to prove the limits on (N_c^1, N_c^2, N_c^3) specified in Eq. (2.18).

When EFCs are used to describe circular orbit constellations, the argument of perigee becomes ill-defined and multiple EFCs describe the same satellite distribution,

creating another equivalency problem.

Theorem C.2. *Given an Elliptical Flower Constellation,*

$$\begin{bmatrix} N_o & 0 & 0 \\ N_c^3 & N_\omega & 0 \\ N_c^1 & N_c^2 & N'_{so} \end{bmatrix} \begin{bmatrix} \Omega_{ijk} \\ \omega_{ijk} \\ M_{ijk} \end{bmatrix} = 2\pi \begin{bmatrix} i \\ k \\ j \end{bmatrix}$$

If the constellation is made of circular orbits ($e = 0$) then this EFC is equivalent to the LFC (with $e = 0$):

$$\begin{bmatrix} N_o & 0 \\ N_c & N_{so} \end{bmatrix} \begin{bmatrix} \Omega_{ij} \\ M_{ij} \end{bmatrix} = 2\pi \begin{bmatrix} i \\ j \end{bmatrix}$$

where

$$N_c = \left[\frac{N_c^1 N_\omega + N_c^3 (N'_{so} - N_c^2)}{\gcd(N_\omega, N'_{so} - N_c^2)} \right] \bmod N_o \tag{2.24}$$

and

$$N_{so} = \frac{N_\omega N'_{so}}{\gcd(N_\omega, N'_{so} - N_c^2)} \tag{2.25}$$

Proof. The EFC equations can be rewritten:

$$\omega = \frac{2\pi k - N_c^3 \Omega}{N_\omega} \tag{2.26}$$

$$M = \frac{2\pi j - N_c^1 \Omega - N_c^2 \omega}{N'_{so}} \tag{2.27}$$

Substituting Eq. (2.26) into Eq. (2.27) yields

$$M = \frac{2\pi j N_\omega - N_c^1 N_\omega \Omega - 2\pi k N_c^2 + N_c^2 N_c^3 \Omega}{N'_{so} N_\omega} \tag{2.28}$$

With zero eccentricity, M and ω are no longer independent, so define $\theta = M + \omega$. Unique values of θ produce unique positions within the constellation. Using

Eqs. (2.26) and (2.28) we find

$$N'_{so}N_\omega\theta = 2\pi\left[N_\omega j + (N'_{so} - N_c^2)k\right] - \left[N_c^3(N'_{so} - N_c^2) + N_c^1 N_\omega\right]\Omega \tag{2.29}$$

Using an integer identity, we can say

$$N_\omega j + (N'_{so} - N_c^2)k = \gcd(N_\omega, N'_{so} - N_c^2)m \tag{2.30}$$

where m is any integer. This allows us to rewrite Eq. (2.29)

$$\left[\frac{N_\omega N'_{so}}{\gcd(N_\omega, N'_{so} - N_c^2)}\right]\theta + \left[\frac{N_c^1 N_\omega + N_c^3(N'_{so} - N_c^2)}{\gcd(N_\omega, N'_{so} - N_c^2)}\right]\Omega = 2\pi m \tag{2.31}$$

which can be simply rewritten into the original LFC equation

$$N_{so}\theta + N_c\Omega = 2\pi m \tag{2.32}$$

Note that, if $\gcd(N_\omega, N'_{so} - N_c^2) \neq 1$ then the circular case of the EFC degenerates as there are not N_s unique slots for satellites. □

Certain properties of the constellation can be easily computed from the general integer (lattice) matrix E.

Theorem C.3. *Given an EFC defined by $E \in \mathbb{Z}^{3\times 3}$, then*

1. *The total number of satellites is $N_s = |\det(E)|$.*
2. *The number of satellites per orbit is $N'_{so} = |\gcd(e_{13}, e_{23}, e_{33})|$.*

Proof. Reduce E to its Hermite Normal Form, E_H, by elementary row operations. Since elementary row operations have no effect on the right hand side of the equations above, they can equivalently be written:

1. The total number of satellites is $N_s = |\det(E_H)| = N_o N_\omega N'_{so} = N_s$.

2. The number of satellites per orbit is

$$\begin{aligned} N'_{so} &= |\gcd(e_{h_{13}}, e_{h_{23}}, e_{h_{33}})| \\ &= \gcd(0, 0, N'_{so}) \\ &= N'_{so} \end{aligned}$$

Note that this gives a physical meaning to the requirement that $\det(E) \neq 0$: otherwise a constellation would have zero satellites. □

Since satellites must have the same argument of perigee to travel on the same repeating ground-track, the number of unique values of argument of perigee for a given EFC is of interest.

Theorem C.4. *The number of unique values of argument of perigee, $N_{u\omega}$, in an EFC is given by*

$$N_{u\omega} = N_\omega \left(\frac{N_o}{\gcd(N_o, N_c^3)} \right) \tag{2.33}$$

Proof. First we look at the sub-matrix, E_s that governs the values of ω when the EFC is written in lower Hermite Normal Form (the last row of E_H, governing the values of mean anomaly, has no impact on the values of ω):

$$E_s = \begin{bmatrix} N_o & 0 \\ N_c^3 & N_\omega \end{bmatrix} \tag{2.34}$$

Matrix E_s can be rewritten into upper Hermite Normal Form using elementary row operations:

$$E'_s = \begin{bmatrix} N_{o\omega} & N_c'^3 \\ 0 & N_{u\omega} \end{bmatrix} \tag{2.35}$$

Clearly, $N_{o\omega}$ is the greatest common denominator of the first column of E'_s. As in Thm. C.3, the elementary row operations do not affect this result, such that it is

also equal to the greatest common denominator of the first column of E_s. Therefore, $N_{o\omega} = \gcd(N_o, N_c^3)$.

We can also define the number of unique orbits, $N_{uo} = N_o N_\omega = \det(E_s)$. Again, the determinant is unchanged by elementary row operations, so $\det(E_s') = N_{o\omega} N_{u\omega} = N_{uo} = N_o N_\omega$. This yields

$$N_{u\omega} = \frac{N_o N_\omega}{N_{o\omega}} = N_\omega \left(\frac{N_o}{\gcd(N_o, N_c^3)} \right) \tag{2.36}$$

□

Theorem C.5. *The satellites in an EFC follow N_{rt} relative trajectories with N_{sr} satellites on each, given by*

$$N_{sr} = \gcd\left[N_{so}' \gcd(N_o, N_c^3), N_d \gcd(N_o, N_c^3), N_c^1 N_d - N_{so}' N_p \right] \tag{2.37}$$

$$N_{rt} = N_s / N_{sr} = m N_{u\omega} \tag{2.38}$$

where $m \geq 1 \in \mathbb{Z}$.

Proof. For two satellites to be on the same relative trajectory, they must have the same argument of perigee. The symmetry of the constellation allows us to evaluate the number of satellites on a single relative trajectory, because that number will be the same on all relative trajectories. Considering just the 0^{th} relative trajectory with all satellites having $\omega = 0$ reveals the requirement

$$\begin{aligned} N_o \Omega &= 2\pi i \\ N_c^3 \Omega &= 2\pi j \end{aligned}$$

which means that we can solve for the values of Ω that result in the same argument of perigee as

$$\Omega = \frac{2\pi l}{\gcd(N_o, N_c^3)}, \quad l \in \mathbb{Z}$$

Given that all satellites satisfying this condition have $\omega = 0$ allows us to write the following requirement for all satellites with the same repeating relative trajectory:

$$\begin{bmatrix} \gcd(N_o, N_c^3) & 0 \\ N_c^1 & N'_{so} \\ N_p & N_d \end{bmatrix} \begin{bmatrix} \Omega \\ M \end{bmatrix} = 2\pi \begin{bmatrix} l \\ j \\ n \end{bmatrix}, \quad l, j, n \in \mathbb{Z}$$

This matrix can be reduced using elementary row and column operations to the simple

$$\begin{bmatrix} \alpha & 0 \\ 0 & \beta \\ 0 & 0 \end{bmatrix} \begin{bmatrix} \Omega \\ M \end{bmatrix} = 2\pi \begin{bmatrix} l \\ j \\ n \end{bmatrix}, \quad l, j, n \in \mathbb{Z}$$

which has $\alpha\beta$ unique solutions. The number of unique solutions of this matrix can be given by the greatest common denominator of the determinants of the 2×2 sub-matrices. Since elementary row and column operations have no effect on the number of solutions or the gcd of the sub-matrix determinants, the number of solutions can be defined as

$$N_{sr} = \gcd\left(\begin{vmatrix} \gcd(N_o, N_c^3) & 0 \\ N_c^1 & N'_{so} \end{vmatrix}, \begin{vmatrix} \gcd(N_o, N_c^3) & 0 \\ N_p & N_d \end{vmatrix}, \begin{vmatrix} N_c^1 & N'_{so} \\ N_p & N_d \end{vmatrix} \right)$$

yielding Eq. (2.37). The number of relative trajectories is clearly $N_{rt} = N_s/N_{sr}$. Substituting $N_{sr} = N'_{so} \gcd(N_o, N_c^3)/m$, where $m \in \mathbb{Z}$ allows us to rewrite this equation in terms of the number of unique values of argument of perigee as $N_{rt} = mN_{u\omega}$. □

Given the desirable properties of having satellites on the same repeating ground-track, a method for achieving the minimum number of unique ground-tracks ($N_{rt} = N_{u\omega}$) is desired.

Theorem C.6. *Letting (N_p, N_d) be two coprime integers satisfying the following for-*

mula:

$$N_p = \lambda \gcd(N_o, N_c^3) + \mu N_c^1 \tag{2.39}$$

$$N_d = \mu N'_{so} \tag{2.40}$$

where $\mu, \lambda \in \mathbb{Z}$ produces exactly $N_{u\omega}$ unique relative trajectories.

Proof. Substituting these equations for N_p and N_d into Eq. (2.37) yields

$$\begin{aligned} N_{sr} &= \gcd\left[N'_{so}g, \mu N'_{so}g, \mu N'_{so}N_c^1 - N'_{so}(\lambda g + \mu N_c^1)\right] \\ &= N'_{so}\gcd\left[g, \mu g, -\lambda g\right] \\ &= N'_{so}g \end{aligned}$$

where $g = \gcd(N_o, N_c^3)$. This value of N_{sr} directly yields $N_{rt} = N_{u\omega}$. □

4. Generalizations

Not only do EFCs share many properties with LFCs, but LFCs are actually a subset of EFCs. An EFC with $N_\omega = 1$, $N_c^2 = 0$, and $N_c^3 = 0$ is equivalent to a LFC. Since the LFC framework also encompasses all Walker constellations as proved in Ref. [26], the EFCs include those as well. The LFCs are represented in the EFC framework (using LFC variable definitions) by the matrix

$$\begin{bmatrix} N_o & 0 & 0 \\ 0 & 1 & 0 \\ N_c & 0 & N_{so} \end{bmatrix} \tag{2.41}$$

Walker constellations are similarly represented (using Walker variable definitions):

$$\begin{bmatrix} P & 0 & 0 \\ 0 & 1 & 0 \\ -F \bmod P & 0 & S \end{bmatrix} \tag{2.42}$$

Dufour [31, 32] introduced elliptical Walker constellations with a single orbit per plane, where the arguments of perigee were distributed according to the equation

$$\omega_{ij} = \omega_0 + \frac{2\pi i G}{N_s} \tag{2.43}$$

where $G \in [0, N_o - 1]$ is a phasing parameter. If the denominator was N_o instead of N_s, we could claim that EFCs also encompassed all of Dufour's elliptical Walker constellations by setting $N_c^3 = 0$, $N_\omega = 1$, and $N_c^2 = -G \bmod N_o$. In fact, Dufour's own limits on the values of G indicate that this is the correct denominator. Additionally, using N_s as the denominator leads to non-uniform constellations, where ω is not uniformly distributed between orbital planes. Whereas the $\Delta\omega$ between subsequent orbital planes is typically $2\pi G/N_s$, the $\Delta\omega$ between the first and last planes is $2\pi G/N_s - 2\pi G/N_{so}$. In the case where $N_s = N_o$ or $G = 0$, the two different denominators produce the same constellation. Of the more than 50 constellations presented in Refs. [31, 32], only one does not satisfy either of those conditions. We thus conclude that EFCs can legitimately be considered a generalization of the elliptical Walker constellations proposed by Dufour.

Also of interest are the elliptical constellations for global coverage developed by Draim in Refs. [24, 25, 33]. Dufour notes that all of these constellations can be described using the elliptical Walker constellation framework, and since all of Draim's constellations in Refs. [24, 25, 33] utilize $N_s = N_o$, they are unquestionably also a subset of Elliptical Flower Constellations. The elliptical Walker constellations are

represented in the EFC framework by:

$$\begin{bmatrix} P & 0 & 0 \\ -G \bmod P & 1 & 0 \\ -F \bmod P & 0 & S \end{bmatrix} \tag{2.44}$$

5. Other Design Considerations

Designing an Elliptical Flower Constellation requires more than selecting the six integer parameters described above. The semi-major axis, eccentricity, and inclination that is common to all satellites must be selected. Additionally, the RAAN (Ω_0), argument of perigee (ω_0), and mean anomaly (M_0) of the first reference satellite can also be selected arbitrarily without affecting the relative phasing within the constellation. We can rewrite Eqn. (2.18) as

$$\begin{bmatrix} N_o & 0 & 0 \\ N_c^3 & N_\omega & 0 \\ N_c^1 & N_c^2 & N'_{so} \end{bmatrix} \begin{bmatrix} \Omega_{ijk} - \Omega_0 \\ \omega_{ijk} - \omega_0 \\ M_{ijk} - M_0 \end{bmatrix} = 2\pi \begin{bmatrix} i \\ k \\ j \end{bmatrix} \tag{2.45}$$

Thus, an EFC requires six integer parameters and six continuous parameters. Essentially, the six continuous parameters define the orbit elements of the 0^{th} satellite, and the six integer parameters phase all other satellites relative to that one. Each of the continuous parameters is subject to particular considerations as described in the following sections.

Semi-major Axis and Eccentricity

The orbit semi-major axis and eccentricity are common among all satellites in the constellation, and are typically bounded by some minimum and maximum altitudes. Typically these bounds are a result of sensor or antennae limitations. Requiring

hardware that can operate at varying altitudes is a significant limitation on the use of elliptic orbits.

The semi-major axis can also be chosen to provide repeating ground-tracks as in the Walker or Lattice Flower constellation theories. Satellites with the same argument of perigee can also be placed on the same repeating ground-track through judicious selection of the parameters (N_p, N_d) as discussed in Thm. C.6.

Inclination

The inclination of the orbits has significant impact on the coverage provided by an EFC. Even in circular orbit constellations, certain inclinations result in satellites theoretically colliding, whereas others permit near perfect phasing as a satellite from one plane passes directly between two satellites from another plane.

Considering two satellites in circular orbits with the same altitude, the closest approach distance between the two satellites, $\rho_{\min}$, can be analytically computed from the equations

$$\Delta F = \Delta M - 2\arctan\left[-\tan(\Delta\Omega/2)\cos i\right] \tag{2.46a}$$

$$\cos\beta = \cos^2 i + \sin^2 i\cos\Delta\Omega \tag{2.46b}$$

$$\rho_{\min} = 2\left|\sqrt{\frac{1-\cos\beta}{2}}\sin(\Delta F/2)\right| \tag{2.46c}$$

where ΔM and $\Delta\Omega$ are the difference in orbit elements of the two satellites and i is the inclination angle common to both [34]. Note that $\rho_{\min}$ must be scaled by the orbit radius to find the physical approach distance. The minimum distance encountered within a constellation of circular orbits can be computed by calculating this approach distance for all pairs of satellites. Perfect juggling requires that no two satellites are ever closer than half the distance between two consecutive satellites in the same orbit.

We can scale the minimum approach distance such that zero corresponds to collision and one corresponds to perfect juggling. Using this scaling, the results for the 27/3/1 Walker constellation are plotted in Fig. 2 as a function of inclination angle. This is the constellation design chosen for the Galileo GNSS system [35]. Note the peak near an inclination of 56°, the chosen inclination for Galileo.

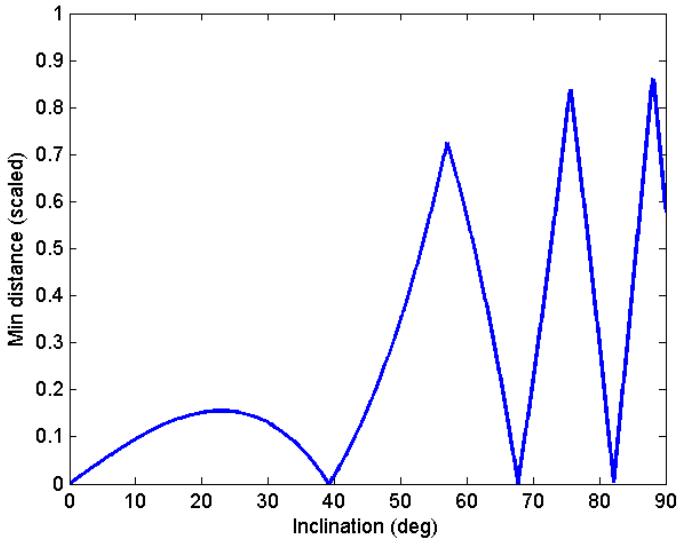

Fig. 2. Minimum encounter distance in the 27/3/1 Walker constellation as a function of inclination.

This indicates that even though inclination is technically a continuous parameter, there exist discrete values of inclination that maintain high levels of uniformity in the distribution of satellites. Equation (2.46) only applies to circular orbits, but similar computations can be made for constellations of elliptic orbits and may prove insightful in the design process. We can also use Eq. (2.46) to address the juggling of apogees and perigees - an issue raised in the previous section. As in the development of Elliptical Flower Constellations, we can consider the arguments of perigee to constitute their own Lattice Flower Constellation, all of which rotate at the same rate, just like a

constellation of circular orbits. Thus, this method must be used to chose an inclination to achieve successful juggling of the apogees and perigees.

Selecting Ω_0, ω_0, and M_0

The values of $(\Omega_0, \omega_0, M_0)$ provide the three angular elements of the reference satellite $(i, j, k) = (0, 0, 0)$. Though each of them could be drawn from $[0, 2\pi)$, each can be further bounded by constellation considerations once the 6 integer parameters have been chosen.

Theorem C.7. *Every initial condition of a given EFC can be described using values of (Ω_0, ω_0, M_0) in the ranges*

$$\Omega_0 \in \left[0, \frac{2\pi}{N_o}\right) \tag{2.47}$$

$$\omega_0 \in \left[0, \frac{2\pi}{N_o N_\omega} \gcd(N_o, N_c^3)\right) \tag{2.48}$$

$$M_0 \in \left[0, \frac{2\pi}{N_s} \gcd(N_o N_\omega, N_c^2 N_o, N_\omega N_c^1 - N_c^2 N_c^3)\right) \tag{2.49}$$

Proof. Assume that the set $\{\Omega^\star_{ijk}, \omega^\star_{ijk}, M^\star_{ijk}\}$ is the set of satellite locations given $(\Omega_0, \omega_0, M_0) = (0, 0, 0)$. Equation (2.45) generates the identical set for particular values of $(\Omega_0, \omega_0, M_0)$ if and only if the following equation is still satisfied:

$$\begin{bmatrix} N_o & 0 & 0 \\ N_c^3 & N_\omega & 0 \\ N_c^1 & N_c^2 & N'_{so} \end{bmatrix} \begin{bmatrix} \Omega^\star_{ijk} - \Omega_0 \\ \omega^\star_{ijk} - \omega_0 \\ M^\star_{ijk} - M_0 \end{bmatrix} = 2\pi \begin{bmatrix} i \\ k \\ j \end{bmatrix} \tag{2.50}$$

This condition can be rewritten as three separate equations involving $(\Omega_0, \omega_0, M_0)$:

$$N_o\Omega_0 = 2\pi i \tag{2.51}$$

$$N_c^3\Omega_0 + N_\omega\omega_0 = 2\pi k \tag{2.52}$$

$$N_c^1\Omega_0 + N_c^2\omega_0 + N'_{so}M_0 = 2\pi j \tag{2.53}$$

The task is to find the minimum values of $(\Omega_0, \omega_0, M_0)$ that satisfy the above equations.

Solving Eq. (2.51) yields:

$$\Omega_0 = \frac{2\pi}{N_o} i \tag{2.54}$$

The smallest value of Ω_0 occurs when $i = 1$, thus establishing the upper limit on Ω_0. Solving Eq. (2.51) for Ω_0 and substituting that into Eq. (2.52) results in:

$$\begin{aligned} \omega_0 &= \frac{2\pi}{N_o N_\omega}(N_o k - N_c^3 i) \\ &= \frac{2\pi}{N_o N_\omega}\gcd(N_o, N_c^3)m \end{aligned}$$

Again, $m = 1$ represents the smallest value of ω_0 before the pattern repeats. Similarly, solving Eqs. (2.51) and (2.52) for Ω_0 and ω_0, respectively, and substituting them into Eq. (2.53) yields the result

$$\begin{aligned} M_0 &= \frac{2\pi}{N_s}\left[N_o N_\omega j - N_c^2 N_o k - (N_c^1 N_\omega - N_c^2 N_c^3)\right] \\ &= \frac{2\pi}{N_s}\gcd(N_o N_\omega, N_c^2 N_o, N_c^1 N_\omega - N_c^2 N_c^3)n \end{aligned}$$

□

All EFCs can be described by values within these ranges due to their uniform, symmetric nature. For general EFCs with a global coverage mission, the design parameters can simply be taken as zero. When zonal or regional coverage is required,

these variables significantly effect coverage. Clearly, ω_0 is significant for critically inclined orbits, even when global coverage is considered, but has no meaning when dealing with circular orbits.

If one is considering global coverage, these ranges may not only be used for design purposes, they can also be used as limits on orbit propagations, thereby reducing computation time. Consider the naive ranges on each parameter

$$\Omega_0 \in \left[0, \frac{2\pi}{N_o}\right), \quad \omega_0 \in \left[0, \frac{2\pi}{N_\omega}\right), \quad M_0 \in \left[0, \frac{2\pi}{N'_{so}}\right) \tag{2.55}$$

These naive bounds can easily be shown to be the worst case bounds allowed bu the optimal bounds of Thm. C.7. First, the bounds on Ω_0 are identical. Second, since the value of N_c^3 is always less than the value of N_o, the maximum value of $\gcd(N_o, N_c^3)$ is N_o, and the maximum value of the optimal bound is $2\pi/N_\omega$. Finally, the gcd in the bounds on M_0 has a maximum value of $N_o N_\omega$ since neither of those parameters is allowed to be zero. Therefore, M_0 is bounded by $2\pi/N'_{so}$ in the worst case.

In the global navigation example of Chapter IV, with 27 satellites in 3 orbital planes, the optimal bounds of Thm. C.7 reduce propagation time by a factor of ≈ 7.5 over these naive bounds when averaged over all 117 EFCs. Some of those 117 EFCs see a reduction in propagation time of a factor of 81. The 150 EFCs with 25 satellites and 5 orbital planes improve propagation times by a factor of ≈ 13.5 on average, with a few improving by a factor of 125!

To complete the picture with respect to other design methods, Walker's phasing parameter in Ref. [15] is equivalent to our M_0. Dufour includes an ω_0 in his elliptical Walker constellations that is a multiple of another integer parameter he introduces, but the range of ω_0 is limited to $[-\pi/2, \pi/2]$ rather than the full allowable range of $[-\pi, \pi]$ [31, 32]. The continuous parameter used here clearly includes the discrete values of Ref. [31, 32].

D. Fast Orbit Propagation

Evaluating a satellite constellation design typically requires the computation of some performance metric over some time span (the period of repetition for repeating ground-track constellations). This is because the performance metrics include complicated constraints, such as sensor field of view (FOV) or minimum elevation angle. The coverage requirements can range from continuous global coverage to maximizing time over target of a specific region. All of these complications preclude the use of any simply analysis of the system performance and require that all satellites be propagated through time, evaluating the performance metric at each time step.

Solving for the position of an object given its orbit element representation is a fundamental problem in celestial mechanics. Whether the orbits are being propagated assuming simple Keplerian motion or more complicated perturbation methods using orbit elements (ie. Lagrange's equations), the orbit propagation problem ultimately rests in solving the transcendental *Kelper's equation* (KE)

$$n(t - t_0) = M = E - e \sin E \tag{2.56}$$

where n is the mean orbital rate, t is the time, t_0 is the time of periapsis passage, M is the mean anomaly, and E is the eccentric anomaly. Mean anomaly is easily solved for during orbit propagation due to its linear dependence on time, but the eccentric anomaly is required to compute satellite positions and velocities. Other orbit propagation methods that rely on numerical integration avoid solving Kepler's equation, but at the much greater expense of evaluating complex equations of motion.

Solving Kepler's equation has been a rite of passage for some of the greatest minds in mathematics since it first appeared about 350 years ago [36]. References [36, 37, 38] provide overviews of the classic methods based on an iterative Newton's method or

truncated series expansion. In recent years, Nijenhuis [39] and Markley [40] have developed advanced techniques for solving KE in only one or two iterations, whereas Fukushima [41] and Feinstein and McLaughlin [42] have developed discretization techniques that utilize computer science techniques to efficiently access large pre-computed data sets.

We performed a comprehensive review of existing methods for solving Kepler's equation, particularly the computation of an initial estimate for use in further iterative solvers. We then developed several new solutions using the fact that most orbit propagations, especially those used for evaluating constellation designs, involve determining orbital position at constant steps in mean anomaly - allowing us to develop solutions based on previous values of eccentric anomaly. Both the existing methods and new methods were analyzed for computational complexity and accuracy.

1. Review of Existing Methods

The literature on solving Kepler's equation typically breaks down the process into the formulation of a starter to compute an initial solution estimate, followed by the application (sometimes iteratively) of a corrector. Odell and Gooding [43] present a survey of a dozen starters, whereas Battin [37] presents several more. Of these simple methods, two in particular stand out. The first is what Odell and Gooding call solution S_7, which is both computationally cheaper and more accurate on average than their solutions S_2, S_3, S_5, S_8, S_{10}, S_{11}, and S_{12}. Solution S_7 is a piecewise function incorporating S_4 and S_6 and is thus more accurate than either of those with similar complexity. The basis for computational complexity and accuracy comparisons is explained in Section 4.

Solution S_7:

1. $0 \leq M < 1 - e$

$$E = \frac{M}{1 - e} \tag{2.57}$$

2. $1 - e \leq M < \pi - 1 - e$

$$S_4 : E = M + e \tag{2.58}$$

3. $\pi - 1 - e \leq M < \pi$

$$S_6 : E = \frac{M + e\pi}{1 + e} \tag{2.59}$$

Only solution S_1 $(E = M)$ is simpler computationally, but it is several orders of magnitude less accurate. Solution S_7 is also simpler and more accurate than any of the additional methods presented by Battin.

The only solution presented by Odell and Gooding or Battin that competes with S_7 is solution S_9 which is significantly more computationally complex, but also more accurate. Solution S_9 is defined as

$$E = M + \frac{e \sin M}{\sqrt{1 + e^2 - 2e \cos M}} \tag{2.60}$$

Taff and Brennan [44] conducted a survey of both starters and iteration methods and identified a starter from Broucke [45] as the most efficient. Our complexity and accuracy analysis of the starters studied by Taff confirms this analysis. Broucke developed upper and lower bounds for the solution based on tangents and chords with the solution space broken up into four sections. Broucke's upper bounds are the basis for solution S_7. By averaging the upper and lower bounds, an efficient starter is achieved with higher accuracy than S_7. The Broucke starter can be written in the form

$$E = \alpha M + \beta \tag{2.61}$$

Table I details the values of α and β for different regions of M.

Table I. Broucke's method parameters

Region	α	β
$0 < M < 1 - e$	$\frac{2\pi-(2+\pi)e}{2\pi-2(2+\pi)e+4e^2}$	0
$1 - e < M < \frac{\pi}{2} - e$	$\frac{\pi-e}{\pi-2e}$	$\frac{e}{2}$
$\frac{\pi}{2} - e < M < \pi - e - 1$	$\frac{\pi+e}{\pi+2e}$	$\frac{3\pi e+2e^2}{2\pi+4e}$
$\pi - e - 1 < M < \pi$	$\frac{2\pi+(2+\pi)e}{2\pi+2(2+\pi)e+4e^2}$	$\frac{e\pi(2+4e+\pi)}{2\pi+2(2+\pi)e+4e^2}$

Beyond these simple starters, both Mikkola [46] and Markley [40] present starters that require the solution of a cubic equation. Both are orders of magnitude more accurate than the three listed above, but the computational cost of the required cube root makes them much less efficient. Though Mikkola requires slightly fewer additions and multiplications than Markley, the computation time is dominated by the transcendental functions and Markley is six times more accurate. We briefly review the equations for Markley's approach here; see Ref. [40] for the derivations.

$$\alpha = \frac{3\pi^2 + 1.6\pi(\pi - M)/(1 + e)}{\pi^2 - 6} \tag{2.62}$$

$$d = 3(1 - e) + \alpha e \tag{2.63}$$

$$q = 2\alpha d(1 - e) - M^2 \tag{2.64}$$

$$r = 3\alpha d(d - 1 + e)M + M^3 \tag{2.65}$$

$$w = \left(r + \sqrt{q^3 + r^2}\right)^{2/3} \tag{2.66}$$

$$E = \frac{1}{d}\left(\frac{2rw}{w^2 + wq + q^2} + M\right) \tag{2.67}$$

Finally, Nijenhuis [39] took the S_7 starter and recognized that it performs poorly in the region $e > 0.55$ and $M < 0.45$ and so replaced S_7 in that region by a slightly modified Mikkola's solution. Throughout the rest of the domain, he refined the S_7

starter using a single iteration of Halley's rational method:

$$E = E - \frac{f}{f' + \frac{1}{2}\delta f''} \tag{2.68}$$

where $\delta = -f/f'$. Nijenhuis defines $f(E) = E - e\mathrm{s}_n(E) - M$, where the sine function has been replaced by the approximation

$$\mathrm{s}_n(x) = x - 0.6605x^3 + 0.00761x^5 \tag{2.69}$$

where $x = E$ for $x < \pi/2$ and $x = \pi - E$ for $x > \pi/2$.

The computational complexity and accuracy of these starters (Broucke, S_9, Markley, and Nijenhuis) will be analyzed and discussed in Section 4 in comparison to the new methods presented here. The application of one or more correction steps using Newton's method, Halley's method, or higher order methods will impact the final solution of the starters in the same way in terms of improved accuracy and increased computational burden. We focus here on more efficient starter methods and refer the reader to Refs. [41, 43, 44] for a discussion of iterative techniques.

2. Sequential Orbit Propagation

For applications such as orbit visualization, preliminary mission analysis, or constellation design, the orbit position and velocity are not solved at arbitrary discrete points. Instead one typically utilizes points equally spaced in time throughout the orbit. Rather than treat each of those points independently, solving Kepler's equation for each, we propose to use the information of previous points to produce approximate solutions at lower computational cost.

The simplest solution of this type would be the simple recursion $E_{k+1} = 2E_k - E_{k-1}$, but this simply amounts to assuming constant steps in ΔE. The slightly more complicated recursion $E_{k+1} = 3E_k - 3E_{k-1} + E_{k-2}$ improves on this estimate, but

both of these recursions are orders of magnitude lower accuracy than the starters reviewed above. Instead, we look at expansions of Kepler's equation and the radius vector to find seven different sequential solutions.

Taylor Expansion of Kepler's Equation

Let us consider the problem of defining a sequence in eccentric anomaly such that the associated sequence of mean anomaly M_k (at times t_k) is such that $(M_k - M_{k-1})$ is equal to an assigned constant difference ΔM, independent from index k. Start by defining the function

$$f(E) = E - e \sin E - M \tag{2.70}$$

To obtain an approximated sequence we can write the Taylor expansion to second order of Kepler's equation as

$$f(E_{k+1}) = f(E_k) + f'(E_k)\Delta E_k + \frac{1}{2} f''(E_k)(\Delta E_k)^2 \tag{2.71}$$

Assuming the previous step was solved perfectly, it follows that $f(E_k) = 0$ and $f(E_{k+1}) = \Delta M$. Substituting in the values of the derivatives, one arrives at

$$\Delta M = (1 - e \cos E_k)\, \Delta E_k + \frac{1}{2}\, e \sin E_k\, (\Delta E_k)^2 \tag{2.72}$$

Taking just the first term of the expansion yields a simple, linear sequence defined by

$$E_{k+1} = E_k + \frac{\Delta M}{1 - e \cos E_k} \tag{2.73}$$

which we will refer to as method M_1. Essentially this equation uses E_k as an initial guess and performs a single iteration of Newton's method. This sequence has the advantage of being very simple computationally, on the order of the S_7 solution or Broucke's method described earlier.

Alternatively, the second order Taylor series can be solved for ΔE_k directly, yielding solution M_2:

$$E_{k+1} = E_k + \frac{\sqrt{(1 - e\cos E_k)^2 + 2\Delta M e \sin E_k} - (1 - e\cos E_k)}{e \sin E_k} \tag{2.74}$$

Note that this is equivalent in form to using E_k as the initial guess and applying a single correction of Halley's irrational form.

Instead of Halley's irrational form, we might instead solve it using Halley's rational form, given in Eq. (2.68). Substituting the correct formulas yields

$$E_{k+1} = E_k + \frac{\Delta M}{(1 - e\cos E_k) + \frac{\Delta M e \sin E_k}{2(1 - e\cos E_k)}} \tag{2.75}$$

which we call solution M_3.

Finally, Battin [37] suggests the use of series reversion to solve Kepler's equation, which can be applied to this second order Taylor series to produce solution M_4:

$$E_{k+1} = E_k + \frac{\Delta M}{1 - e\cos E_k} - \frac{e \sin E_k}{2(1 - e\cos E_k)} \left(\frac{\Delta M}{1 - e\cos E_k} \right)^2 \tag{2.76}$$

These three second order solutions are more computationally complex than the linear form (similar to S_9), but significantly more accurate. Note that in all three cases, knowing the value of f to be ΔM saves its costly computation involving the sine function.

Since evaluation of the orbit position requires evaluation of sine and cosine of each value of eccentric anomaly, the use of those functions in solutions M_1-M_4 do not represent additional computation, as opposed to the sine and cosine of mean anomaly seen in S_9.

Taylor Expansion of the Radius Vector

Alternatively, the propagation phase can be performed by evaluating the radius at time $t_k + \Delta t$, through Taylor expansion. The series is

$$\boldsymbol{r}(t_k + \Delta t) = \sum_{n=0}^{\infty} \left. \frac{d^n \boldsymbol{r}}{dt^n} \right|_{t_k} \frac{\Delta t^n}{n!} \tag{2.77}$$

where, for the elliptical case, the radius can be expressed in term of eccentric anomaly

$$\boldsymbol{r} = a \begin{bmatrix} \cos E - e \\ \sqrt{1 - e^2} \, \sin E \end{bmatrix} \tag{2.78}$$

The derivatives appearing in the series expansion can be evaluated as

$$\frac{d\boldsymbol{r}}{dt} = \frac{d\boldsymbol{r}}{dE} \frac{dE}{dt} \qquad \text{where} \qquad \frac{dE}{dt} = \frac{n}{1 - e \, \cos E} \tag{2.79}$$

For instance, keeping just the first three terms (position, velocity, and acceleration) of the expansion given in Eq. (2.77) we obtain

$$\boldsymbol{r}_{k+1} \approx \boldsymbol{r}_k + \dot{\boldsymbol{r}} \, \Delta t + \frac{1}{2} \ddot{\boldsymbol{r}} \, \Delta t^2 \tag{2.80}$$

where, using Eq. (2.79), we can express position, velocity, and acceleration in term of eccentric anomaly as

$$\begin{aligned} \boldsymbol{r} &= a \begin{bmatrix} \cos E - e \\ \sqrt{1 - e^2} \, \sin E \end{bmatrix} \\ \dot{\boldsymbol{r}} &= \frac{a \, n}{(1 - e \, \cos E)} \begin{bmatrix} -\sin E \\ \sqrt{1 - e^2} \, \cos E \end{bmatrix} \\ \ddot{\boldsymbol{r}} &= -\frac{a \, n^2}{(1 - e \, \cos E)^3} \begin{bmatrix} \cos E - e \\ \sqrt{1 - e^2} \, \sin E \end{bmatrix} \end{aligned} \tag{2.81}$$

Substituting Eq. (2.81) in Eq. (2.80) we obtain our formulation to perform the orbit propagation step

$$\begin{aligned} \cos E_{k+1} &\approx \cos E_k - \frac{\sin E_k}{(1 - e\,\cos E_k)}\,\Delta M - \frac{1}{2}\,\frac{(\cos E_k - e)}{(1 - e\,\cos E_k)^3}\,\Delta M^2 \\ \sin E_{k+1} &\approx \sin E_k + \frac{\cos E_k}{(1 - e\,\cos E_k)}\,\Delta M - \frac{1}{2}\,\frac{\sin E_k}{(1 - e\,\cos E_k)^3}\,\Delta M^2 \end{aligned} \tag{2.82}$$

Since these two equations are not independent, each must be normalized by $L = \sqrt{\cos^2 E_{k+1} + \sin^2 E_{k+1}}$ at each time step. As in the previous section, we define a linear update, M_5, using only the first two terms and a second order update, M_6, using all three. The advantage of this formulation is that it requires no trig function evaluations to obtain the position and velocity of the satellite.

3. Expansion of the Difference Form of KE

Yet another approach involves the expansion of the difference form of Kepler's equation, which can be written as

$$\Delta M = \Delta E_k - e\cos E_k \sin \Delta E_k + e \sin E_k (1 - \cos \Delta E_k) \tag{2.83}$$

where we define $\Delta E_k = E_{k+1} - E_k$. Assuming $\Delta E_k = \Delta E_{k-1} + \delta$, and substituting into this equation, we can write

$$\begin{aligned} \Delta M = \Delta E_{k-1} + \delta \;&-\; e\cos E_k(\sin \Delta E_{k-1} \cos \delta + \sin \delta \cos \Delta E_{k-1}) \\ &+\; e \sin E_k (1 - \cos \Delta E_{k-1} \cos \delta + \sin \Delta E_{k-1} \sin \delta) \end{aligned} \tag{2.84}$$

Assuming that δ is small (a reasonable assumption for small values of ΔM, particularly at small to moderate values of eccentricity) allows us to solve for δ as

$$\delta = \frac{\Delta M - \Delta E_{k-1} + e\,(\sin(E_k + \Delta E_{k-1}) - \sin E_k)}{1 - e\cos(E_k + \Delta E_{k-1})} \tag{2.85}$$

We can now define a quadratically recursive update method, M_7, as

$$E_{k+1} = E_k + \Delta E_{k-1} + \delta \tag{2.86}$$

The calculation of δ is computationally burdensome, but not without benefit as seen in Section 4.

Initial Step

The proposed solutions utilizing sequences are sensitive to errors in the initial step since this error can propagate through to all other steps. The second order forms reduce to the linear form for $E_0 = 0$ (or have no solution in the case of M_2), given by

$$E_1 = \frac{\Delta M}{1 - e} \tag{2.87}$$

This is the same equation used by S_7 for small values of M, but as Nijenhuis found, it performs poorly for eccentricities larger than about 0.55. So instead, we seek a more accurate initial step at the price of increased computational complexity for that single initial step. One option would be to utilize Markley's or Mikkola's solutions, but instead we simply use the third order Taylor expansion to find a formula accurate in the region $M < 5°$. The third order expansion of Kepler's equation can be written

$$\Delta M = (1 - e)E + \frac{eE^3}{6} \tag{2.88}$$

which yields

$$r = \frac{3\Delta M}{e} \tag{2.89}$$

$$q = \frac{2(1 - e)}{e} \tag{2.90}$$

$$E_1 = \frac{2rw}{w^2 + wq + q^2} \tag{2.91}$$

where w is defined as in Eq. (2.66). This provides a solution just as accurate as Markley or Mikkola in the specified range but with lower complexity. Clearly this equation fails for $e = 0$, but in that case $E_1 = \Delta M$ is the exact solution. This equation is used for the initial step in all solutions M_1-M_7 in the numerical tests of Section 4.

4. Numerical Analysis

In the following discussion, Markley's solution refers to just the starter presented here and does not include his high order correction. Similarly, the Nijenhuis solution refers to his refined starter.

Algorithmic Complexity

We note that the information required for orbit propagation is not E itself, but rather the sine and cosine of E, meaning any solution that solves for E must include the evaluation of those two transcendental functions in any complexity analysis.

To support the proposed algorithms, the computational complexity of required mathematical operations [30] is evaluated. Tables II and III provide summaries of the number of evaluations for each method and the run-time bit complexity (using big-$\mathcal{O}$ notation) for the three kind of operations involved: a) addition or subtraction, b) multiplication or division or square root,[1] and c) the trigonometric functions. In these tables, n represents the number of digits for the specific operation (32 for single and 64 for double precision). For both the Broucke and Nijenhuis solutions, the listed complexity is the average over the range $0 \leq e \leq 1$ and $0 \leq M \leq \pi$. Only operations that must be computed for every value of M was considered. Quantities such as α

[1]The run-time bit complexity for multiplication appearing in Tables II and III is associated with the Schönhage-Strassen algorithm [47].

and β in Broucke's solution (Eq. (2.61)) that depend only on constants and e can be computed just once for an entire orbit propagation, so those operations were ignored.

Table II. Algorithmic complexity of existing methods

Operations	Complexity	Broucke	S_9	Markley[2]	Nijenhuis
$+,\ -$	n	1.8	3	12	10.9
$*,\ /,\ \sqrt{}$	$n\ \log(n)\ [\log\log(n)]$	1	4	22	14.2
sin, cos	$M(n)\ \log(n)$	2	4	2	2

Table III. Algorithmic complexity of sequential methods

Operations	Complexity	M_1	M_2	M_3	M_4	M_5	M_6	M_7
$+,\ -$	n	2	4	3	3	3	7	7
$*,\ /,\ \sqrt{}$	$n\ \log(n)\ [\log\log(n)]$	2	6	4	6	8	14	3
sin, cos	$M(n)\ \log(n)$	2	2	2	2	0	0	4

To produce these complexity tables, each algorithm was evaluated for the minimum possible evaluations by pre-computing constants and simplifying equations where possible. The cost of conditional statements or assignment statements was not evaluated and may have a slight impact on computation time. All algorithms that require a value for M include the cost of evaluating $M_{k+1} = M_k + \Delta M$.

It is clear from these tables that Markley's and Nijenhuis' methods are significantly more complex than any of the other solutions. Since the trigonometric functions are so much more costly than multiplication and division, it is also clear that S_9 is more complex than any of the proposed second order solutions (M_2-M_4). The relationship between methods M_5-M_6 and methods M_1-M_4 is less clear, but tests using MATLAB Profiler suggest that M_5 is comparable to M_1 and M_6 is comparable to

[2]Also requires a cube root for all values of (M, e)

M_2-M_4 in run-time complexity. Direct comparison of times has been avoided because such times are affected by choice of processor, operating system, coding language, etc.

Accuracy

Each algorithm was evaluated on a fine grid over the range $M \in [0, \pi]$ to assess accuracy. Many authors stress the performance of their Kepler's solver in the region near $e = 1$, but this condition is rarely encountered in practice, so we evaluated over the entire range $e \in [0, 0.99]$. The sequential starters were evaluated using a step-size of $\Delta M = 1^\circ$ and $\Delta M = 5^\circ$ since the accuracy degrades as the step-size increases. Again, since the end-goal is orbit propagation, each solution for E was converted into a solution for the satellite position, and the error in that position as a percentage of the semi-major axis was used to evaluate accuracy. This feels more intuitive than relative errors in E and also more practical.

Figure 3 shows contour plots of the accuracy results of the existing methods. The mean and maximum errors encountered are listed in Table IV. Clearly Broucke and S_9 have issues in the high eccentricity, low mean anomaly range which is what led Nijenhuis to evaluate that region separately.

Table IV. Error in position propagation as percent of semi-major axis of existing methods

Error	Broucke	S_9	Markley	Nijenhuis
Mean (%)	1.97	0.60	0.01	0.03
Maximum (%)	17.26	29.98	0.04	0.94

Note that the Markley solution is far and away the most accurate, and even though Nijenhuis has replaced the most troublesome region, the maximum error en-

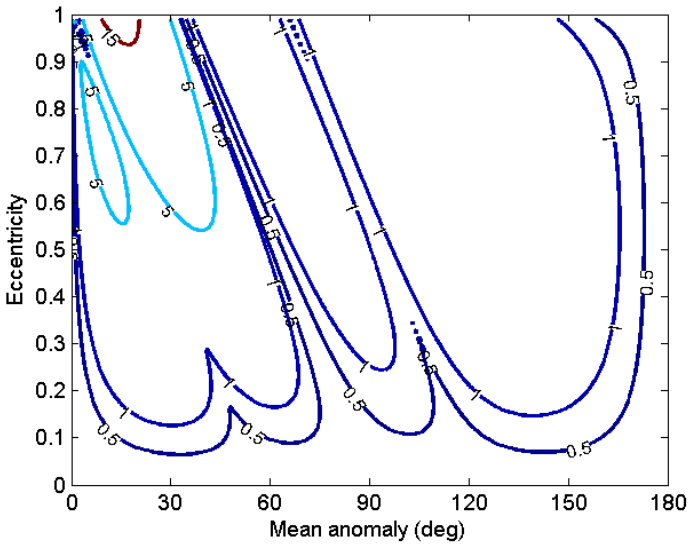

(a) Broucke's solution

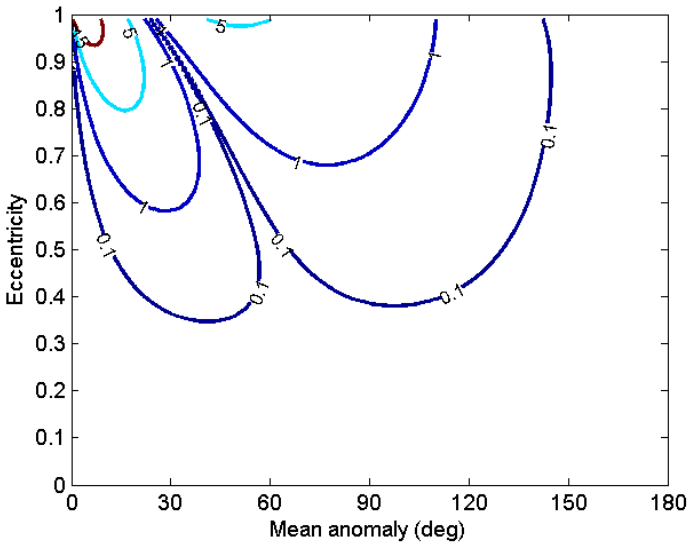

(b) Solution S_9 from Ref. [43]

Fig. 3. Error in position propagation as percent of semi-major axis of existing methods.

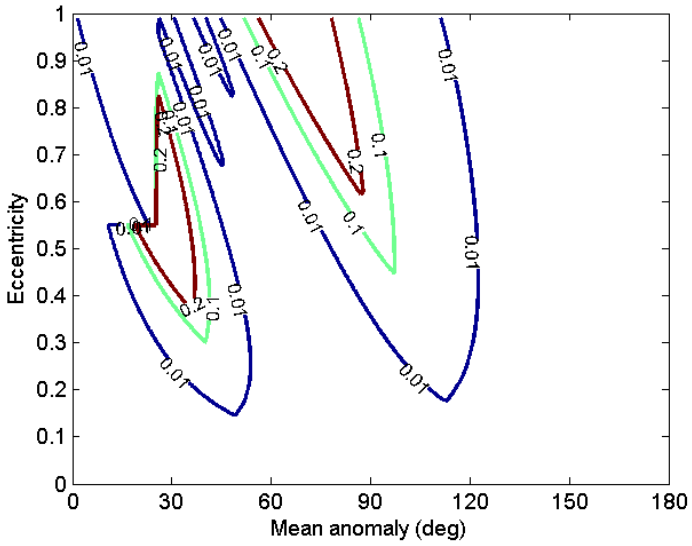

(c) Nijenhuis' solution

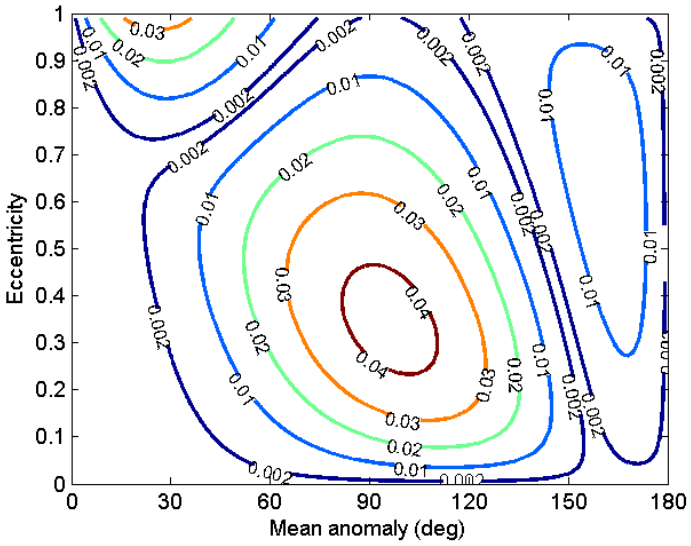

(d) Markley's solution

Fig. 3. (cont.) Error in position propagation as percent of semi-major axis of existing methods.

countered is more than an order of magnitude larger than Markley.

Figures 4-10 show the accuracies for the new sequential starters, with the errors summarized in Table V.

Table V. Error in position propagation as percent of semi-major axis of sequential methods

Error	M_1	M_2	M_3	M_4	M_5	M_6	M_7
Mean (%) ($\Delta M = 1°$)	0.58	0.01	0.01	0.03	0.56	0.03	0.03
Maximum (%) ($\Delta M = 1°$)	3.21	0.26	0.38	1.48	3.09	1.39	5.68
Mean (%) ($\Delta M = 5°$)	2.48	0.11	0.10	0.35	2.05	0.35	0.45
Maximum (%) ($\Delta M = 5°$)	7.87	0.62	1.26	4.02	6.84	3.20	13.96

The behaviors of M_1 and M_5 are nearly identical, with a slight edge to M_5. Similarly, M_4 and M_6 are nearly identical, with a slight edge to M_6. Since M_5 and M_6 do not require evaluation of trig functions, they appear to be better candidates than M_1 or M_4 respectively. Further, solution M_4 is more computationally complex than M_3 and also significantly less accurate, so its utility is questionable. Solutions M_2 and M_3 perform comparably, but since M_3 has the lower computational complexity, it is preferred over M_2.

Solution M_7 appears from Table V to be less accurate than any of the second order methods, but Fig. 10 shows that this is largely due to its poor performance for large eccentricities (as expected). Since most satellites operate with low to moderate values of eccentricity, the performance of these methods in that range is of particular interest. Table VI shows the performance of Markley's starter, method M_3, and method M_7 in the restricted eccentricity range $e \in [0, 0.55]$ with both 1° and 5° step-sizes. In this range of eccentricity, M_3 outperforms Markley for small values of ΔM and is competitive for larger values of ΔM. Method M_7 outperforms both Markley

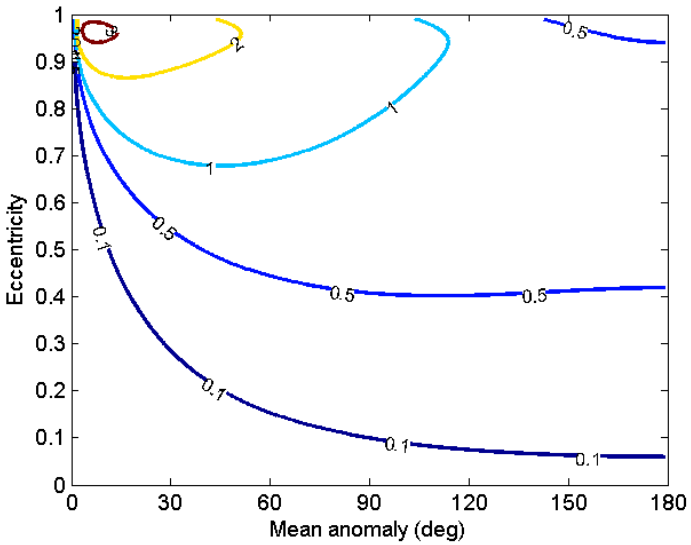

(a) $\Delta M = 1^\circ$

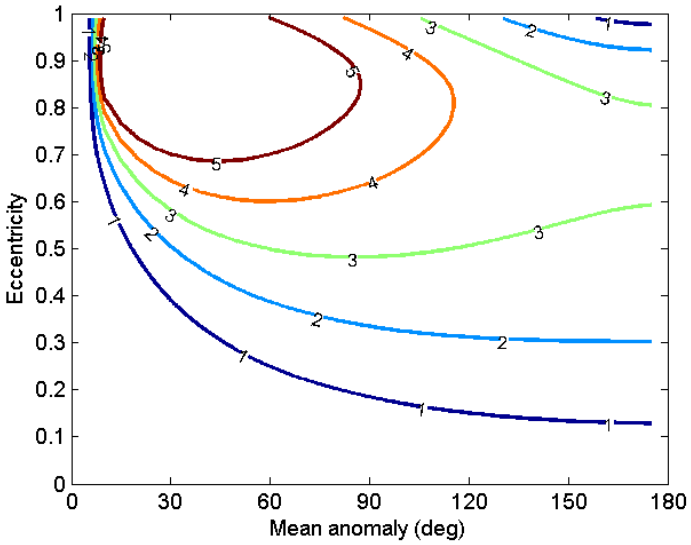

(b) $\Delta M = 5^\circ$

Fig. 4. Error in position propagation as percent of semi-major axis of method M_1.

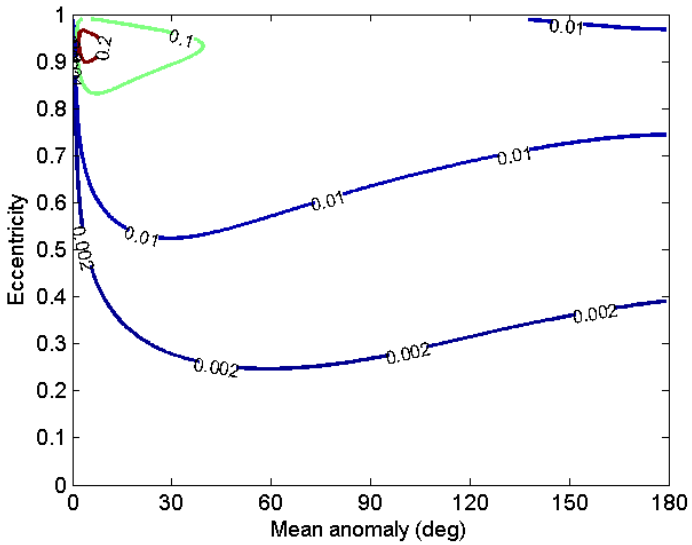

(a) $\Delta M = 1^\circ$

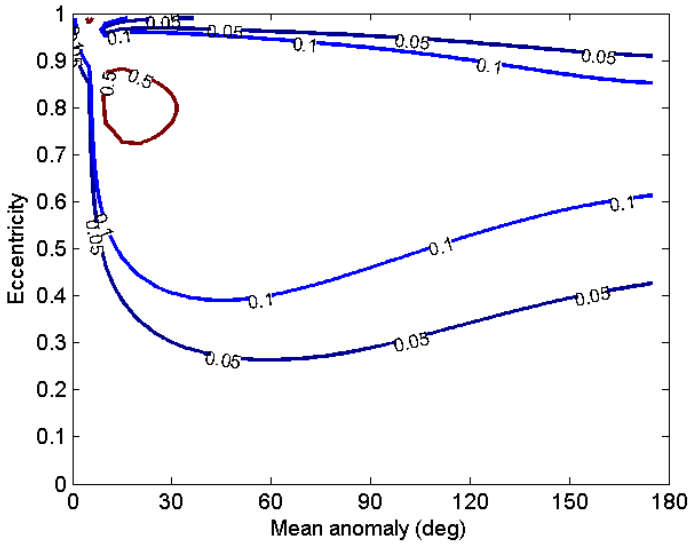

(b) $\Delta M = 5^\circ$

Fig. 5. Error in position propagation as percent of semi-major axis of method M_2.

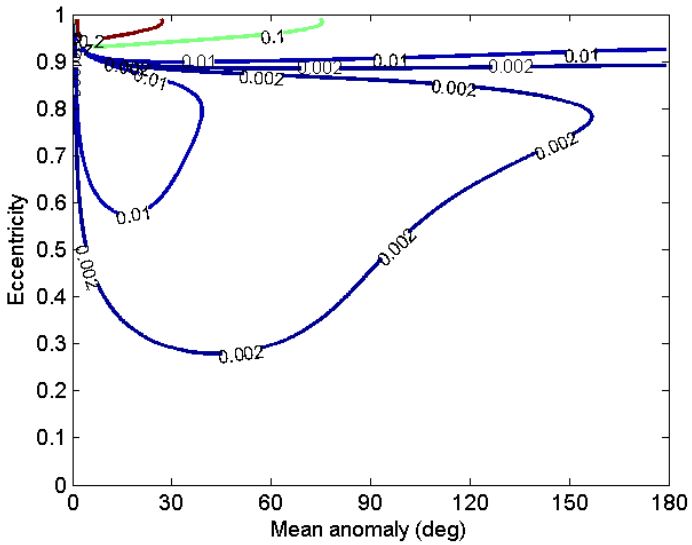

(a) $\Delta M = 1^\circ$

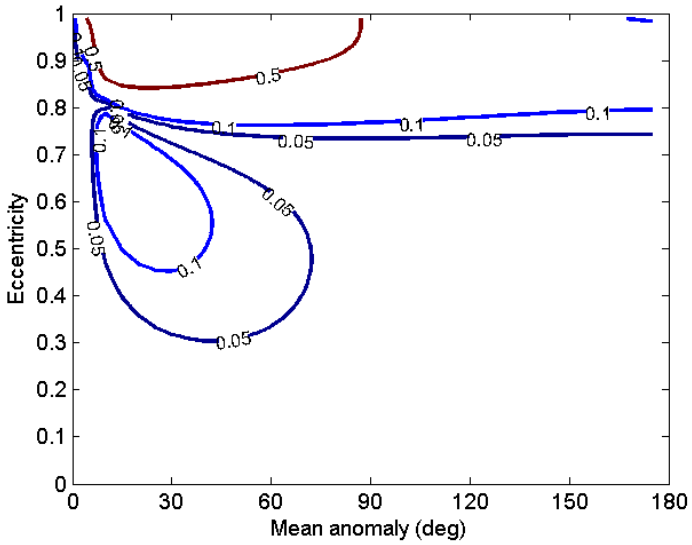

(b) $\Delta M = 5^\circ$

Fig. 6. Error in position propagation as percent of semi-major axis of method M_3.

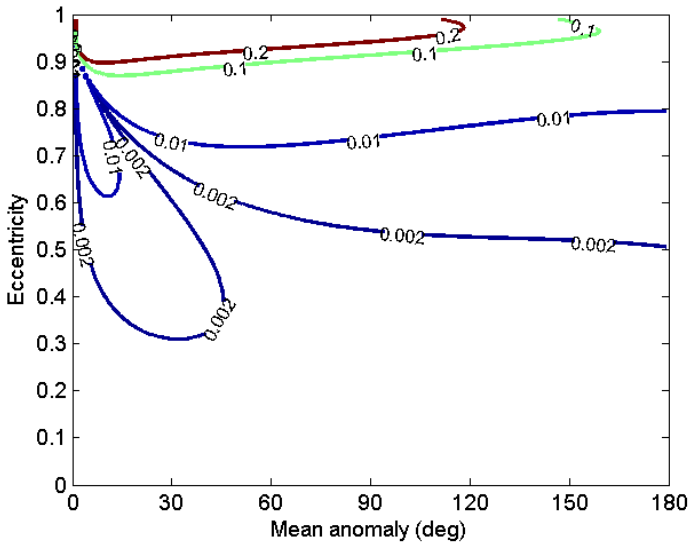

(a) $\Delta M = 1°$

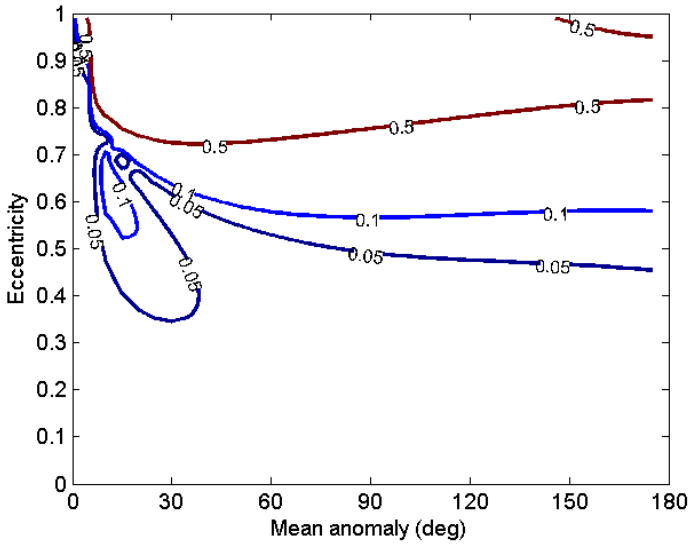

(b) $\Delta M = 5°$

Fig. 7. Error in position propagation as percent of semi-major axis of method M_4.

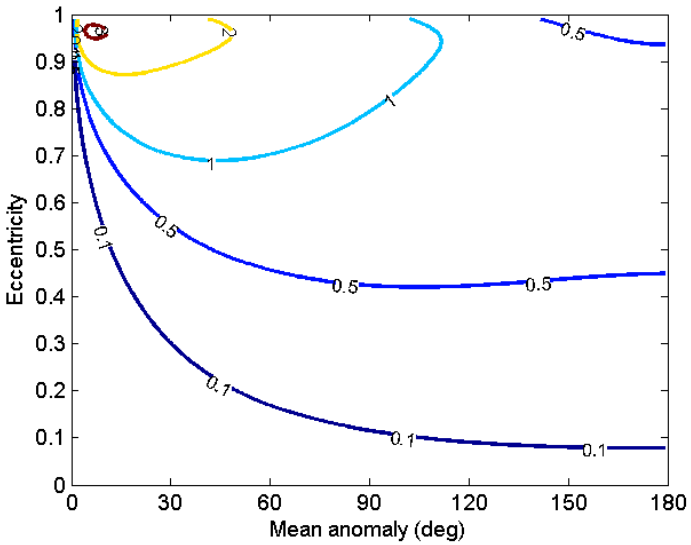

(a) $\Delta M = 1°$

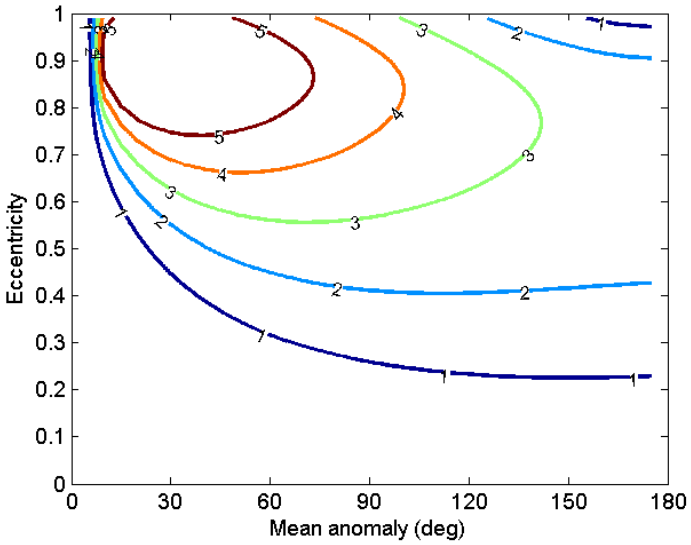

(b) $\Delta M = 5°$

Fig. 8. Error in position propagation as percent of semi-major axis of method M_5.

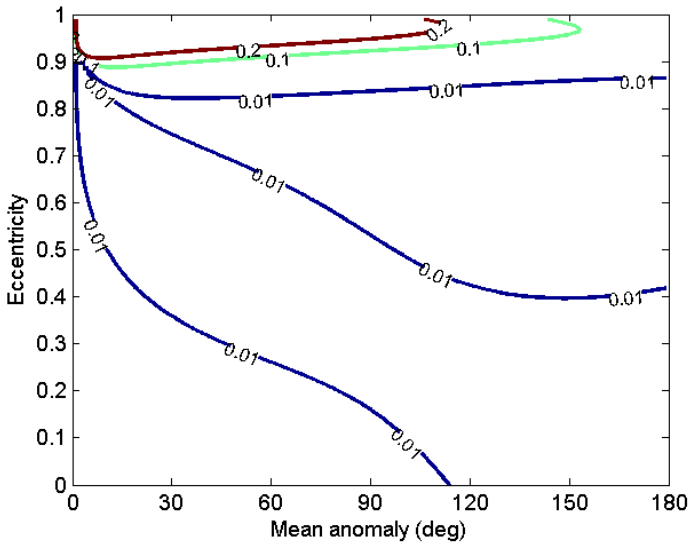

(a) $\Delta M = 1°$

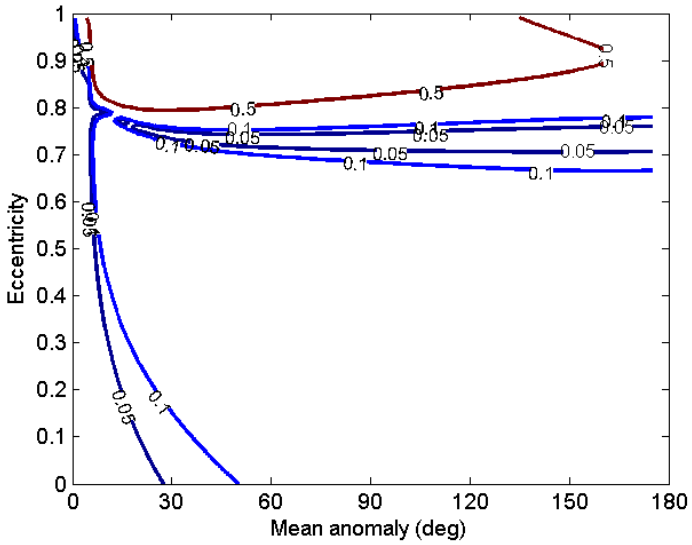

(b) $\Delta M = 5°$

Fig. 9. Error in position propagation as percent of semi-major axis of method M_6.

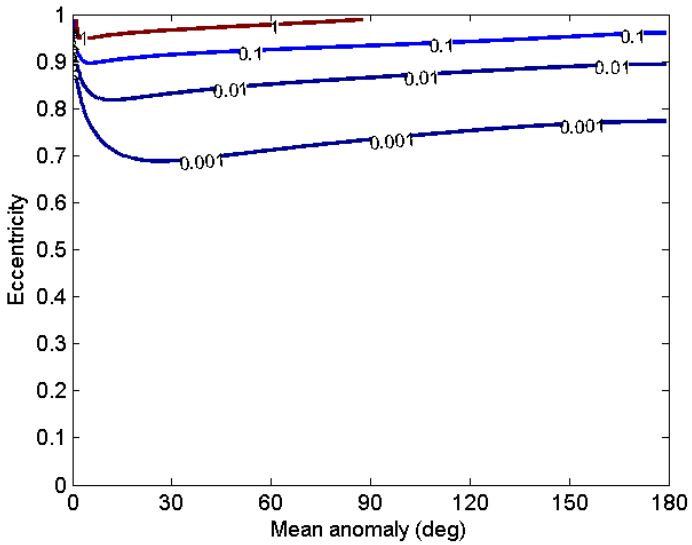

(a) $\Delta M = 1^\circ$

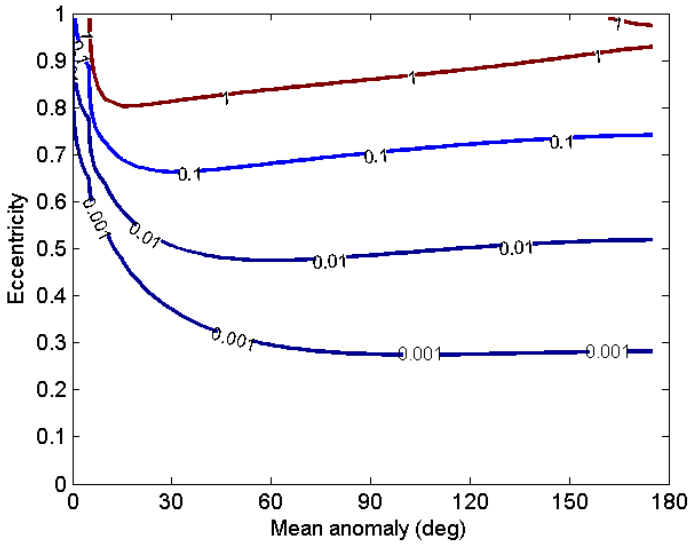

(b) $\Delta M = 5^\circ$

Fig. 10. Error in position propagation as percent of semi-major axis of method M_7.

and M_3 for both values of ΔM, and with $\Delta M = 1°$, M_7 outperforms Markley by several orders of magnitude!

Table VI. Error in position propagation as percent of semi-major axis for small to moderate eccentricities

Error	Markley	$M_3\,(1°)$	$M_3\,(5°)$	$M_7\,(1°)$	$M_7\,(5°)$
Mean (%)	1.46×10^{-2}	1.26×10^{-3}	2.32×10^{-2}	1.96×10^{-5}	2.56×10^{-3}
Max (%)	4.32×10^{-2}	8.65×10^{-3}	1.53×10^{-1}	1.71×10^{-4}	2.32×10^{-2}

Discussion

All solutions in Refs. [37, 43, 44] were evaluated using similar complexity and accuracy analysis to eliminate all but Broucke's solution and S_9. We have only considered the accuracy and complexity of starter equations. Any iterative method may be applied to these starters to achieve required accuracy, including discretized solutions which offer improved efficiencies as seen in Refs. [41, 42]. The required accuracies are application dependent, but in many cases, the accuracy achieved with the sequential starters proposed here may be sufficient without subsequent iteration - allowing for extremely fast orbit propagation.

In cases where high propagation accuracy is needed, not only will iterative methods be required, but osculating orbit elements may be involved. In these cases, the orbit elements change so slightly over a single orbit that these simple starters using mean orbit elements will still provide an excellent starting point for the iterative methods used to provide high fidelity. Note that the application of a single iteration at each step of these sequential methods not only improves the estimate at that point, but it also improves the estimate at every subsequent step as shown in Ref. [48]. As such, an iterative method applied to these sequential starters will improve overall

solution accuracy more than the same iterative method applied to a non-sequential starter.

Both M_1 and M_5 considerably outperform Broucke's solution at comparable complexity, even for large step-sizes in ΔM. Solution S_9 is outperformed in both accuracy and complexity by methods M_1-M_6. These sequential starter values outperform all other published simple starters.

Comparison to Nijenhuis' method reveals that methods M_2-M_4 and M_6 have comparable accuracy at lower complexity for small step-sizes ($\Delta M = 1^\circ$). At larger step-sizes, Nijenhuis' method is slightly more accurate but at the cost of significant computational overhead. Just as Nijenhuis refines the simple S_7 starter, the sequential starters presented here could be refined to yield solutions more accurate than those of Nijenhuis but with the same computational complexity.

A similar observation can be made about Markley's solution. None of the sequential starters challenge Markley for accuracy over the entire range of eccentricity, but the computational burden of Markley is so great that the sequential starters could be improved using a single iteration of any of a number of methods to provide solutions with better accuracy than Markley but similar computational complexity. For small to moderate values of eccentricity ($e < 0.55$), solutions M_3 and M_7 outperform Markley by orders of magnitude.

E. Conclusions

Constellation design is too complex of a problem to solve by brute force, hence the use of design frameworks that utilize only a handful of design parameters to specify an entire constellation of satellites. The Walker constellations, the most popular today, are the simplest of these representations, using only three parameters and circular

orbits. The Flower Constellations and Lattice Flower Constellations of Mortari and Avendaño expand on Walker constellations by including eccentric orbits - enabling new capabilities and improved efficiencies in constellation design.

We present here a new framework for constellation design, the *Elliptical Flower Constellations*. Elliptical Flower Constellations are defined by six integer parameters, allowing for increased design flexibility. Like the Lattice Flower Constellations, EFCs have a rigorous mathematical basis that enables easy computation of various properties of the constellation.

The Elliptical Flower Constellations are a clear extension of the framework of Lattice Flower Constellations, and it is tempting to consider even higher order models, incorporating any of the other orbital parameters into a 4×4 matrix. The reason this has not been done here is that the other parameters, semi-major axis, eccentricity, and inclination, all affect the perturbations experienced by the individual satellites. The J_2 effect would tend to destroy a constellation that allowed satellites to vary in any of those three parameters. Similarly, atmospheric drag could incur substantially different station-keeping costs on satellites with different perigee altitudes. These effects can be overcome through active station-keeping but typically at unreasonable fuel costs. In practice, these three parameters must be held constant over the entire constellation to maintain a uniformly distributed, symmetric constellation.

The Elliptical Flower Constellations include as subsets: Lattice Flower Constellations, Walker constellations, elliptical Walker constellations, and Draim's uniform, elliptical, global coverage constellations. Importantly, this new framework enables the use of non-critically inclined elliptic orbits for global coverage.

To efficiently analyze EFCs (or any other constellation), a new method of orbit propagation is presented to reduce time spent on orbit propagation when analyzing the coverage metrics of a constellation. This new approach utilizes a sequential

estimate for the values of eccentric anomaly when solving for Kepler's equation. Compared to the four best solutions to KE found in the literature, the new methods are generally of lower computational complexity and higher accuracy.

CHAPTER III

CONSTELLATION TRANSFERS

In considering constellation reconfiguration, we seek to solve not an orbit transfer problem, but the *constellation transfer* problem. The optimal assignment of each satellite in the initial constellation to a slot in the final constellation must be solved, along with the optimal orbit transfer for each of those assignments. The optimal assignment depends directly on some cost associated with each possible orbit transfer, whether that be time, fuel, a combination of the two, or some other metric (such as coverage during transfer). To solve the assignment problem rigorously, we must calculate the cost associated with every possible orbit transfer - some n^2 orbit transfers when the constellation consists of n satellites. Unlike the standard orbit transfer problem, the combinatorial nature of constellation transfer *demands* an efficient solution to each orbit transfer problem.

One reasonable cost function for defining the optimal constellation transfer is the minimization of the total fuel used by all satellites in the constellation. This cost function can reduce the generalized assignment problem to the simple linear assignment problem (LAP). This formulation and an efficient solution to it is provided in Section A. To solve the optimal orbit transfer problem, a new method is developed in Section B to solve for the optimal two-impulse maneuver with fixed initial and final states. This new method provides an approximately optimal solution by solving a quartic equation, which can be solved in closed form. To solve the general two-impulse orbit transfer problem where initial and final positions can be freely chosen, the recently developed Learning Approach (LA) to sampling optimization [17, 18, 19] is used along with the previous solution method to quickly and accurately determine the global minimum. Section C describes some slight modifications to the LA algorithm

and its application to the specific problem of two-impulse orbit transfer. Finally, Section D provides some concluding remarks about the constellation transfer problem.

A. Assignment Problems

The question of which satellite in the initial constellation maps to which slot in the final constellation can easily be formulated as an assignment problem. Generalized assignment problems come in many shapes and sizes, from simple linear assignment problems to the NP-hard traveling salesman problem. Luckily, the minimum total fuel constellation transfer can be solved using the relatively simple linear assignment problem formulation (alternative formulations and exceptions are provided at the end of this section).

1. Linear Assignment Problem

The linear assignment problem can be stated as: given n persons (agents, satellites) and n objects (tasks, slots), match them on a one-to-one basis to maximize the cost function

$$J = \sum_{i=1}^{n} \sum_{j=1}^{n} C_{ij} X_{ij} \tag{3.1}$$

$$X_{ij} = 0 \quad \forall \quad j \neq j_i, \quad X_{ij_i} = 1$$

where C_{ij} represents the benefit of agent i being assigned to task j. Solving for the permutation matrix X_{ij} is the task of any algorithm seeking to solve the LAP. Of course, in constellation transfers, we seek to minimize the fuel cost, rather than maximize some benefit, which simply requires negating the cost function J.

The linear assignment problem can handle a mismatch in the number of agents and the number of tasks by adding columns or rows of zeros to the matrix C_{ij}. In the case of constellation reconfiguration, a final constellation with more slots than

satellites currently on orbit would effectively have more tasks than agents and would require additional columns of zeros in C_{ij} to compensate.

2. Auction Algorithm

The auction algorithm is the most efficient method for solving the linear assignment problem and features guaranteed convergence. The naive auction algorithm was first proposed by Bertsekas in 1979 and is briefly summarized here. A good tutorial of the auction algorithm can be found in Ref. [11].

First, assign an arbitrary price P_j to each task (typically zero). Next, define the value of completing task j to agent i, V_{ij}, as the difference between the benefit and the price:

$$V_{ij} = C_{ij} - P_j \tag{3.2}$$

We will consider an agent to be "happy" if its assigned task j_i satisfies

$$V_{ij_i} = \max_j V_{ij} \tag{3.3}$$

The naive auction algorithm chooses an "unhappy" agent and assigns it to the task that satisfies Eq. (3.3). The price of that task is then increased according to

$$P_{j_i} = P_{j_i} + \left(V_{ij_i} - \max_{j \neq j_i} V_{ij} \right) \tag{3.4}$$

The "bid" of the agent is effectively the difference in value between its best task and its second best task.

In order to assign the optimal task to the "unhappy" agent, another agent had to be reassigned to a new task - potentially making it unhappy. The auction algorithm iterates through until no unhappy agents remain and the prices for all tasks have converged.

The problem with the naive auction algorithm is that if two tasks have the same benefit for a given agent, it will bid zero for that task. Thus, the price will not change, and an unending bidding war between two agents bidding zero for the same task could result. To avoid this problem, the bid is augmented by some value ϵ and agents are defined as "almost happy" when

$$V_{ij_i} \geq \max_j V_{ij} - \epsilon \tag{3.5}$$

The auction algorithm iterates until all agents are almost happy. Smaller values of ϵ lead to results closer to optimal, whereas larger values lead to faster convergence. It is readily shown that the auction algorithm results in a final cost $J^\star$ within $n\epsilon$ of optimal. See Ref. [11] for a discussion on dynamic values of ϵ as the algorithm moves toward convergence and for a proof of optimality.

3. Alternative Formulations

Casting the constellation transfer problem as one that seeks to minimize the total fuel use with no restrictions on which satellite ends up where leads to the simple LAP with the auction algorithm as the obvious approach to obtain a solution. However, other cost functions may be equally valid and some restrictions may apply.

If one seeks to minimize the maximum fuel expended by any single satellite (or minimize the maximum transfer time), the formulation yields the linear bottleneck assignment problem (LBAP). Quadratic cost functions could also be considered, yielding quadratic assignment problems (QAPs). The LBAPs can be solved efficiently, whereas the QAP has no efficient solution to date. For information on these and other assignment problems, see Refs. [49, 50, 51, 52, 53].

Restrictions on the placements of the satellites may also complicate the picture. For instance, if the reconfiguration is a phased deployment, and there are multiple

satellites on each launch vehicle, the cost of one satellite on the launch vehicle to achieve a specific orbit is dependent on the assignment of all other spacecraft on the launch vehicle. The LAP can be solved repeatedly, converging toward a solution consistent with such constraints, as done in Ref. [1], but this is an inelegant solution. Advances in solving more complicated assignment problems will lead to more options for the constellation reconfiguration engineer.

B. Minimum Δv^2 Lambert's Problem

Given the position of a satellite at two different, specified times provides all of the information required to solve for the Keplerian orbit between those two positions in the specified amount of time, a problem known as Lambert's problem. This two-point boundary value problem is used throughout celestial mechanics for a variety of purposes, and there is vast existing literature on efficiently solving Lambert's problem [37, 38, 54]. One typical use is interplanetary trajectory design, where Lambert's problem is solved for varying departure and arrival dates between two planets (the dates define the initial and final positions from the planetary ephemeris) to optimize for fuel cost. Alternatively, one can use the solution of Lambert's problem to solve the angles-only orbit determination problem [54].

If the initial and final positions of the satellite lie on two different orbits, then the solution of Lambert's problem can be considered the transfer orbit between the two at the prescribed takeoff and arrival times, and the fuel cost calculated. But Lambert's problem in the classic formulation has a unique solution - it does not permit any additional optimization unless Lambert's problem is solved repeatedly for different boundary conditions. Instead, many researchers have cast the problem of the two-impulse orbit transfer as the "minimum Δv_{tot} Lambert's problem", where

time of flight is unconstrained and the solution is the transfer orbit that minimizes the sum of the Δv's applied [55, 56, 57, 58, 59]. All existing methods for solving this problem involve either some iterative technique, or provide a high-order polynomial that requires numerical techniques to solve for the roots.

In contrast to the iterative methods and numerical techniques, we seek a method with constant computation time and guaranteed convergence for the combinatory constellation transfer problem. We propose to solve a variation on the minimum Δv_{tot} Lambert's problem, which we call the Δv_{tot}^2 Lambert's problem, utilizing the cost function

$$\Delta v_{\text{tot}}^2 = |\Delta \boldsymbol{v}_1|^2 + |\Delta \boldsymbol{v}_2|^2, \tag{3.6}$$

where $\Delta \boldsymbol{v}_1$ and $\Delta \boldsymbol{v}_2$ represent the initial and final orbit transfer impulses, respectively. Using this function, remarkably, a closed form solution can be found, while the errors between this cost function and the Δv_{tot} cost function are bounded.

This section presents a unique approach that ultimately produces a quartic equation whose roots are the solution to the cost function of Eq. (3.6). Handling multiple solutions and the difference between the Δv_{tot} and Δv_{tot}^2 solutions are then discussed. The unique case of $\boldsymbol{r}_1$ and $\boldsymbol{r}_2$ being collinear creates a singularity, and an analytic solution for this case is derived. A numerical example demonstrates the accuracy of this approach.

1. Problem Definition

Given a satellite on some initial orbit defined by position $\boldsymbol{r}_1$ and velocity $\boldsymbol{v}_1$ and some final orbit defined by $\boldsymbol{r}_2$ and $\boldsymbol{v}_2$, solve for the transfer orbit between them that minimizes the cost function of Eq. (3.6). We define the velocities of the transfer orbit

to be $\boldsymbol{w}_1$ and $\boldsymbol{w}_2$ such that the cost function can be rewritten

$$\Delta v_{\text{tot}}^2 = |\boldsymbol{w}_1 - \boldsymbol{v}_1|^2 + |\boldsymbol{v}_2 - \boldsymbol{w}_2|^2 \tag{3.7}$$

In other words, the satellite starts at position $\boldsymbol{r}_1$ with velocity $\boldsymbol{v}_1$, and after an impulsive (instantaneous) burn, moves onto the transfer orbit at position $\boldsymbol{r}_1$ but velocity $\boldsymbol{w}_1$. After some unspecified coast time, the satellite arrives at $\boldsymbol{r}_2$ with velocity $\boldsymbol{w}_2$, where it executes a second impulsive burn to achieve the desired velocity $\boldsymbol{v}_2$.

2. Approach

The approach is based on Battin's formulation for the terminal velocity vectors of a transfer orbit [37], which is briefly reviewed here. First, we know the F&G solution for orbit propagation, given position vectors $\boldsymbol{r}_i$ and velocity vectors $\boldsymbol{w}_i$:

$$\boldsymbol{r}_2 = F\boldsymbol{r}_1 + G\boldsymbol{w}_1 \tag{3.8}$$

$$\boldsymbol{w}_2 = F_t\boldsymbol{r}_1 + G_t\boldsymbol{w}_1 \tag{3.9}$$

Using both this formulation and the inverse formulation, the two position vectors can be written as

$$\boldsymbol{r}_1 = G_t\boldsymbol{r}_2 - G\boldsymbol{w}_2 \tag{3.10}$$

$$\boldsymbol{r}_2 = F\boldsymbol{r}_1 + G\boldsymbol{w}_1 \tag{3.11}$$

We define the following unit vectors

$$\hat{\boldsymbol{r}}_i = \frac{\boldsymbol{r}_i}{r_i}, \text{ where } r_i = |\boldsymbol{r}_i| \tag{3.12}$$

$$\hat{\boldsymbol{c}} = \frac{\boldsymbol{r}_2 - \boldsymbol{r}_1}{c}, \text{ where } c = |\boldsymbol{r}_2 - \boldsymbol{r}_1| \tag{3.13}$$

$$\hat{\boldsymbol{h}} = \frac{\hat{\boldsymbol{r}}_1 \times \hat{\boldsymbol{r}}_2}{|\hat{\boldsymbol{r}}_1 \times \hat{\boldsymbol{r}}_2|} \tag{3.14}$$

Battin then defines the following scalar variables

$$w_c = \frac{c\sqrt{\mu p}}{r_1 r_2 \sin\Delta\varphi} \tag{3.15}$$

$$w_\rho = \sqrt{\frac{\mu}{p}}\frac{1-\cos\Delta\varphi}{\sin\Delta\varphi} \tag{3.16}$$

where p is the semilatus rectum of the transfer orbit, and $\Delta\varphi$ is the angle between the two position vectors (true anomaly variation on the transfer orbit). Combining these definitions with those of F, G, F_t, and G_t allows the velocities to be written as

$$\boldsymbol{w}_1 = w_c\hat{\boldsymbol{c}} + w_\rho\hat{\boldsymbol{r}}_1 \tag{3.17}$$

$$\boldsymbol{w}_2 = w_c\hat{\boldsymbol{c}} - w_\rho\hat{\boldsymbol{r}}_2 \tag{3.18}$$

The important result is that the following product is a constant dependent only on the geometry of the position vectors:

$$w_c w_\rho = \frac{\mu c}{2r_1 r_2}\sec^2\frac{\Delta\varphi}{2} \tag{3.19}$$

We define the constant $K = w_c w_\rho$, which can also be calculated as

$$K = \frac{\mu c}{r_1 r_2 + \boldsymbol{r}_1\cdot\boldsymbol{r}_2} \tag{3.20}$$

We then define the initial (before impulse) velocity vectors $\boldsymbol{v}_i$ in the same frame as the transfer velocities ($\boldsymbol{w}_i$)

$$\boldsymbol{v}_i = v_{i\zeta}\hat{\boldsymbol{c}} + v_{i\rho}\hat{\boldsymbol{r}}_i + v_{ih}\hat{\boldsymbol{h}} \tag{3.21}$$

It is important to note that these unit vectors are not orthogonal, so computing the magnitude of these velocity vectors cannot be done by simply summing the squares of the components. Nor can the components simply be computed by dotting the

velocity vector with the unit vectors. We can compute the $\Delta \boldsymbol{v}_i$'s as

$$\Delta \boldsymbol{v}_1 = \boldsymbol{w}_1 - \boldsymbol{v}_1 \tag{3.22}$$

$$\Delta \boldsymbol{v}_2 = \boldsymbol{v}_2 - \boldsymbol{w}_2 \tag{3.23}$$

$$\Delta \boldsymbol{v}_1 = (w_c - v_{1\zeta})\,\hat{\boldsymbol{c}} + \left(\frac{K}{w_c} - v_{1\rho}\right)\hat{\boldsymbol{r}}_1 - v_{1h}\hat{\boldsymbol{h}} \tag{3.24}$$

$$\Delta \boldsymbol{v}_2 = (v_{2\zeta} - w_c)\,\hat{\boldsymbol{c}} + \left(v_{2\rho} + \frac{K}{w_c}\right)\hat{\boldsymbol{r}}_2 + v_{2h}\hat{\boldsymbol{h}} \tag{3.25}$$

We define a cost function $J = |\Delta \boldsymbol{v}_1|^2 + |\Delta \boldsymbol{v}_2|^2$. With some manipulation of the above equations, one finds:

$$J = v_1^2 + v_2^2 + 2K(\cos\theta_1 - \cos\theta_2) + 2w_c^2 + 2\frac{K^2}{w_c^2} - 2\left(v_{1c} + v_{2c}\right)w_c - 2\frac{K}{w_c}\left(v_{1r} - v_{2r}\right) \tag{3.26}$$

where v_1 and v_2 are the magnitudes of the initial velocity vectors, $\cos\theta_i = \hat{\boldsymbol{c}} \cdot \hat{\boldsymbol{r}}_i$, $v_{ic} = \boldsymbol{v}_i \cdot \hat{\boldsymbol{c}}$, and $v_{ir} = \boldsymbol{v}_i \cdot \hat{\boldsymbol{r}}_i$.

Since the first three terms of J are constants, and the remaining terms are all multiplied by 2, we ignore constants and redefine the cost function G which we seek to minimize:

$$G = \frac{1}{w_c^2}\left[w_c^4 - \left(v_{1c} + v_{2c}\right)w_c^3 - K\left(v_{1r} - v_{2r}\right)w_c + K^2\right] \tag{3.27}$$

The first derivative of this cost function is given by

$$\frac{dG}{dw_c} = \frac{1}{w_c^3}\left[2w_c^4 - (v_{1c} + v_{2c})w_c^3 + K(v_{1r} - v_{2r})w_c - 2K^2\right] \tag{3.28}$$

Setting this derivative to zero to find the extremum of G yields a quartic of the form

$$w_c^4 + c_3 w_c^3 + c_1 w_c + c_0 = 0 \tag{3.29}$$

where

$$\begin{aligned} c_3 &= -\frac{v_{1c} + v_{2c}}{2} \\ c_1 &= \frac{K\left(v_{1r} - v_{2r}\right)}{2} \\ c_0 &= -K^2 \end{aligned}$$

This quartic equation can be solved analytically using Ferrari's method (see Ref. [60]). Since c_0 is always less than zero and the initial quartic term is positive, there will always be at least two real solutions to this quartic polynomial. Considering Eq. (3.28), it is clear that as $w_c \to \infty$, $\frac{dG}{dw_c} \to \infty$, whereas as $w_c \to 0$ from the positive side of zero, $\frac{dG}{dw_c} \to -\infty$. As such, there exists at least one real solution of Eq. (3.29) that is positive. Similarly, as $w_c \to -\infty$, $\frac{dG}{dw_c} \to -\infty$, whereas as $w_c \to 0$ from the negative side of zero, $\frac{dG}{dw_c} \to \infty$. Again, this proves the existence at least one real solution of Eq. (3.29) that is negative. Both of these solution points are guaranteed to have a positive slope (ie. $\frac{d^2G}{dw_c^2} > 0$) and so they are both minima. The positive and negative solutions represent local minima in prograde and retrograde directions, respectively. Rarely this equation yields four real solutions, in which case three local minima and one local maxima exist. Comparing these solutions provides the desired global minimum.

3. Multiple Solutions and Error Analysis

The method presented here transforms the optimal transfer into a single parameter minimization. To better demonstrate what is happening when multiple solutions occur and the difference between the minimum Δv_{tot} and minimum Δv_{tot}^2 solutions, consider Fig. 11. This particular case is a special case that has four real solutions to the quartic described above and is diagrammed in Fig. 11a, with orbital elements

Table VII. Orbit parameters for four solution case

Orbital element	Initial orbit	Final orbit
Perigee altitude (km)	386.8	7000.0
Apogee altitude (km)	9235.9	7000.0
R.A.A.N.	0	0
Argument of perigee	$-164.44°$	0
Inclination	$180.00°$	0
True anomaly	$73.85°$	0

listed in Table VII. Though this type of transfer situation is unlikely to occur in practice, it is useful to investigate from a mathematical viewpoint.

Figure 11b has as its axes the magnitude of the two burns, and the dashed (red) and dotted (blue) lines represent feasible transfers between the two specified orbits. For the minimum Δv_{tot} optimization, minima and maxima exist where these two curves are tangent to a line with slope of -1 as shown in the figure. Minimum Δv_{tot}^2 optimization, alternatively, has solutions anywhere those two curves are tangent to a circular arc. Triangles and circles show minima and maxima of Δv_{tot} and Δv_{tot}^2 respectively.

Consider solution 4 indicated in Fig. 11 where a significant difference exists between the Δv_{tot} and Δv_{tot}^2 solutions. Despite the vastly different transfers, the error in total Δv_{tot} cost is small - represented by the perpendicular distance of the Δv_{tot}^2 solution from the linear cost contour passing through the Δv_{tot} solution.

Minimization of Δv_{tot} means fuel minimization while Δv_{tot}^2 minimization does not, but the error is bounded, as shown here. Assume that the minimum Δv_{tot} and Δv_{tot}^2 require two different two-impulse maneuvers, p and q, respectively. It is clear that $\Delta v_{\text{tot}}(p) \leq \Delta v_{\text{tot}}(q)$ and that $\Delta v_{\text{tot}}^2(q) \leq \Delta v_{\text{tot}}^2(p)$. Using the elementary

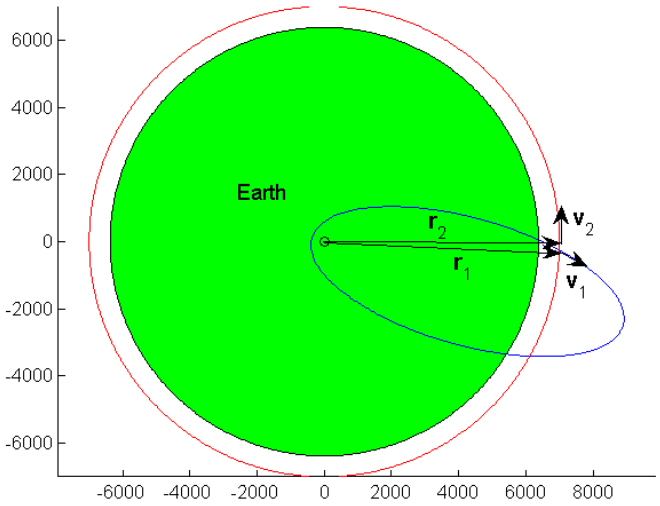

(a) Diagram of initial and final orbits.

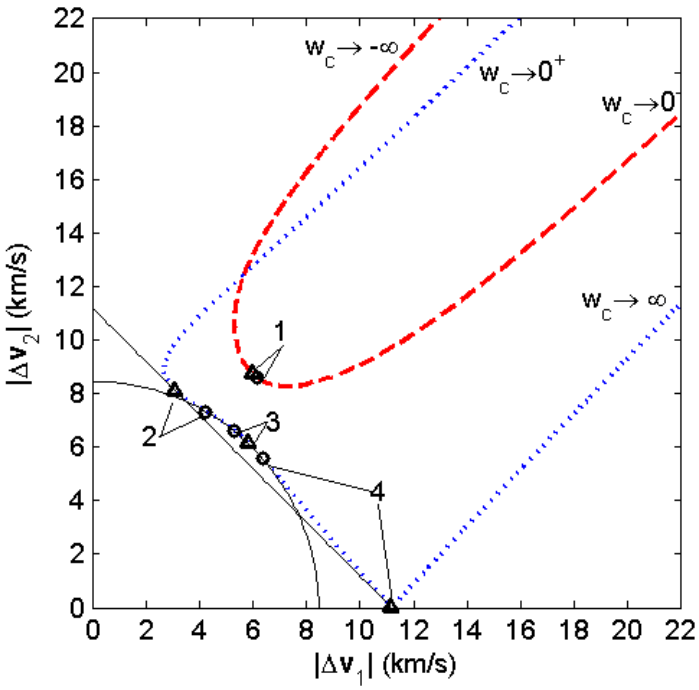

(b) Dashed (red) and dotted (blue) lines represent feasible transfers, parameterized by w_c. Triangles and circles show minima and maxima of Δv_{tot} and Δv_{tot}^2 respectively.

Fig. 11. Special transfer case with four real roots.

Table VIII. Orbit parameters range

Orbital element	from	to
Perigee altitude, h_p (km)	350	36,000
Apogee altitude (km)	h_p	36,000
R.A.A.N.	0	360°
Argument of perigee	0	360°
Inclination	0	180°
True anomaly	0	360°

inequalities, $|a| + |b| \leq \sqrt{2(a^2 + b^2)}$ and $\sqrt{a^2 + b^2} \leq |a| + |b|$, we can derive the following estimation

$$\Delta v_{\text{tot}}(q) \leq \sqrt{2\Delta v_{\text{tot}}^2(q)} \leq \sqrt{2\Delta v_{\text{tot}}^2(p)} \leq \sqrt{2}\Delta v_{\text{tot}}(p). \tag{3.30}$$

which implies a maximum cost overestimate of 41.4% using the Δv_{tot}^2 optimality. In practice, Eq. (3.30) overestimates this difference. To provide a better answer, the results of a Monte Carlo approach is provided in Fig. 12. These results are obtained with one million random tests, using random orbit and orbital positions with the ranges provided in Table VIII. We calculate error as the percent difference in the costs $\Delta v_{\text{tot}}(p)$ and $\Delta v_{\text{tot}}(q)$. They show that 74.3% of the cases resulted in errors of less than 1%, and 95.4% of the cases had less than 5% error. The maximum error achieved in these million cases was 15.8%. Despite efforts to maximize this error and identify cases where maximal error may occur, we have been unable to find a case that exceeds 20% error. Thus, the inequality of Eq. (3.30) is highly conservative (pessimistic) as regards the degree of sub-optimality incurred by minimization of Δv_{tot}^2 instead of Δv_{tot}.

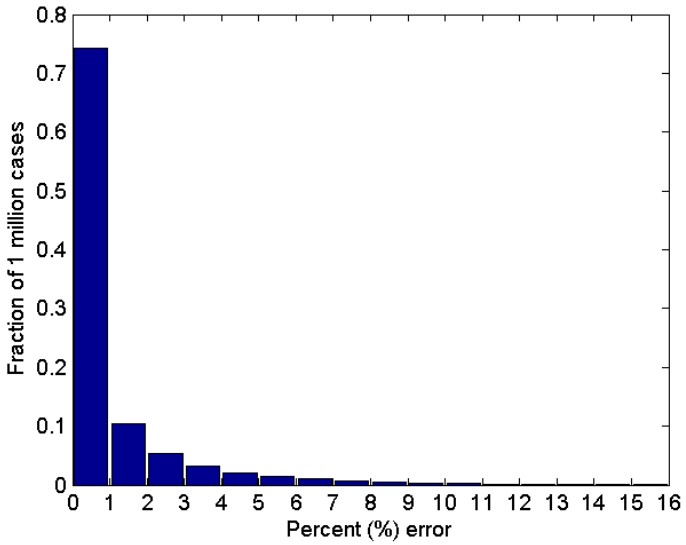

Fig. 12. Histogram of percent error in $|\Delta \boldsymbol{v}_1| + |\Delta \boldsymbol{v}_2|$ using the $J = |\Delta \boldsymbol{v}_1|^2 + |\Delta \boldsymbol{v}_2|^2$ cost function over one million random transfers.

4. Singularity

This method becomes singular when the departure and arrival radii become collinear. When this happens, the value of K, as defined by Eq. (3.19), goes to infinity. When the radii point in opposite directions, as in the Hohmann transfer case, an additional design parameter - the angle of the orbit transfer plane - is introduced. When the radii point in the same direction, the motion becomes rectilinear and a new quartic equation must be solved. Both of these cases are treated in this section.

Collinear Radii in Opposite Directions

Consider the following equation for the magnitude of the orbit radius:

$$r_i = \frac{p}{1 + e\cos\varphi_i} \tag{3.31}$$

where p is the semilatus rectum, e is the eccentricity, and φ is the true anomaly. For a transfer between two collinear radii pointing in opposite directions, the final true anomaly on the transfer orbit can be simply written as $\varphi_2 = \varphi_1 + \pi$, and the orbit radii can be written in terms of the transfer orbit elements as

$$r_1 = \frac{p}{1 + e\cos\varphi_1} \tag{3.32}$$

$$r_2 = \frac{p}{1 - e\cos\varphi_1} \tag{3.33}$$

which allows us to solve for p of the transfer orbit as the harmonic mean

$$p = \frac{2r_1 r_2}{r_1 + r_2} \tag{3.34}$$

Given that $h = \sqrt{\mu p}$, the angular momentum of the transfer orbit can be solved for explicitly using only the orbit radii.

We can decompose the transfer velocities into two components, one parallel to the orbit radii, w_{ir}, and one perpendicular to the orbit radii, $w_{i\perp}$. The radial velocity component of an orbit is given by [37]:

$$w_{1r} = \frac{\mu e \sin\varphi_1}{h} \tag{3.35}$$

$$w_{2r} = \frac{\mu e \sin\varphi_2}{h} = \frac{\mu e \sin(\varphi_1 + \pi)}{h} = \frac{-\mu e \sin\varphi_1}{h} \tag{3.36}$$

such that we can define $w_r = w_{1r} = -w_{2r}$. To solve for $w_{i\perp}$, we simply use the definition of angular momentum:

$$h = |\boldsymbol{r}_i \times \boldsymbol{w_i}| = r_i w_{i\perp} \tag{3.37}$$

The direction of $w_{i\perp}$ has an additional degree of freedom that serves to define the plane of the orbit transfer. We define the angle between the transfer orbit plane and the initial orbit plane as θ.

We introduce a reference frame, $\mathcal{O}_1$, based on the initial orbit, defined by the vectors $\{\hat{\boldsymbol{r}}_1, \hat{\boldsymbol{s}}_1, \hat{\boldsymbol{h}}_1\}$ where $\hat{\boldsymbol{h}}_1 = \frac{\hat{\boldsymbol{r}}_1 \times \hat{\boldsymbol{v}}_1}{|\hat{\boldsymbol{r}}_1 \times \hat{\boldsymbol{v}}_1|}$ and $\hat{\boldsymbol{s}}_1 = \hat{\boldsymbol{h}}_1 \times \hat{\boldsymbol{r}}_1$. The initial, transfer, and final velocity vectors can all be coordinatized in this $\mathcal{O}_1$ frame as follows:

$$\boldsymbol{v}_1 = \begin{bmatrix} v_{1r} \\ v_{1s} \\ 0 \end{bmatrix} = \begin{bmatrix} \boldsymbol{v}_1 \cdot \hat{\boldsymbol{r}}_1 \\ \boldsymbol{v}_1 \cdot \hat{\boldsymbol{s}}_1 \\ 0 \end{bmatrix} \tag{3.38}$$

$$\boldsymbol{v}_2 = \begin{bmatrix} v_{2r} \\ v_{2s} \\ v_{2h} \end{bmatrix} = \begin{bmatrix} \boldsymbol{v}_2 \cdot \hat{\boldsymbol{r}}_1 \\ \boldsymbol{v}_2 \cdot \hat{\boldsymbol{s}}_1 \\ \boldsymbol{v}_2 \cdot \hat{\boldsymbol{h}}_1 \end{bmatrix} \tag{3.39}$$

$$\boldsymbol{w}_1 = \begin{bmatrix} w_r \\ w_{1\perp} \cos\theta \\ -w_{1\perp} \sin\theta \end{bmatrix} \tag{3.40}$$

$$\boldsymbol{w}_2 = \begin{bmatrix} w_r \\ -w_{2\perp} \cos\theta \\ w_{2\perp} \sin\theta \end{bmatrix} \tag{3.41}$$

Expanding the cost function $J = |\Delta\boldsymbol{v}_1|^2 + |\Delta\boldsymbol{v}_2|^2$ yields

$$J = v_1^2 + v_2^2 + w_{1\perp}^2 + w_{2\perp}^2 + 2w_r^2 - 2\left[(v_{1r} + v_{2r})w_r + (v_{1s}w_{1\perp} - v_{2s}w_{2\perp})\cos\theta + v_{2h}w_{2\perp}\sin\theta\right] \tag{3.42}$$

Again, after removing the first four terms which are constant, and removing the common factor of two, a slightly modified cost function can be defined that we seek to minimize:

$$G = w_r^2 - (v_{1r} + v_{2r})w_r - (v_{1s}w_{1\perp} - v_{2s}w_{2\perp})\cos\theta - v_{2h}w_{2\perp}\sin\theta \tag{3.43}$$

Taking the first derivative of G with respect to the two optimization variables w_r and

θ and substituting in the values of $w_{i\perp}$ from Eq. (3.37) yields the following optimality conditions:

$$w_r = \frac{v_{1r} + v_{2r}}{2} \tag{3.44}$$

$$\tan\theta = \frac{r_1 v_{2h}}{r_2 v_{1s} - r_1 v_{2s}} \tag{3.45}$$

The angle θ has two possible solutions in different quadrants, and these must both be checked to find the minimum.

Collinear Radii in the Same Direction

Alternatively, a singularity can occur when the angle between the two radius vectors is zero - they are collinear and pointed in the same direction. In this case, the transfer orbit devolves into a rectilinear orbit. To solve the rectilinear orbit case we first note the form of the transfer velocities:

$$\boldsymbol{w}_i = w_i \hat{\boldsymbol{r}} \tag{3.46}$$

The only unknowns of the transfer are the two magnitudes, w_i. Second, we look at the energy, α, of the orbit through the vis-viva equation:

$$\alpha_i = \frac{2}{r_i} - \frac{w_i^2}{\mu} \tag{3.47}$$

Note that this is a generic form, allowing for elliptic, parabolic, and hyperbolic orbits. By setting $\alpha_1 = \alpha_2$, we can reduce the problem to a single unknown w_i. Note that the sign of w_i is known for the inner location (closest to the Earth) since passing through the Earth must be restricted, but the sign of the outer location velocity is unknown. For this reason we introduce the subscript I to refer to the inner location and O for the outer location in place of the 1 and 2 subscripts. For instance, if $r_1 < r_2$, then we equate $r_I = r_1$ and $r_O = r_2$.

We break the initial and final velocities into components along the radial direction and normal to the radial direction:

$$\boldsymbol{v}_i = v_{ir}\hat{\boldsymbol{r}} + v_{it}\hat{\boldsymbol{t}}_i \tag{3.48}$$

such that

$$\Delta\boldsymbol{v}_1 = (w_1 - v_{1r})\,\hat{\boldsymbol{r}} - v_{1t}\hat{\boldsymbol{t}}_1 \tag{3.49}$$

$$\Delta\boldsymbol{v}_2 = (v_{2r} - w_2)\,\hat{\boldsymbol{r}} + v_{2t}\hat{\boldsymbol{t}}_2 \tag{3.50}$$

This yields the cost equation:

$$J = v_1^2 + v_2^2 + w_1^2 + w_2^2 - 2\,(w_1 v_{1r} + w_2 v_{2r}) \tag{3.51}$$

Using Eq. (3.47) to solve for one of the unknown transfer velocities and making some simplifications, we can define the equivalent cost function:

$$G = w_O^2 - w_O v_{Or} \pm v_{Ir}\sqrt{w_O^2 + 4K} \tag{3.52}$$

where we define K equivalent to before in Eq. (3.20) and the $\pm$ sign depends on whether the initial position is the outer or inner point respectively. Taking the derivative of G, we find the optimality condition:

$$\frac{\partial G}{\partial w_O} = 2w_O - v_{Or} \pm \frac{v_{Ir} w_O}{\sqrt{w_O^2 + 4K}} = 0 \tag{3.53}$$

This equation can then be transformed into the following quartic equation:

$$w_O^4 + c_3 w_O^3 + c_2 w_O^2 + c_1 w_O + c_0 = 0 \tag{3.54}$$

where

$$\begin{aligned} c_3 &= -v_{Or} \\ c_2 &= 4K + \frac{v_{Or}^2 - v_{Ir}^2}{4} \\ c_1 &= -4Kv_{Or} \\ c_0 &= Kv_{Or}^2 \end{aligned}$$

Note that not all solutions of this equation are solutions of Eq. (3.53), but all solutions of Eq. (3.53) are also solutions of this equation. We also note that Eq. (3.53) is guaranteed to have at least one real solution, because it is continuous and goes from negative infinity to positive infinity as w_O varies over that range. Thus, the quartic is also guaranteed to have at least one real solution, which means Eq. (3.54) must have two or four real roots. Checking all of the real solutions to minimize the cost function solves this singular case.

5. Pork-chop Example

Using the general theory (and the theory developed for the singular case presented in the previous section) it is possible to produce "pork-chops" and to identify the best departure and arrival orbital positions for the two-impulse orbit transfer problem between two generic elliptic orbits. For two orbits randomly selected, as specified by Table IX, Fig. 13 show the contour plots for the minimum Δv_{tot} transfer cost (left plot) and the associated minimum Δv_{tot}^2 transfer cost (right plot). The two plots are nearly identical, indicating that the Δv_{tot}^2 minimization is sufficient for finding optimal transfer locations. Figure 14 shows the percent difference between the two plots.

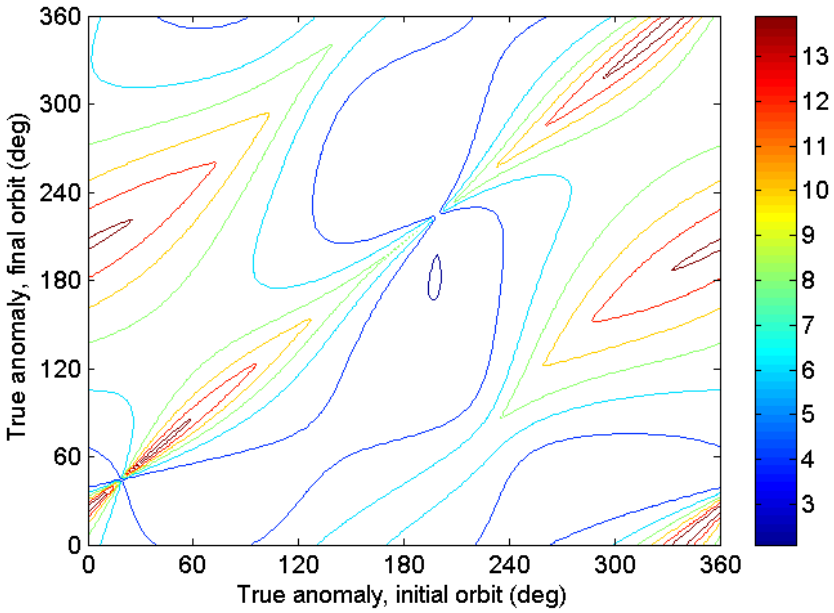

(a) Δv_{tot} optimal

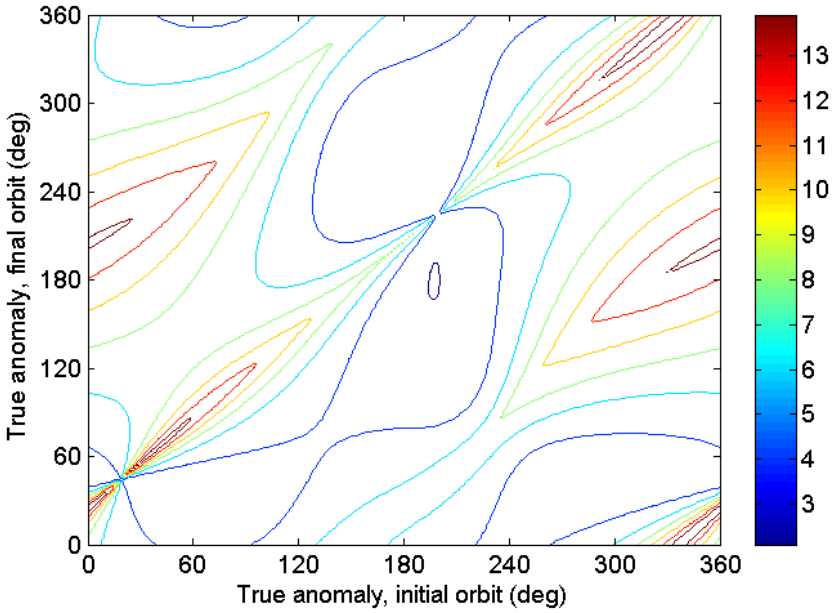

(b) Δv_{tot}^2 optimal

Fig. 13. Contour plots showing $|\Delta \boldsymbol{v}_1| + |\Delta \boldsymbol{v}_2|$ cost using the Δv_{tot} optimality (left) and Δv_{tot}^2 optimality (right) over the ranges of true anomaly for initial and final orbit.

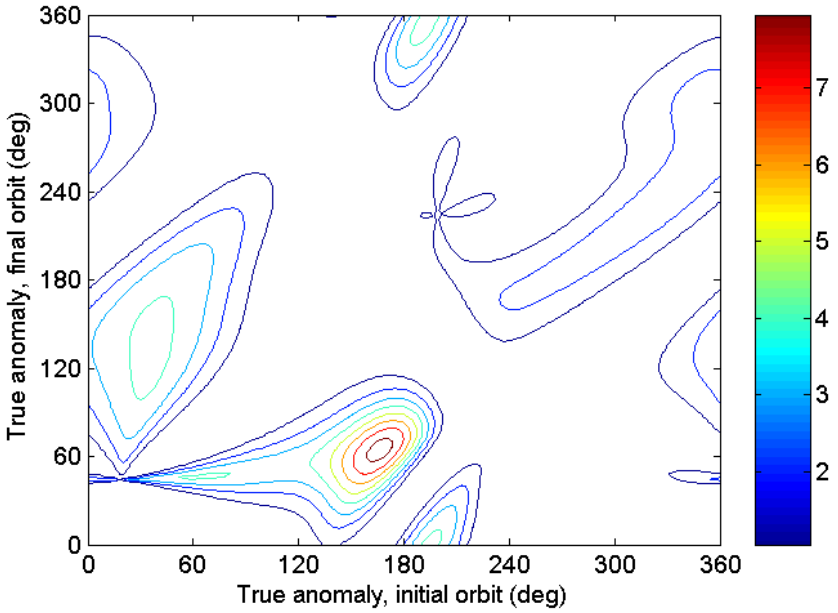

Fig. 14. Percent error in $|\Delta \boldsymbol{v}_1| + |\Delta \boldsymbol{v}_2|$ using the Δv_{tot}^2 optimality.

Table IX. Orbit parameters for pork-chop plots

Orbital element	Initial orbit	Final orbit
Perigee altitude (km)	10,236.2	26,158.9
Apogee altitude (km)	54,495.6	29,659.0
R.A.A.N.	83.86°	103.27°
Argument of perigee	18.54°	159.13°
Inclination	33.39°	57.08°

C. Optimal Two-Impulse Transfers

The method presented in the previous section solves for the optimal two-impulse transfer when the initial and final states are fixed and time is free. In the constellation transfer problem, the initial and final states are freely chosen so long as they lie on the state-space of the initial and final orbit. In other words, the true anomaly for departure and the true anomaly for arrival are additional optimization variables. As shown in Fig. 13, the cost function over these variables has many local minima that precludes the use of traditional optimization methods.

Methods such as the Genetic Algorithm (GA), Particle Swarm Optimization (PSO), or Simulated Annealing (SA) can be used to solve for global minima in complicated, multi-variable optimization problems, but both have a number of parameters to tune to produce the desired results [61, 62]. Alternatively, Henderson and Mortari have developed a Learning Approach (LA) to sampling optimization algorithm to solve these problems that requires no tuning [17, 18, 19]. Several refinements to the LA algorithm are presented here, and it is then applied to the general optimal two-impulse transfer problem.

1. Learning Approach to Sampling Optimization

The Learning Approach to sampling optimization is based on rejection sampling (or accept-reject method) developed by von Neumann [63]. A brief review of the LA method is presented here. First, we start with a cost function $J(\boldsymbol{x})$ where $\boldsymbol{x}$ is an n-d vector of design variables. The domain of the optimization problem is restricted by some minimum and maximum values such that $\boldsymbol{x} \in [\boldsymbol{x}^-, \boldsymbol{x}^+]$. Initially, the range of the cost function must be defined on some interval $J(\boldsymbol{x}) \in [J^-, J^+]$. The cost function is then evaluated at the boundary points of the specified domain and these

values are stored in a database.

The LA algorithm then generates a random point, $\boldsymbol{x}_r$, within the domain using a uniform distribution. The points within the database are used to approximate the value of the cost function at the randomly generated point, $\hat{J}(\boldsymbol{x}_r)$. Next, a random value y is generated over the specified range of the cost function. If $y > \hat{J}(\boldsymbol{x}_r)$ then the point is accepted, and the cost function is evaluated at $\boldsymbol{x}_r$ and added to the database. Otherwise, the point is simply rejected and no cost function evaluation takes place. The process of generating random points within the domain and accepting some and rejecting others continues until a specified number of points have been accepted.

The way the LA algorithm works is essentially that the database acts as a piecewise approximation to the cost function. The regions where the approximate cost function are low will have small values of $\hat{J}(\boldsymbol{x}_r)$ and are thus more likely to be accepted. As more points are added, the database approximation becomes more and more accurate and the point selection accelerates towards accepting points near the true minima of the cost function. Still, no region of the domain has zero probability of being accepted, so the entire domain is explored.

2. Refinements

Though the learning-adaptive algorithm is simple in theory, the implementation can cause headaches. Two issues had to be addressed before the LA algorithm could be applied to the impulsive transfer problem and before it could be efficiently used to solve the constellation transfer problem. First, the question of how to organize the generated points into a database had to be addressed. Secondly, limits on the cost function J were required to select random values for the accept-reject sampling.

Delaunay Triangulation

The problem of how to organize all of the data associated with this algorithm is critical to the efficiency of the overall method. An unorganized database requiring extensive searches will slow the process down so much it would be better to simply choose points at random and evaluate all of them to find the global minimum. The clumping of the samples poses additional problems because the database must handle non-uniform distributions, and the continuous addition of new samples means the database method must be efficient for dynamic datasets.

The k-vector approach described in Ref. [64] is extremely efficient, but it requires a uniform dataset for maximum efficiency. Additionally, much of its efficiency is based on significant pre-computing, so it works best on a static dataset. Quad-tree databases are extremely popular, but again they work best on uniform datasets [65]. As the dataset becomes non-uniform, a balancing operation must take place, decreasing its efficiency. A K-D tree (extension of quad-tree to n dimensions) implementation with automatic tree balancing has been developed for the LA algorithm in Ref. [66], but we seek a simpler and more elegant solution for this limited 2-D application.

One method stands out for its ability to handle non-uniform, dynamic datasets: Delaunay triangulation [67]. Not only is the efficiency of a Delaunay triangulation unaffected by clustering, there is a method for constructing Delaunay triangulations by adding one point at a time that ties for the best expected run-time complexity on average. Delaunay triangulation takes points in $\mathbb{R}^2$ and generates a series of edges connecting those points to create a convex shape filled with triangles (Delaunay tesselation does a similar thing for higher dimension spaces). In general, an infinite number of triangulations exist, but Delaunay triangulations maximize the minimum angle of any triangle. In other words, Delaunay triangulation prefers equilateral

triangles to long, skinny triangles. Note that Delaunay triangulations are the dual of Voronoi diagrams [67].

This yields an additional favorable property of Delaunay triangulations (or tesselations) in that the three vertices of a triangle are often the nearest neighbors of all the points residing within that triangle. As such, the points on the vertices can be used in a simple linear interpolation to solve for the needed estimate of J in the LA algorithm. These many advantages led to the use of the Delaunay triangulation as the database method for this problem.

Generating y-values

A fine balance must be struck between the number of points rejected and the number accepted. Higher numbers of rejected points provide better local convergence, but restrict the LA algorithm's ability to explore the entire domain. Despite the efficiency of the Delaunay database method, running a search on every generated point to locate the triangle that encloses it followed by a linear interpolation can take significant time when the rejection rate is too high.

To accomplish the accept-reject sampling, a random variable y must be generated based on the expected limits of the cost-function J. The original formulation of the LA algorithm called for either a uniform distribution or a log-normal distribution to generate a point within the range $[J^-, J^+]$ [17]. The log-normal distribution has the advantage of preferring low values of y, thereby weighting more heavily the regions of local minima. Ref. [19] further recommended that those limits for an orbital transfer problem be $J^- = 0$ and $J^+ = \max J(\boldsymbol{x}_i)$, where $\boldsymbol{x}_i$ are all data points in the data base. Note that a stricter lower limit reduces the number of spurious points rejected because they are lower than the global minimum, whereas a stricter upper limit improves the behavior of the LA algorithm of focusing efforts on the minima.

Instead of the aforementioned limits and distributions, we adopted the following for generating values of y:

$$y = (J_{med} - J_{min})|z| + J_{min} \tag{3.55}$$

where J_{med} and J_{min} are the median and minimum values of J in the database respectively, and z is a zero-mean Gaussian random variable with $\sigma = 1$. This approach has many advantages. First, like the log-normal scale, it tends to produce smaller values of y, but the scaling is more intuitive to understand. Second, using the median value of the database forces the sampling to become stricter as more points are added, thus improving the convergence towards minima. Third, since the values $\hat{J}(\boldsymbol{x}_r)$ are linearly interpolated from the values in the database, $\hat{J}(\boldsymbol{x}_r)$ is strictly greater than $\min J(\boldsymbol{x}_i)$, so values of y below that level will *always* be rejected if generated.

Note that since this work was completed, Henderson and Mortari have proposed several additional alternatives for generating y-values, similar to the one used here. They have also performed extensive testing on a variety of benchmark problems using these different formulations. For the authoritative analysis on the LA algorithm, refer to Henderson's forthcoming dissertation.

Tuning LA for Orbit Transfers

To improve performance, a few other tweaks have been made to the rejection sampling method, given a target of n accepted points. Though this fine-tuning of the LA algorithm is generally applicable to all problems, we make no claims as to improvements in performance on any problem other than the optimal orbit transfer problem studied here.

First, an initial set of points is accepted regardless of the accept-reject criteria to fill out the domain - typically the first 1%-5% of n. Second, rather than using

J_{med} in Eq. (3.55), J_{max} is used for the first 10% of the points, allowing for more of the domain to be searched initially. Lastly, when a point is generated, the size of the triangle that encloses it is evaluated. If the size of that triangle is more than 10 times the average triangle size (number of triangles is approximately twice the number of points in the database), then the point is accepted, regardless of the other accept-reject criteria. This guarantees that the LA algorithm does not exclude huge swaths of the domain that may need to be investigated. Without this additional criterion, many cases were witnessed where a triangle had vertices at three peaks in the cost function domain and the entire valley enclosed by that triangle went unsearched.

3. Application to Two-Impulse Transfers

We define the *general two-impulse orbit transfer* as follows. A satellite exists on some initial orbit and must move to some final orbit. Both orbits can be arbitrarily defined in shape, size, and orientation. The transfer departure point lies anywhere on the initial orbit and the transfer arrival point lies anywhere on the final orbit. As such the true anomalies of the departure and arrival points are independent optimization variables. The time of flight is also unconstrained, permitting a third optimization variable. The approach here is to solve the free time of flight optimization problem using the method presented in Section B, then use the Learning Approach optimization technique to solve for the optimal initial and final true anomalies.

Satellite Phasing

Free time of flight and arbitrary initial and final position along an orbit clearly ignores the critical issue of phasing along the orbit. This can be rectified with a combination of three methods.

First, in-plane rephasing of a satellite simply entails boosting into a slightly larger

orbit or dropping down into a slightly smaller one. After a number of revolutions, the satellite is reinserted into the target orbit with the correct phasing. As the amount of time spent on those phasing revolutions is allowed to increase towards infinity, the fuel cost of the rephasing goes to zero. Even with non-infinite time, the costs of in-plane rephasing are small enough to be neglected compared to the other orbit shape changes and reorientations.

Second, if the initial and final orbit have different semi-major axes, the departure time can be chosen such that the phasing is correct. Again, it may take infinite time before the phasing becomes correct, and it may be impossible if the two orbital periods are rational multiples of one another, but choosing the departure time can minimize the rephasing effort required.

Lastly, the transfer orbit presents another opportunity to effect the phasing, provided it has a different semi-major axis than the other two orbits. The transfer can be allowed to extend to multiple revolutions without affecting the fuel requirements.

Describing Initial and Final Orbits

Typically the size, shape, and orientation of a general orbit can be described using a set of five orbit parameters: semi-major axis, eccentricity, inclination, right ascension of the ascending node (RAAN), and argument of perigee. The general orbit transfer problem only requires information about the relative orientation between the two orbits - not both inertial orientations. This allows a reduced set of parameters to be used to describe the orbit transfer problem.

First, the inclination of the initial orbit can be set to zero without loss of generality. Additionally, the RAAN of both orbits can be set to zero. The relative orientation of the two orbits will be handled completely by the values of the argument of periapsis. Given a direction cosine matrix (DCM), $[C_{IN}(\Omega_i, i_i, \omega_i)]$, that rotates a vector

from the inertial frame into the initial orbit frame and a direction cosine matrix, $[C_{FN}(\Omega_f, i_f, \omega_f)]$, that rotates a vector from the inertial frame into the final orbit frame, the DCM describing the relative orientation between the two orbits can be computed as

$$[C] = [C_{FN}][C_{IN}]^{\mathrm{T}} \tag{3.56}$$

The relative orbit elements can be calculated from the elements of this matrix as follows:

$$\omega_i = -\tan^{-1}\left(\frac{C_{31}}{-C_{32}}\right) \tag{3.57}$$

$$i_f = \cos^{-1}(C_{33}) \tag{3.58}$$

$$\omega_f = \tan^{-1}\left(\frac{C_{13}}{C_{23}}\right) \tag{3.59}$$

This simplification means that the general orbit transfer problem can be described using only the seven variables $\{a_i, e_i, \omega_i, a_f, e_f, i_f, \omega_f\}$, rather than the typical ten parameters required to define the size and orientation of two general orbits. This reduced space will be used in the Monte Carlo tests later in this section.

Simple Example

To better understand how the LA optimization technique solves the orbit transfer problem, we return to the example transfer presented at the end of the previous section in Fig. 13. Since the LA method relies on random sampling, we will compare it to randomly sampling the domain with a uniform distribution. The LA algorithm initializes with 10 randomly selected points, where all points are accepted, to provide a reasonable initial approximation of the cost function, so Fig. 15 shows that after 10 points, both the LA and the uniform distribution are identical.

As more points are added to the database, the LA algorithm focuses more on the

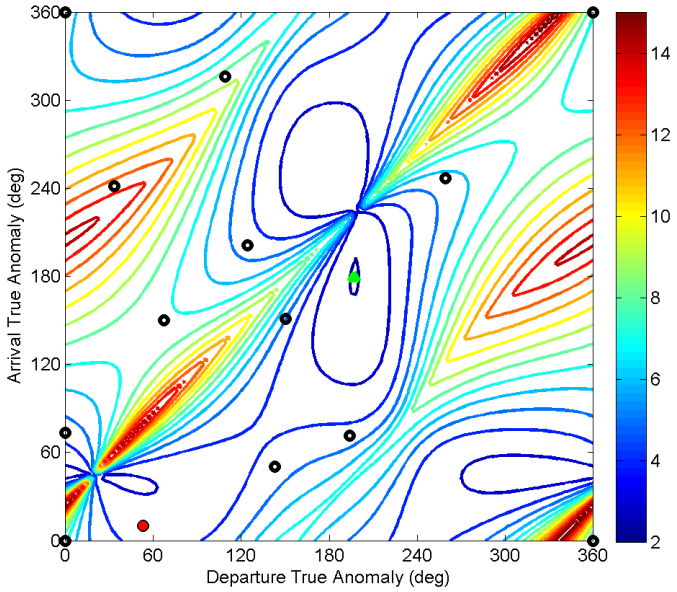

(a) LA sampling

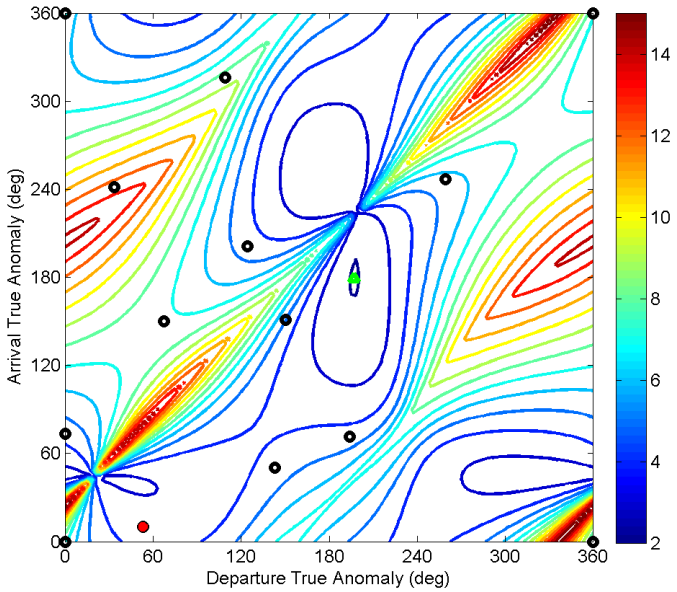

(b) Random sampling

Fig. 15. Initial distribution of 10 points for both the LA sampling algorithm and a purely random sampling algorithm. The LA algorithm accepts the first 10 points regardless of accept-reject criterion.

minima. Figures 16 and 17 show the distributions of both techniques at 100 points, 200 points, 300 points, and 400 points. The points noted by circles (black) represent accepted points. The filled in circle (red) represents the current best solution in the database at each stage, whereas the triangle (green) represents the true global minimum of this particular transfer.

In this particular case, both methods arrive approximately at the true global minimum, though the LA algorithm performs slightly better. The LA algorithm arrives at a cost 1.8% off of the true minimum cost at a distance of 4.7° from the minimum, whereas the random sampling algorithm is 5.3% off the true minimum cost at a distance of 6.3°.

Monte Carlo Results

To further test the LA sampling algorithm as it applies to the two-impulse transfer problem, a Monte Carlo test was run. One thousand (1,000) different sets of initial and final orbits, as defined by the seven parameters $\{a_i, e_i, \omega_i, a_f, e_f, i_f, \omega_f\}$ described earlier, were run through the LA sampling algorithm and also through a simple random sampling algorithm that accepted all points. A brute force grid search was used to initialize multiple local minima searches, the results of which were used to determine the true global minimum of the Δv_{tot}^2 cost function. The minimum value reported by both the LA sampling and random sampling algorithms were then compared to these global minimum values.

Figure 18 shows the percent error in the value of the Δv_{tot}^2 cost function between the true global minimum and that found by the two different algorithms. The average error over all test cases was 1.0% for the LA algorithm with 96.0% of the cases below 5% error, versus 2.9% average error and only 81.9% below the 5% threshold for the random algorithm. The maximum error encountered was 12.2% and 35.4%

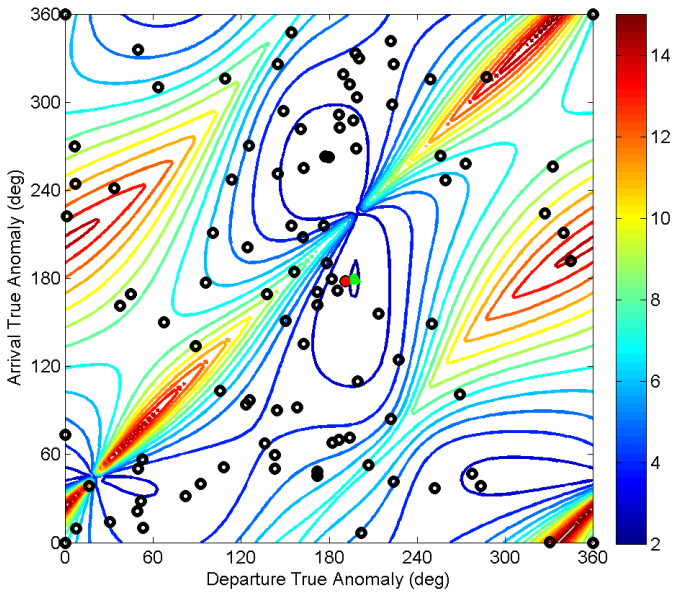

(a) 100 points

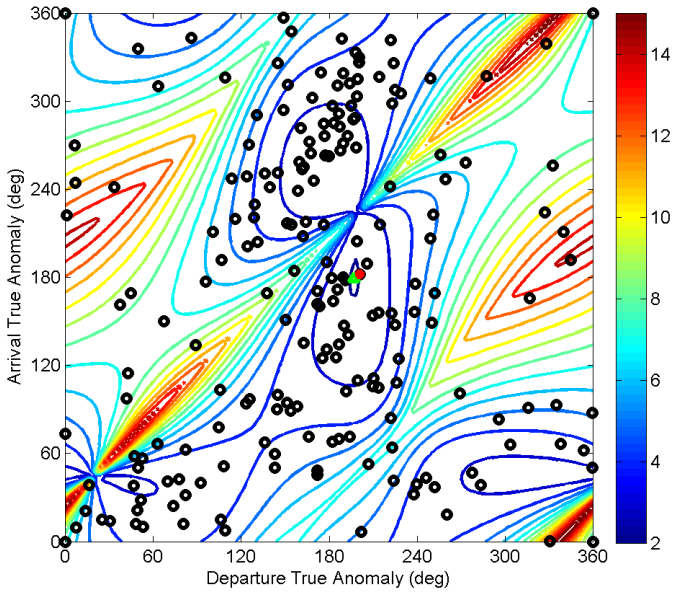

(b) 200 points

Fig. 16. Accepted points for the LA sampling algorithm.

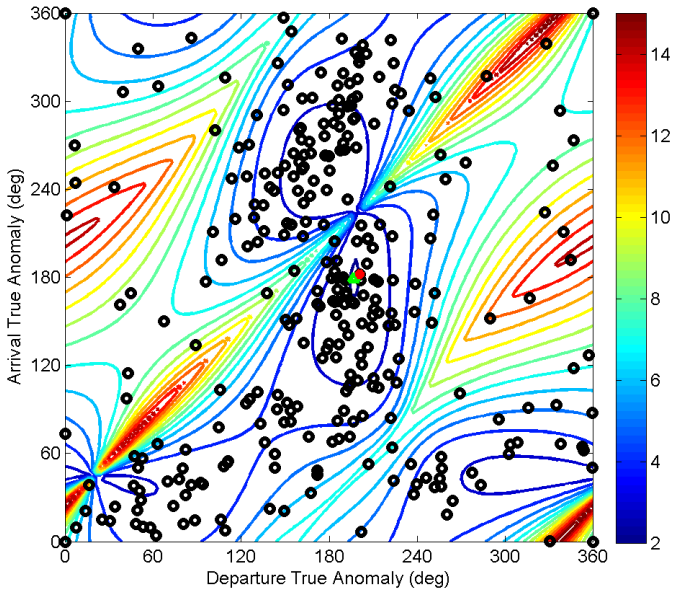

(c) 300 points

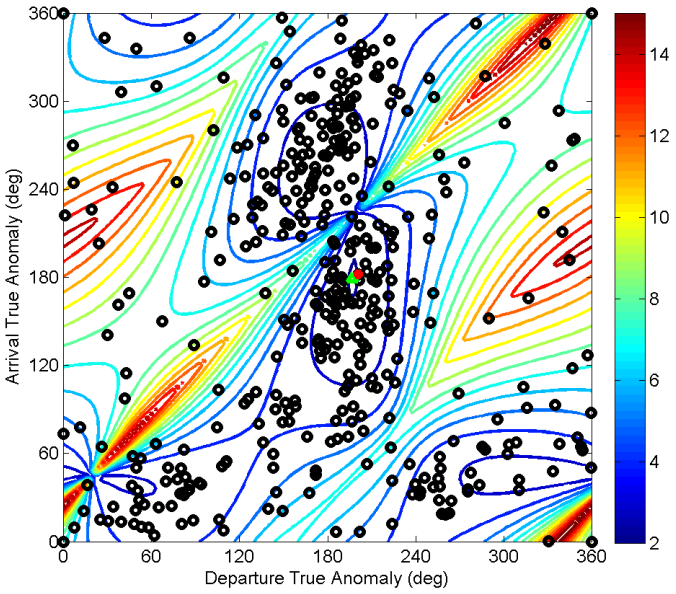

(d) 400 points

Fig. 16. (cont.) Accepted points for the LA sampling algorithm.

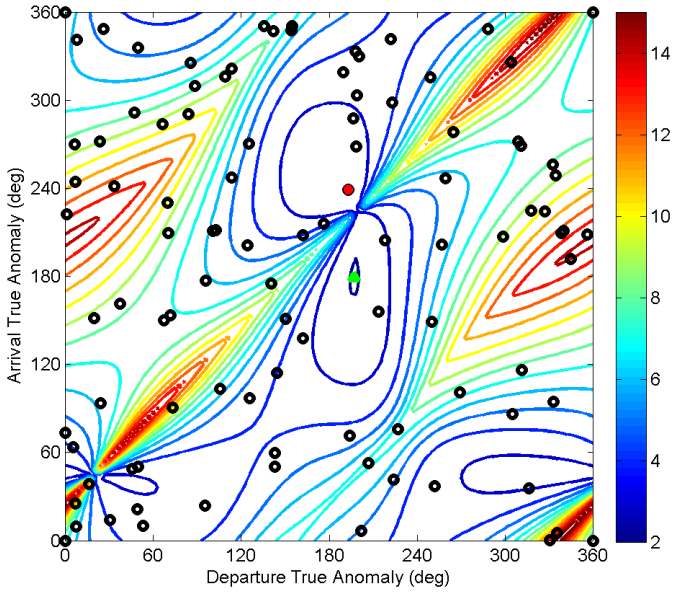

(a) 100 points

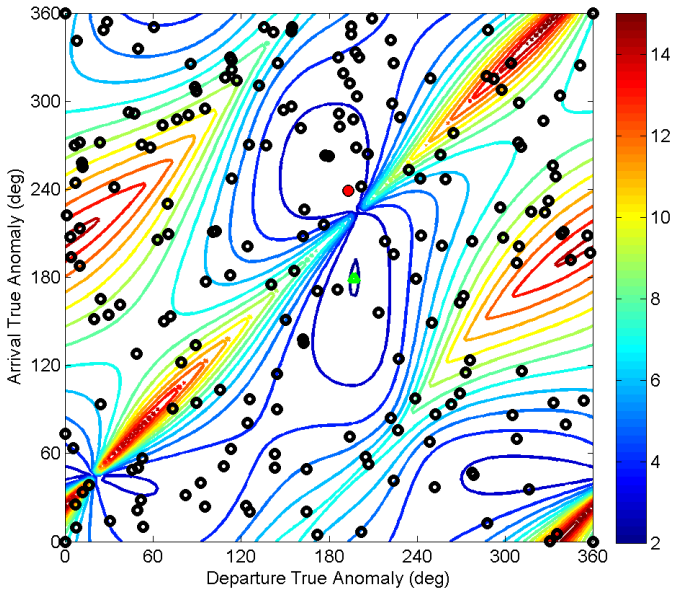

(b) 200 points

Fig. 17. Accepted points for the random sampling algorithm.

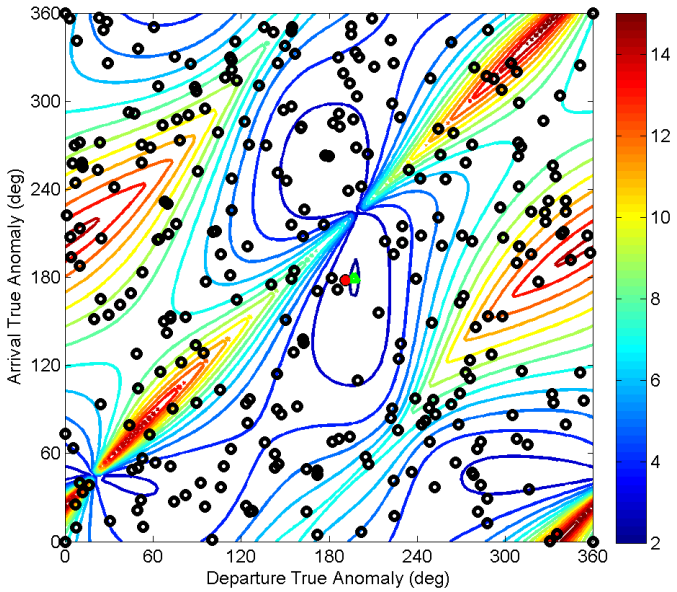

(c) 300 points

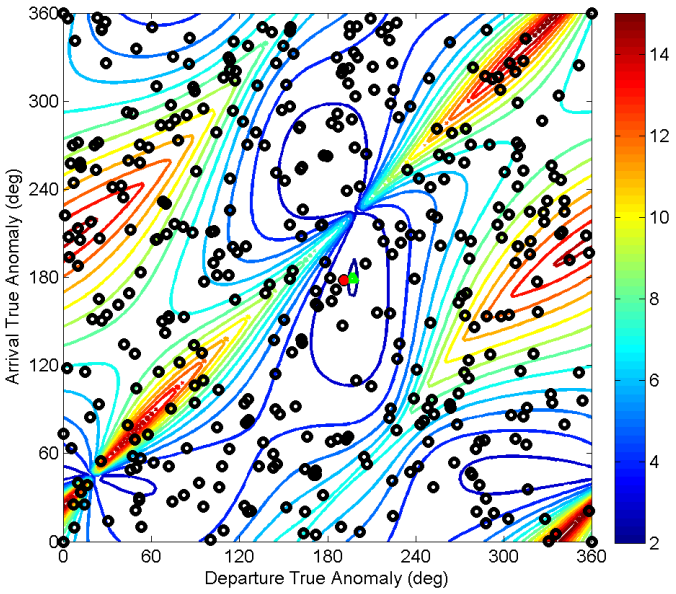

(d) 400 points

Fig. 17. (cont.) Accepted points for the random sampling algorithm.

respectively. It is concluded that the LA algorithm outperforms the random sampling algorithm by about a factor of three in this application.

For the constellation transfer problem, correctly computing the cost function is of utmost importance, but it is still interesting to see how far off in true anomaly space the true global minimum was from the global minimum computed by each algorithm. Figure 19 shows the error in true anomaly space in degrees between the calculated locations of the global minimum. For the LA algorithm, 71.2% of the reported global minima are within 10° of the true global minima, compared to only 43.6% for the random algorithm. Despite the large number of cases with large errors in global minimum location, the errors in the cost function remain low - a look at the relationship between the two errors reveals very little correlation - indicating that when the location error is large, the algorithm has converged on a local minimum that is only slightly worse than the global optimum.

When considering the entire constellation transfer problem, we have introduced the Δv_{tot}^2 cost function to minimize computational cost, but this has some error built into it, as discussed in the previous section. Since no global search routine, including the LA method presented here, can guarantee convergence to the true global minimum, a valid question is to ask what are the end-to-end errors. That is, the output of the LA algorithm is a slightly sub-optimal solution of a slightly approximated cost function, so what is the error of that final solution compared to the true optimal value accrording to the desired Δv_{tot} cost function? Figures 20 and 21 show the same results as the Figs. 18 and 19, but with respect to the Δv_{tot} cost function.

Despite the slightly sub-optimal result using an approximated cost function, the LA sampling algorithm still averages only 1.3% error from optimal over the 1,000 test cases and has 95.9% of the test cases within 5% error!

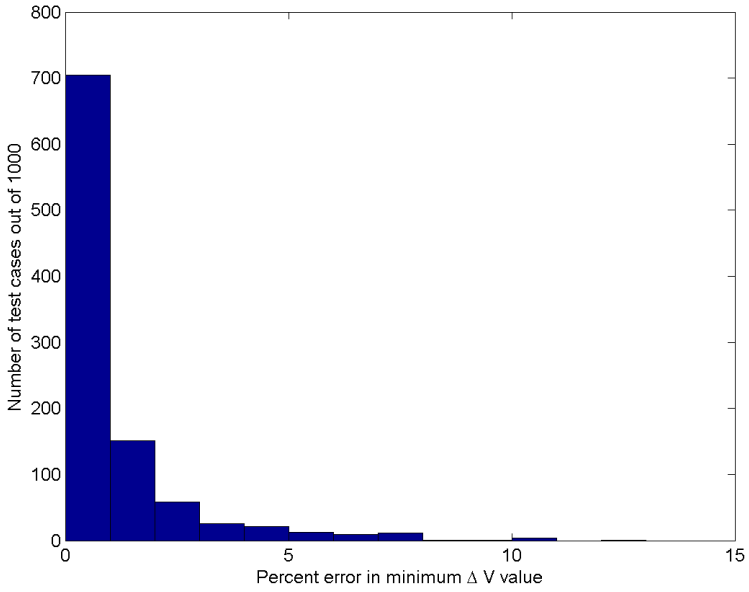

(a) LA sampling

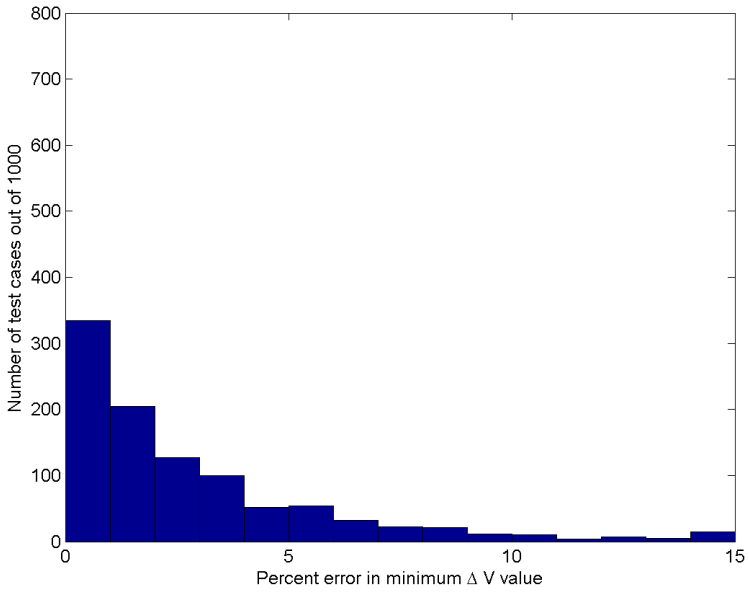

(b) Random sampling

Fig. 18. Percent error of the minimum Δv value using the Δv_{tot}^2 cost function.

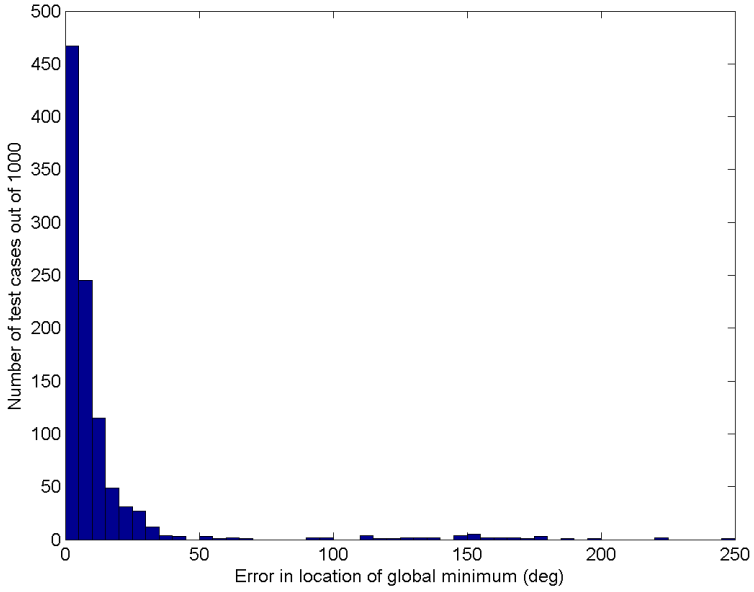

(a) LA sampling

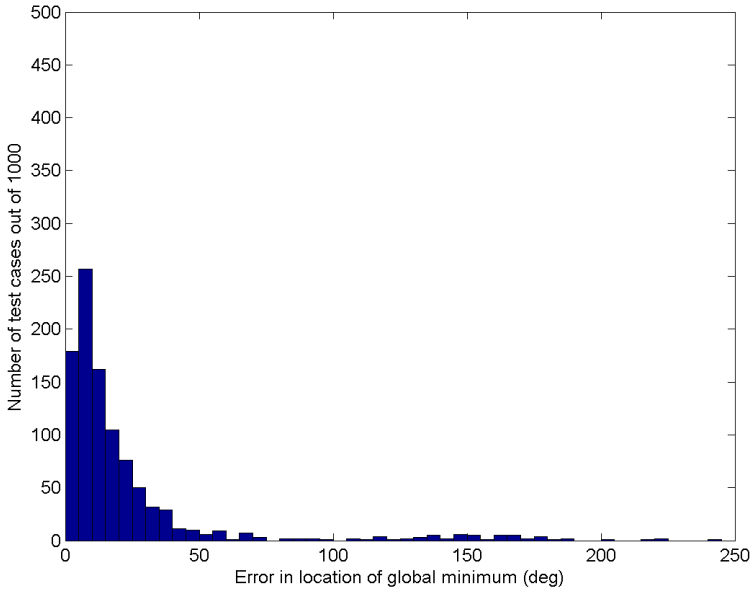

(b) Random sampling

Fig. 19. Error in degrees of the location of the global minimum using the Δv_{tot}^2 cost function.

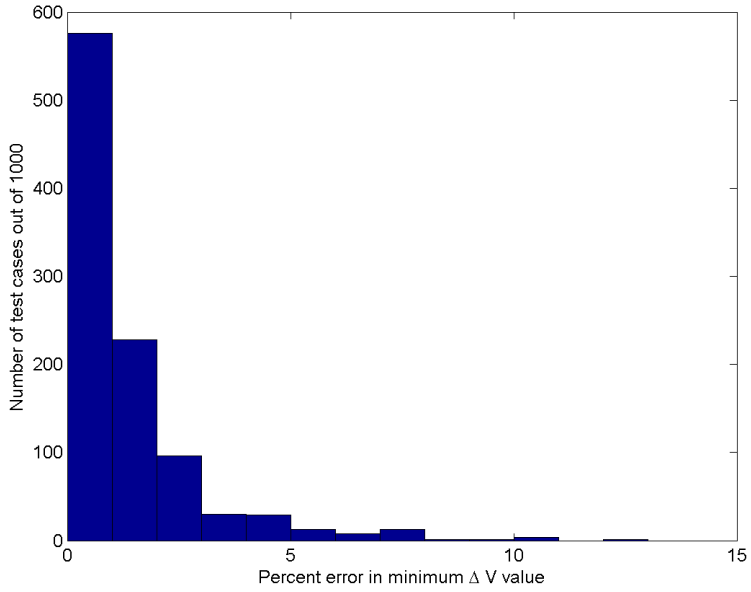

(a) LA sampling

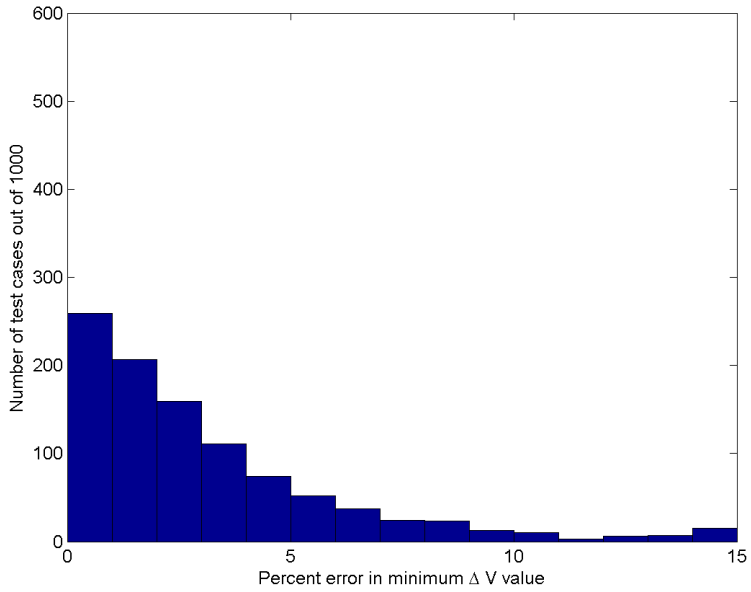

(b) Random sampling

Fig. 20. Percent error of the minimum ΔV value using the Δv_{tot} cost function.

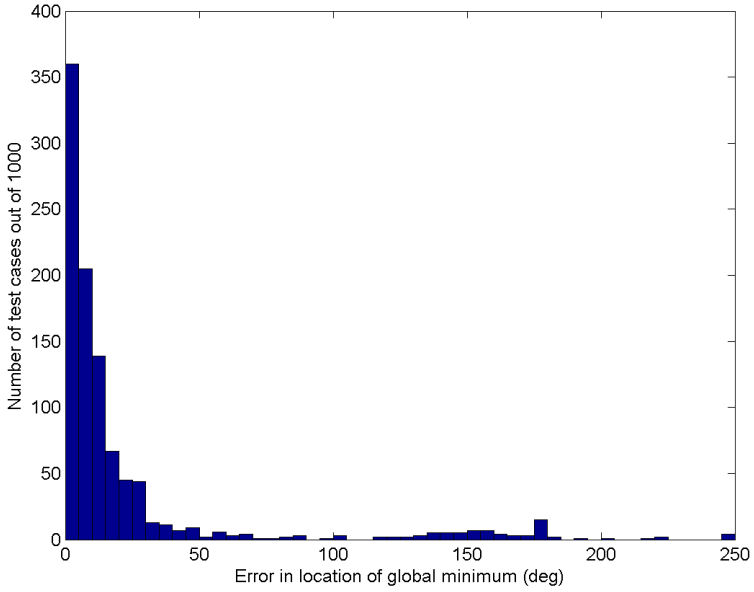

(a) LA sampling

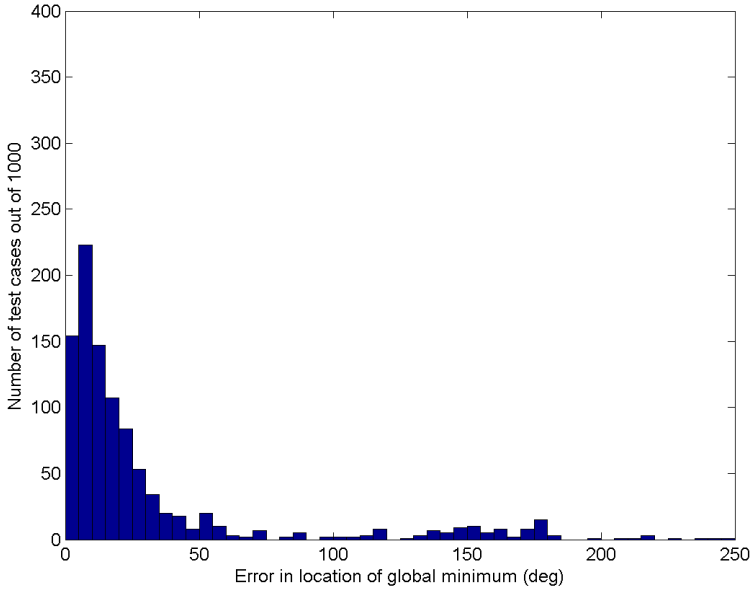

(b) Random sampling

Fig. 21. Error in degrees of the location of the global minimum using the Δv_{tot} cost function.

D. Conclusions

The general constellation transfer problem can be defined as selecting the optimal assignment of satellites in an initial constellation to satellite slots in a final constellation while simultaneously solving for the optimal orbit transfers for those assignments. This chapter has shown how the constellation transfer problem can be formulated and solved as a linear assignment problem, although this formulation requires the optimal orbit transfer problem to be solved for every combination of initial satellite position and final constellation slot.

To efficiently solve these orbit transfer problems, this chapter then presented a closed-form solution for the minimum Δv_{tot}^2 Lambert's problem. The resulting procedure constitutes an easy tool to implement that can be useful when extensive minimum Δv_{tot} problems must be solved. Since the method does not require any iterations, the number of steps for the whole procedure (complexity) is constant. This is a crucial property when the algorithm has to be extensively used within the constellation transfer framework or other optimization routines. The solution provided by minimizing Δv_{tot}^2 does not always minimize the fuel consumption, but it represents a good approximation, and it can be used as the starting point for finding (e.g. using gradient descent approach) the true optimal two-impulse maneuver with minimum Δv_{tot}. The difference between Δv_{tot}^2 and Δv_{tot} minimizations is numerically found to be bounded with a maximum value lower than 20%.

An efficient solution to the Δv_{tot}^2 Lambert's problem, however, is only part of what is needed to solve the general orbit transfer problem. Allowing the initial and final positions to vary about the initial and final orbit presents a difficult global optimization problem with multiple local minima. The newly developed Learning Approach to sampling optimization was applied to the two-impulse orbit transfer

problem. Section 2 introduced some modifications and improvements to the LA algorithm to improve its overall performance. The LA algorithm was demonstrated to outperform a simpler random sampling approach and to efficiently solve the global optimization problem with only 400 evaluations of the Δv_{tot}^2 cost function.

CHAPTER IV

CASE STUDIES

Chapters II and III provided the development of several new techniques critical to efficiently solving the constellation design and constellation transfer problems. Though each method was assessed individually within those chapters, here we look at three particular case studies to emphasize their utility. First, we consider the problem of designing a constellation for a global navigation satellite system (GNSS). Using the European Galileo GNSS design as a baseline, we design an Elliptical Flower Constellation demonstrating superior performance for the same launch costs. In the second example, we consider the design of a new Iridium LEO communications constellation (Iridium recently announced plans to launch a new constellation by 2014 [68]). Compared to an optimal Walker constellation design, the EFC design provides improved global coverage to minimize downtime for satellite phone users. Lastly, we design two Lattice Flower Constellations to provide regional coverage over two different sites, then solve the constellation transfer problem using the minimum Δv_{tot}^2 and auction algorithm approaches discussed in Chapter III.

A. Global Navigation Satellite System

To examine the effectiveness of the Elliptical Flower Constellation framework for designing a global coverage constellation, we first use the example of global navigation. Flower Constellations were first studied for use in GNSS by Park [69], who found improvements over the Galileo GNSS constellation by using a combination of two Harmonic Flower Constellations found by trial and error. Tonetti [70] ran a Genetic Algorithm (GA) to improve upon Park's results. Both of these Flower Constellations were designed for 30 satellites and utilized large numbers of orbital planes (15 and

30 respectively), which is unattractive from a launch and operational standpoint. Alternatively, Bruccoleri [71] found a Harmonic Flower Constellation with 24 satellites that showed improved performance over the GPS constellation. All three studies considered only circular orbits rather than be restricted to a critically inclined Flower Constellation with elliptic orbits. In this study, we consider both 27 and 25 satellite EFCs. We have not considered the combination of two or more EFCs into the same constellation, as was done in Ref. [69], but this may yield additional improved results.

1. Cost Function

As a cost function to drive these design studies, we consider the Geometric Dilution of Precision (GDOP), a measure of the accuracy of a GNSS solution. The lower the value of GDOP, the more accurate is the GNSS solution. GDOP is dependent entirely on the geometry of the satellites within view of a specific ground site and relies on the visibility matrix, given by

$$A = \begin{bmatrix} \hat{\boldsymbol{r}}_1^{\mathrm{T}} & 1 \\ \hat{\boldsymbol{r}}_2^{\mathrm{T}} & 1 \\ \vdots & \vdots \\ \hat{\boldsymbol{r}}_n^{\mathrm{T}} & 1 \end{bmatrix} \tag{4.1}$$

where $\hat{\boldsymbol{r}}_i$ is the unit vector from ground site to the i^{th} satellite, and n is the number of visible satellites. We defined a minimum elevation angle of 10° to determine satellite visibility in this simulation. We define the matrix $H = A^{\mathrm{T}}A$. GDOP can then be calculated

$$\text{GDOP} = \sqrt{\text{tr}\left(H^{-1}\right)} \tag{4.2}$$

This compact equation is simple, but requires a matrix inverse for every point (in time and space) that needs to be evaluated, so here we derive a new equation with

faster computation. Since the trace of a matrix is the sum of its eigenvalues, and the eigenvalues of a matrix inverse are the inverses of the original matrix eigenvalues, we can rewrite the computation of GDOP as

$$\text{GDOP} = \sqrt{\sum_i \frac{1}{\lambda_i}} \tag{4.3}$$

where λ_i are the eigenvalues of H. Note that $\sum_i \lambda_i = 2n$. This alternate form of GDOP calculation reduced computation time in MATLAB by more than a factor of two.

To evaluate the accuracy of a given GNSS constellation, 1,000 points were distributed uniformly around a spherical Earth. The constellation was propagated using an initial argument of perigee of zero with 5° steps in mean anomaly, and GDOP was calculated for all ground sites at each of those times. The initial argument of perigee was then rotated in 5° steps with mean anomaly propagation performed at each step. This is a useful approximation of the behavior of the constellation due to the low rate of rotation of argument of perigee as compared to mean anomaly. The values of GDOP from all of these evaluations were then averaged, and the GA sought to minimize this mean GDOP value.

2. Design Study: 27 Satellites

In this study, we compare performance to the Galileo constellation, designed as a 27/3/1 Walker constellation at 56° inclination and semi-major axis of 29,600 km [35, 72]. Initial design studies based on a variety of performance and operational considerations led to this particular selection of the number of satellites and number of orbital planes, so those were held constant in this design study. Once those numbers are fixed, the Walker constellation framework allows for just two design variables: the phasing parameter F and the inclination angle. The phasing parameter is restricted

to just 3 possible values. In contrast, the new EFC framework allows for 117 unique combinations of the parameters $\{N_\omega,\, N'_{so},\, N_c^1,\, N_c^2,\, N_c^3\}$ and permits eccentricity to vary in addition to the inclination angle. Additionally, elliptic orbits are cheaper to launch into than circular orbits of the same semi-major axis, so holding launch cost constant allows EFCs with higher altitudes. Thus, the search space is significantly expanded, yet still contains the original Galileo constellation design.

Preliminary analysis to reduce the design space consisted of evaluating all 117 EFCs over four values of eccentricity and eleven values of inclination:

$$e \in [0.1, 0.2, 0.3, 0.4], \quad i \in [45^\circ, 47^\circ, \ldots, 65^\circ]$$

Circular orbits were not considered because they all collapse to LFC/Walker constellations per Thm. C.2. The inclination range was chosen to place the Galileo optimal inclination of 56° in the middle. The semi-major axis was held fixed at 29,655 km, corresponding to a repetition time of 17 orbits in 10 days. A satellite was considered in view if it was at least 10° above the horizon (grazing angle).

The constellations were evaluated for both mean GDOP and maximum GDOP encountered throughout the propagation. As a first cut, only solutions with a maximum GDOP below 6 were accepted (corresponding to the original requirements for the GPS constellation [73, 74]). There were 9 EFCs out of the original 117 that satisfied this requirement at a variety of inclinations and eccentricities, all of the form

$$\begin{bmatrix} N_o & 0 & 0 \\ N_c^3 & N_\omega & 0 \\ N_c^1 & N_c^2 & N'_{so} \end{bmatrix} = \begin{bmatrix} 3 & 0 & 0 \\ N_c^3 & 9 & 0 \\ N_c^1 & 0 & 1 \end{bmatrix}$$

All of the minima for mean GDOP occurred in the inclination range $i \in [53^\circ, 59^\circ]$ over the full range of eccentricity.

This initial analysis was completed at a fixed altitude, but one advantage of elliptical orbits is their ability to launch into larger orbits for the same launch cost. To demonstrate this fact, consider the simple example of launching into a circular parking orbit at an altitude of 200 km. Figure 22 shows the cost in Δv for a two-impulse maneuver into final orbits of varying semi-major axis and eccentricity. Clearly, as eccentricity increases for a constant semi-major axis, the impulse requirement falls.

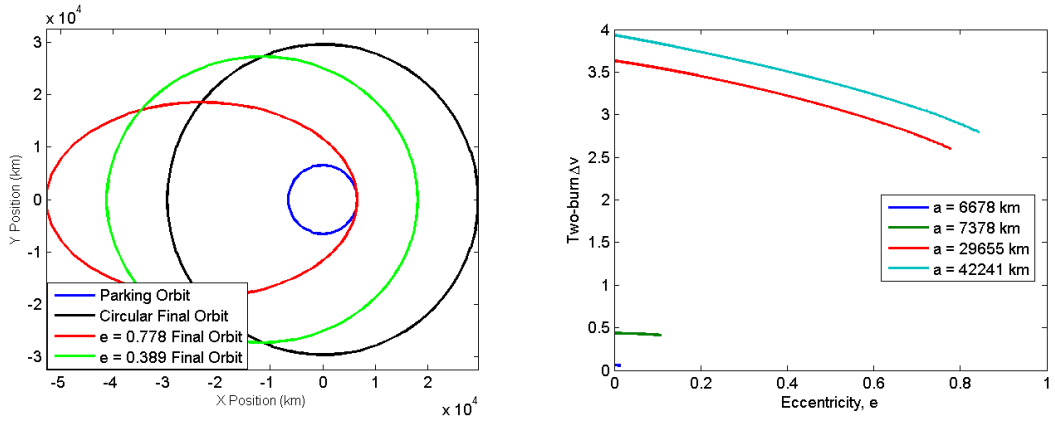

(a) Orbit transfer illustration for the case of a=29,655 km

(b) Δv requirements

Fig. 22. Demonstrating the lower Δv requirements for elliptic orbits vs. circular orbits of the same semi-major axis

The GIOVE-A and GIOVE-B satellites, launched as test vehicles for Galileo, launched into 190 km altitude circular parking orbits at an inclination of 51.8° [75]. They were then boosted into their final orbit using a simple two-burn maneuver. Using the limiting case of a 60° final inclination, a minimum eccentricity required to launch into an orbit of a given semi-major axis with the same two-burn maneuver cost as Galileo can be calculated. The minimum Δv_{tot}^2 algorithm of Chapter III was used for this computation assuming 180° transfer angle.

Following the design guidelines laid out by the Galileo constellation design en-

gineers, we seek a constellation with a repeating ground-track with repetition times between 5 and 10 days. Shorter repetition times lead to the build up of perturbations as the satellites pass over the same gravitational disturbances repeatedly, whereas longer repetition times pose operational challenges. Given these limitations and the desire to keep the apogee below GEO, we selected nine values of semi-major axis. Table X shows the different values of semi-major axis, minimum eccentricity (for the same launch cost), and maximum eccentricity (for apogee below GEO). Only values of semi-major axis larger than the planned Galileo system were considered because Ref. [72] shows that performance improves as altitude increases (though with diminishing returns, and they considered only circular orbits).

Table X. Values of semi-major axis used for GNSS optimization

N_p	N_d	a (km)	$e_{\min}$	$e_{\max}$
17	10	29,655	0.045	0.424
13	8	30,561	0.078	0.382
8	5	30,878	0.089	0.368
11	7	31,252	0.101	0.351
14	9	31,464	0.107	0.342
13	9	33,057	0.151	0.277
10	7	33,302	0.157	0.268
7	5	33,753	0.168	0.251
11	8	34,161	0.177	0.236

For the second stage of the design study, another brute force grid search was completed with inclination selected from $i \in [52^\circ, 53^\circ, \ldots, 60^\circ]$, semi-major axis and $e = e_{\min}$ selected from Table X, and the EFC parameters selected from the 9 EFCs

down-selected in the first stage.

After selecting the optimal inclination angle for each EFC at each altitude, one EFC outperformed all others at all altitudes:

$$\begin{bmatrix} N_o & 0 & 0 \\ N_c^3 & N_\omega & 0 \\ N_c^1 & N_c^2 & N'_{so} \end{bmatrix} = \begin{bmatrix} 3 & 0 & 0 \\ 2 & 9 & 0 \\ 0 & 0 & 1 \end{bmatrix}$$

As expected, the best performance occurred at the maximum altitude with $a = 34,161$ km and $e = 0.177$. The optimal inclination was the same as that of Galileo: 56°. The mean GDOP of Galileo was calculated to be 2.32, whereas the mean GDOP of this EFC designed constellation is 2.24 - an improvement of 3.5%. Given an inclination of only 56° (as opposed to 60°), the minimum eccentricity to achieve the same launch cost to this much larger orbit is 0.150. The mean GDOP varies only slightly (by 0.005) over the allowable eccentricity range, so eccentricity can be chosen based on other considerations. For instance, small eccentricity is attractive from an operational perspective, whereas larger eccentricity increases the allowable on-orbit satellite dry mass.

This EFC exhibits an interesting property: the satellites share the same geometry of the Galileo constellation at all times, they simply vary in altitude over time. The geometry is not an exact match, as the rotation of the argument of perigee perturbs it somewhat, but the two constellations bear great resemblance to one another. This "breathing" behavior, where the EFC mimics an LFC but with varying altitude, will occur for any EFC of the form

$$\begin{bmatrix} N_o & 0 & 0 \\ N_c^3 & N_\omega & 0 \\ N_c^1 & N_c^2 & N'_{so} \end{bmatrix} = \begin{bmatrix} N_o & 0 & 0 \\ N_c & N_{so} & 0 \\ 0 & 0 & 1 \end{bmatrix}$$

where N_o, N_{so}, and N_c are the parameters of the associated LFC.

The results of this study indicate that the Galileo constellation, at a semi-major axis of almost 30,000 km and 27 satellites, is very nearly optimal. The original designers chose a design point near the knee of the curve where increasing number of satellites or altitude met with diminishing returns [35], which is why the EFC design could only slightly improve upon the original Galileo design.

3. Design Study: 25 Satellites

The ultimate goal of a constellation designer is a constellation that maximizes performance while minimizing total system cost. Toward that end, reducing the number of satellites in a constellation, thereby eliminating its hardware and launch vehicle costs is one of the most effective means of reducing costs. We consider here the problem of designing an EFC with 25 satellites, divided into 5 orbital planes, to see what performance can be achieved while reducing the number of satellites by two.

The design approach is the same as in the previous section. For the 25 satellite, 5 plane case, there exist 150 unique EFCs, and these were all studied over a range of eccentricities and inclinations at the original Galileo altitude. The maximum GDOPs encountered by the 25 satellite constellations were significantly higher than the original 27 satellite study, so the initial results were pared down by requiring the mean GDOP to be less than 3 and the maximum GDOP to be less than 16. This left 8 different EFCs which were effective at a variety of eccentricities and inclinations. Table XI shows the configuration parameters for these 8 EFCs, all of which had $N_\omega = 5$.

When the altitude was allowed to vary as in the previous section (with $e = e_{\min}$), the maximum altitude was again the most effective. Unlike the 27 satellite case, however, there was significant variation in GDOP as a function of eccentricity, so each of the 8 EFCs were analyzed over a range of eccentricities at the maximum

Table XI. Elliptical Flower Constellation parameters for 25 satellite GNSS

N_c^1	N_c^2	N_c^3
0	2	3
3	2	2
4	2	2
3	3	4
4	3	3
3	4	3
4	4	2
4	4	4

altitude.

The best 25 satellite constellation was found to be inclined at 55° with an eccentricity of 0.207 and EFC parameters

$$\begin{bmatrix} N_o & 0 & 0 \\ N_c^3 & N_\omega & 0 \\ N_c^1 & N_c^2 & N'_{so} \end{bmatrix} = \begin{bmatrix} 5 & 0 & 0 \\ 4 & 5 & 0 \\ 4 & 4 & 1 \end{bmatrix}$$

The mean GDOP experienced with this constellation was 2.49, compared to the 2.24 of the 27 satellite EFC in the previous section. This 10% reduction in mean accuracy is significant, but may be warranted given the reduced costs of a 25 satellite constellation. Of course, if the spare satellite strategy employed is to place one spare satellite in every orbital plane, then both the 27 satellite, 3 plane constellation and this 25 satellite, 5 plane constellation require 30 total satellites on orbit. The major shortcoming of the 25 satellite constellation is its maximum GDOP of 9.11, compared

to a maximum GDOP of 3.87 for the 27 satellite EFC. A value above 6 is considered unusable [73], so there are times at which users would be unable to get a fix using this system. One conclusion is that the Galileo constellation as currently designed is very well optimized!

B. Iridium Design

The Iridium constellation was initially launched in 1997-1998 to provide global satellite phone service. The anticipated consumer demand never materialized due to the explosion of cell phones, and the company quickly went bankrupt in 1999 [76]. The bankrupt company was purchased for pennies on the dollar and service was restarted in 2001, with a focus on commercial and government customers with needs to communicate in remote areas of the world. In February 2007, Iridium announced a plan to launch a new constellation of satellites in 2014 to replace the existing one. The new satellites will have increased bandwidth capabilities, as well as several scientific instruments on board to measure the atmosphere [68].

The original Iridium constellation consisted of 66 satellites in 6 planes in a streets-of-coverage design pattern. Iridium has announced that the new constellation will also have 66 satellites in 6 planes at the same altitude - 781 km - but have not released details of the constellation design. To compare the efficacy of the Elliptical Flower Constellation approach, both an optimal Walker constellation and EFC were designed with the announced number of satellites, orbital planes, and semi-major axis.

A brute force search was conducted through the 6 available Walker constellations and the 396 EFCs. The eccentricity for the EFCs was set to 0.07, which yields a perigee altitude of ≈ 300 km. Satellites below that altitude are subject to significant atmospheric drag, so that established the maximum allowable eccentricity. The in-

clination of all of the constellations was varied between 40° and 90° in 2° increments. As in the GNSS example, 1,000 points were distributed uniformly about a spherical Earth, and satellite visibility required a minimum elevation angle of 5°.

The optimal Walker constellation was a 66/6/2 at an inclination of 64°. The optimal EFC had an inclination of 62° and EFC parameters

$$\begin{bmatrix} N_o & 0 & 0 \\ N_c^3 & N_\omega & 0 \\ N_c^1 & N_c^2 & N'_{so} \end{bmatrix} = \begin{bmatrix} 6 & 0 & 0 \\ 0 & 11 & 0 \\ 1 & 6 & 1 \end{bmatrix}$$

The constellations were propagated with 5° steps in mean anomaly, and every point on the Earth's surface was evaluated for single satellite visibility at each time step. We define the *failure rate* to be the sum total, both spatially and temporally, of the number of points with no satellite visibility divided by the total number of point evaluations. A failure rate of zero corresponds to continuous global coverage. The optimal Walker constellation exhibited a failure rate of 2.8% compared to a failure rate of only 0.9% for the EFC - a factor of 3 improvement.

A simple coverage metric was used to optimize these constellations, and streets-of-coverage designs were not considered. Still, this simple example shows the power of using EFCs for global coverage over the traditional Walker constellation design methodology. Whereas the GNSS example showed the utility of eccentric orbits due to lower launch costs, this example illustrates how eccentric orbits can improve coverage due to their larger mean altitude. The mean orbital radius of a satellite when averaged over time is equal to $a(1+e^2/2)$. So increasing eccentricity while maintaining semi-major axis results in a larger mean altitude, thereby improving coverage. In this case, optimizing the design using EFCs leads to significant advantages over the optimal Walker constellation.

C. Surveillance Reconfiguration

The previous two examples demonstrated the advantages of using EFCs over traditional Walker constellations. In this section, we complete an example of solving the constellation transfer problem. Two Lattice Flower Constellations were independently designed to optimize coverage over either Baghdad, Iraq or Kabul, Afghanistan, and then the constellation transfer tools of Chapter III were applied to optimize the transfer between them. This is an example of changing mission requirements motivating constellation reconfiguration.

1. Constellation Design

The following scenario is not based on any existing needs or capabilities, but is merely meant to be representative of a possible situation calling for constellation reconfiguration. Assume that the U.S. seeks to deploy a constellation of satellites for surveillance and reconnaissance of particular sites and has enabled this constellation to be reconfigurable by incorporating high-impulse thrusters into the satellite design. This constellation consists of 6 satellites in an unspecified number of planes and with a repeating ground-track that repeats every day after 12 orbital periods ($a = 8,059$ km).

Initially the constellation is designed to provide coverage of Baghdad, Iraq, located at 33°20′0″N and 44°26′0″E. Later, the mission changes to require coverage of Kabul, Afghanistan at 34°31′59″N and 69°9′58″E. Since this is a regional coverage requirement, LFCs are better suited than EFCs to tackle this problem. Only critically inclined orbits were considered to allow for the use of elliptical orbits without concern for J_2 effects.

Genetic Algorithm

The design space includes a combination of integer and real valued variables and the cost function is very non-linear with multiple minima. Genetic Algorithms (GAs) have been widely used for such problems and are implemented for this problem using MATLAB's Genetic Algorithms Toolbox. A complete description of GAs is beyond the scope of this paper, but here is a brief explanation.

An initial population is randomly generated where each member of the population is represented by a chromosome comprised of genes representing each design variable. In this problem, the chromosome is defined as an index number indicating one of the 12 integer parameter combinations, an eccentricity value ranging between 0 and 0.171, an argument of perigee on the interval $[0°, 360°)$, and two scale factors between 0 and 1 to vary the mean anomaly and RAAN of the 0^{th} satellite. A scale factor of 0 corresponds to those parameters being zero, whereas a scale factor of 1 corresponds to the maximum values of M and Ω as calculated by Thm. C.7. Eccentricity was restricted to maintain perigee above 300 km altitude.

A fitness (cost) function is evaluated for each member of the population. In this problem, we seek to maximize the amount of time within view of the target latitude and longitude. A new population is then generated by recombining and mutating the "fittest" members of the original population. Each population is known as a generation, and each generation represents an iteration of the optimization program. The average fitness of the population typically improves with each generation as the population evolves toward the optimal solution. The mutation enables the population to escape local minima in search of the global minimum, whereas the recombination (known as cross-over) averages the best solutions of the population to converge towards minima.

Design Results

Satellite visibility for this problem was restricted to satellites above 5° elevation angle and ground sites within the 45° field of view (FOV) of a nadir pointing sensor. Clearly the FOV is the limiting requirement, but a minimum elevation angle must be specified simply to avoid satellites "seeing" a ground site through the Earth.

We denote the constellation designed for Baghdad coverage as *Constellation B* and the constellation designed for Kabul coverage as *Constellation K*. The optimal parameters for these constellations, as found by the GA, are given in Table XII. Note that an argument of perigee of 270° places the apogee at the northernmost point of the orbit, and that both constellations converged to nearly the maximum eccentricity allowed to maximize coverage.

Table XII. GA generated LFC designs for coverage of Baghdad and Kabul

Parameter	Constellation B	Constellation K
N_o	6	6
N_{so}	1	1
N_c	0	0
e	0.168	0.170
ω	258.5°	273.9°
Ω_0	41.4°	30.9°
M_0	221.6°	272.7°

The amount of time each site is visible over the course of a single day by each constellation is given by Table XIII. The ground-tracks of both constellations are sufficiently dense that both sites are covered by both constellations, but the optimal constellation provides an improvement of more than 10% in both cases.

Table XIII. View time per day of each site by each constellation in minutes

Site	Constellation B	Constellation K
Baghdad	90	74
Kabul	84	94

2. Constellation Transfer

The first step in solving the constellation transfer problem was to solve for the required Δv for each of the 36 different orbit transfers between the 6 satellites of Constellation B and the 6 satellites of Constellation K. As described in Chapter III, the phasing of the satellites was ignored, and the Learning Approach to sampling optimization was combined with the minimum Δv_{tot}^2 methodology to rapidly compute the Δv's presented in Table XIV.

Table XIV. Required Δv to transfer from one slot in Constellation B (B_i) to another slot in Constellation K (K_i) in km/s. Optimal assignment in bold.

	K_1	K_2	K_3	K_4	K_5	K_6
B_1	12.82	10.26	6.19	**1.02**	4.62	9.27
B_2	9.38	12.96	10.22	6.20	**1.02**	4.69
B_3	4.64	9.38	12.91	10.33	6.26	**1.02**
B_4	**1.05**	4.63	9.32	12.92	10.23	6.28
B_5	6.21	**1.02**	4.63	9.35	12.94	10.24
B_6	10.21	6.22	**1.02**	4.57	9.31	12.83

A few things are immediately obvious from Table XIV. First, the optimal assignment, shown in bold, is individually optimal for every satellite. The auction

algorithm was initialized with a random assignment, and it quickly converged on the correct assignment. Note that not all constellation transfer assignments will be this straightforward and the auction algorithm is a useful tool for automating the assignment process. Secondly, the uniformity of the LFCs is clearly evident from the repeated values throughout the table. The near perfect agreement between the values validates the optimal Δv calculation method.

Whether the total Δv cost of 6.14 km/s is justified by the $> 10\%$ improvement in coverage time is left to the fictitious customer. This example demonstrates the solution to the entire constellation reconfiguration problem, from constellation design to constellation transfer using the methods outlined in Chapters II and III.

D. Conclusions

This chapter presented two case studies on using the Elliptical Flower Constellations for constellation design, and then a third case study on the entire constellation reconfiguration problem. All three examples demonstrated improvements over standard design and analysis methodologies.

The first example investigated the Galileo GNSS constellation and utilized the fact that elliptical orbits are cheaper to launch into than circular orbits of the same semi-major axis to find an EFC at a higher altitude with improved performance. The 3.5% improvement in mean positioning accuracy using EFCs was achieved despite the high degree of optimality found within the original Galileo design. The GNSS design study converged on an EFC with an almost identical distribution to that of the original Galileo constellation, highlighting one of the advantages of the EFC framework: since it generalizes Walker constellations, LFCs, and many of Draim's elliptic constellations, it can converge on one of those designs if that design is indeed

optimal.

The second example focused on the Iridium communications constellation which sought continuous global coverage from a LEO constellation of 66 satellites in 6 orbital planes. An optimal EFC with an eccentricity of only 0.07 was found that reduced the failure rate of the constellation by a factor of three when compared to the optimal Walker constellation.

The third and final example considered a constellation designed for regional coverage of a specific site being reconfigured to provide coverage of a different site. The entire constellation design and constellation transfer process was demonstrated. The computation methods for calculating optimal Δv costs were shown to be reliable and repeatable, and the auction algorithm successfully chose the optimal transfer assignment.

CHAPTER V

CONCLUSION

A. Summary

Satellite constellations provide capabilities above and beyond those achievable by terrestrial or single satellite systems. Their feasibility, capability, and cost effectiveness can all be enhanced through *constellation reconfiguration*. Whether by phasing up deployment to meet growing demand, or by repositioning the constellation to account for changing mission requirements, or by re-optimizing after the loss of one or more satellites, constellation reconfiguration improves the optimality of the system throughout its lifetime.

Constellation reconfiguration can be broken into two separate (but not necessarily independent) problems: *constellation design* and *constellation transfer*. Both problems are combinatorial in nature and require new, more efficient methods to solve them. This dissertation has presented a number of new approaches to make the constellation reconfiguration problem more tractable.

1. Constellation Design

The constellation design problem has been dominated by the streets-of-coverage and Walker constellation design methodologies for the last 40 years. The recent development of Flower Constellations by Mortari has offered the constellation designer a new framework that permits elliptic orbits and specializes in repeating ground-track constellations. The Lattice Flower Constellations (LFCs), a subset of the original Flower Constellation theory, provide uniform constellations that can be seen as generalizing Walker constellations to include elliptical orbits.

The first major contribution of this work to constellation design methodology has been the development of the Elliptical Flower Constellation (EFC) framework. The EFC framework produces constellations with satellites uniformly distributed not only in (Ω, M)-space as in Walker constellations or LFCs, but in the extended (Ω, ω, M)-space. Distributing satellites in multiple orbits with different arguments of perigee within the same plane enables the use of eccentric orbits for global coverage constellations without restricting the inclination to the non-J_2-perturbed critical inclination.

Design studies of both global navigation satellite systems and satellite phone communications systems revealed that EFCs offer significantly improved performance over the popular Walker constellations. This is possible through two main mechanisms. First, elliptical orbits are cheaper to launch into than circular orbits of the same semi-major axis, so the use of elliptical orbits in EFCs allows for larger orbits (and the attendant improved coverage) than the circular orbits of Walker. Second, elliptical orbits average a greater mean altitude than circular orbits of the same semi-major axis, so even constellations of the same size will see improved coverage using elliptical orbits.

One of the major powers of the EFC framework is that it generalizes all known constellation design methods for producing uniform constellations. Not only do they generalize Walker constellations and LFCs, they also generalize the elliptical Walker constellations of Dufour and the uniform, global coverage constellations of Draim. As such, even if elliptical orbits do not offer a benefit for a given application, an EFC-based design algorithm will converge to the optimal Walker constellation or LFC, as dictated by the performance index and imposed constraints.

The second major contribution of this work in the area of constellation design was the development of a new approach to orbit propagation. Given the combinatorial nature of constellation design and the large number of satellites within each

constellation, orbit propagation often consumes the majority of analysis time. The new methods focus on solving Kepler's equation in a sequential manner, using results from earlier in the orbit to improve the estimates at later times. Seven different methods were presented, and each was more accurate and less computationally complex than the best existing methods in literature. The result is that a number of them can be used for initial mission analysis and design where low fidelity but high speeds are needed. Where higher fidelity is needed, the new methods still offer the best starting estimates for initializing iterative solving techniques.

2. Constellation Transfer

To complete an optimal constellation reconfiguration, all satellites within the initial constellation must perform an optimal orbit transfer into a slot in the final constellation. Designing all of those orbit transfers and assigning satellites slots in the final constellation constitutes the *constellation transfer* problem. Like the constellation design problem, constellation transfer is combinatorial in nature and requires efficient methods for rapid exploration of the design space.

If the goal of the constellation transfer optimization is to minimize total fuel expenditure (or some other total measure), the assignment problem reduces to the simple Linear Assignment Problem (LAP) which can be efficiently solved by the auction algorithm. Solving the LAP or more general assignment problems requires that the cost be computed for every individual orbit transfer, thus requiring an efficient method for solving the optimal orbit transfer problem.

Considering the optimal impulsive orbit transfer where initial and final states are fixed but time is free to minimize fuel expenditure, existing methods use iterative techniques or require root-solving high-order (6+) polynomials. This dissertation developed a new method for calculating an approximately optimal orbit transfer re-

quiring the solution of only a 4^{th} order polynomial, with no iterations. Rather than minimizing the sum of Δv, the new method minimizes the sum of Δv^2. The errors of this method were shown to be bounded and typically small, and the improved efficiency over existing methods speeds computation of optimal two-impulse maneuvers.

In the constellation transfer problem, the phasing of the satellites can be safely ignored, because the cost of rephasing is insignificant compared to other orbit transfer costs. Thus, the optimal departure and arrival points on the initial and final orbits must be chosen to optimize for fuel expenditure. The domain includes multiple local minima, requiring the use of advanced optimization techniques. The recently developed Learning Approach (LA) to sampling optimization was applied to the orbit transfer problem utilizing the Δv_{tot}^2 method to evaluate the cost at the sampled departure and arrival points. Several modifications specifically designed to enhance the LA algorithm when applied to the two-impulse orbit transfer were presented, and Monte Carlo tests proved the efficacy of the approach.

A full end-to-end constellation reconfiguration problem was presented to demonstrate the effectiveness of the constellation transfer methods developed here, as well as that of the auction algorithm in finding the optimal assignment. The methods presented constitute a complete tool to automate the solution of the constellation transfer problem in an efficient manner.

B. Future Work

The constellation design and transfer problems have been treated independently in this dissertation, but in reality an optimal constellation reconfiguration would require solving both problems simultaneously. Solving each piece independently leads to a sub-optimal whole. For optimal (and practical) constellation reconfiguration, constel-

lations must be designed with transfer in mind. Phased deployment or satellite failure scenarios can be designed for, though designing multiple constellations and transfers simultaneously magnifies the computational burden. Parallel computing offers some hope that this problem will become tractable. Designing constellations in the face of changing mission requirements remains an unaddressed problem.

As the constellation reconfiguration problem moves toward a complete solution, incorporating multiple constellation designs and transfers simultaneously, effort should be directed toward multi-objective optimization. The coverage metrics for each constellation and the transfer costs for each transfer could be considered as unique objectives for which the designer is seeking some Pareto optimal solution.

With progress towards solving the complete, end-to-end reconfiguration problem comes the need to perform end-to-end constellation reconfiguration studies to demonstrate the advantage of reconfigurability. Though the theoretical benefits of constellation reconfiguration are easy to see, quantitative benefits need to be shown before constellation reconfiguration will become practically realized.

1. Constellation Design

The theory of EFCs is substantially developed in this work, but EFCs would benefit from a detailed study enumerating and classifying the "good" EFC designs, just as Walker did for his constellations. Certain sets of EFC parameters will provide more uniform global coverage than others, and will be optimal at a discrete number of inclinations. Perhaps some general rules exist that would help the constellation designer eliminate some EFCs out of hand, thereby reducing the design space and enabling faster design studies.

Alongside the classification of "good" EFC designs is the identification of missions where EFCs provide the most substantial benefits over more traditional meth-

ods. From the case studies presented here, it is clear that very robust constellations, such as Galileo, can be improved upon by using EFCs, but not as much as constellations on the edge of providing global coverage, like Iridium, which see substantial improvements. It seems EFCs would be particularly well-suited for applications requiring non-continuous global coverage. For instance, many commercial companies today offer Earth imagery from their own satellite constellations which provide imagery at the customer's request of anywhere in the world within a given time frame. The improved coverage offered by EFCs could reduce the time between imaging passes while also providing variable resolution imagery.

In many applications, particularly regional coverage, uniform satellite distributions may not be desirable. The orbital parameters in the EFC framework are distributed such that there is linear spacing between satellites. What if non-linear, but still periodic distributions were permitted instead? For instance what if RAAN was distributed such that $\Omega_i = (2\pi i^2/N_o^2)$? The pattern would still repeat, but the planes are non-uniformly spaced. The EFC framework could be modified on the right hand side to be something besides $2\pi i$ ($2\pi i^2/N_o$ in this example). In principle, an infinity of periodic patterns could be considered. Perhaps these non-uniform constellations would provide additional benefits for regional coverage problems.

2. Constellation Transfer

The work presented here solves the two-impulse constellation transfer problem, but many other options are available. Staying with impulsive trajectories, n-impulse transfers offer superior performance, but are much more difficult to compute. Satellites with low-thrust capabilities are arguably better suited to multiple reconfigurations, but some rapid algorithm for minimizing flight time to complete an orbit transfer needs to be developed. Alternatively, the J_2 effect can be utilized to redis-

tribute both RAAN and argument of perigee by making changes to eccentricity and semi-major axis, which varies those rates with respect to the other satellites in the constellation. These different constellation transfer methods must be addressed.

In addition to allowing for different transfer methods, different transfer metrics could be used to formulate different assignment problems. For instance, it may be beneficial to minimize the maximum Δv experienced by any one satellite, rather than minimizing the sum total, which leads to the Linear Bottleneck Assignment Problem (LBAP). More complicated metrics, like ones that combine time of flight and fuel cost in a non-linear way lead to more complicated general assignment problems, but advanced techniques do exist to approximately solve them.

Lastly, there are several issues that were not addressed surrounding the constellation transfer problem. Multiple satellites on the same launch vehicle create issues for the assignment problem, since they will typically all launch into the same (but unspecified) orbital plane. The scheduling of the transfers must be dealt with, including which satellites transfer when, and this could be dependent on some coverage metric that the constellation attempts to maintain while transferring.

C. Conclusion

In time, reconfiguring constellations to maintain optimality throughout their lifetime will be realized. While many open questions remain in the constellation reconfiguration problem, the tools developed and presented in this work significantly improve the efficiency with which that problem can be solved. These methods also apply to the more general constellation design and orbit transfer problems, providing all satellite systems engineers with new tools for producing enhanced constellation capabilities and reducing computation time.

REFERENCES

[1] Scialom, U., "Optimization of Satellite Constellation Reconfiguration," M.S. Thesis, August 2003, Massachusetts Institute of Technology, Cambridge, MA.

[2] Siddiqi, A., Mellein, J., and de Weck, O. L., "Optimal Reconfigurations for Increasing Capacity of Communication Satellite Constellations," *Proceedings of 46th AIAA Structures, Structural Dynamics & Materials Conference*, Austin, TX, April 2005, AIAA Paper 2005-2065.

[3] Abdelkhalik, O. O. and Mortari, D., "Orbit Design for Ground Surveillance Using Genetic Algorithms," *Journal of Guidance, Control, and Dynamics*, Vol. 29, No. 5, September–October 2006, pp. 1231–1235.

[4] Ely, T., Crossley, W., and Williams, E., "Satellite Constellation Design for Zonal Coverage Using Genetic Algorithms," *Journal of the Astronautical Sciences*, Vol. 47, No. 3, December 1999, pp. 207–228.

[5] Ulybyshev, Y., "Satellite Constellation Design for Complex Coverage," *Journal of Spacecraft and Rockets*, Vol. 45, No. 4, 2008, pp. 843–849.

[6] Wertz, J., *Mission Geometry; Orbit and Constellation Design and Management*, Microcosm Press, El Segundo, CA, 2001.

[7] de Weck, O. L., de Neufville, R., and Chaize, M., "Staged Deployment of Communications Satellite Constellations in Low Earth Orbit," *Journal of Aerospace Computing, Information, and Communication*, Vol. 1, No. 3, March 2004, pp. 119–136.

[8] de Weck, O. L., Scialom, U., and Siddiqi, A., "Optimal Reconfiguration of Satellite Constellations with the Auction Algorithm," *Acta Astronautica*, Vol. 62, No. 2, 2007, pp. 112–130.

[9] Ferringer, M., Spencer, D., Reed, P., Clifton, R., and Thompson, T., "Pareto-hypervolumes for the Reconfiguration of Satellite Constellations," *Proceedings of the AIAA/AAS Astrodynamics Specialist Conference*, Honolulu, HI, August 2008, AIAA Paper 2008-6611.

[10] Ferringer, M., Spencer, D., and Reed, P., "Many-objective Reconfiguration of Operational Satellite Constellations with the Large-cluster Epsilon Non-dominated Sorting Genetic Algorithm-II," *Proceedings of the Eleventh Conference of Congress on Evolutionary Computation*, Trondheim, Norway, 2009, pp. 340–349.

[11] Bertsekas, D. P., "The Auction Algorithm for Assignment and Other Network Flow Problems: A Tutorial," *Interfaces*, Vol. 20, No. 4, July-August 1990, pp. 133–149.

[12] Fonseca, C. and Fleming, P., "An Overview of Evolutionary Algorithms in Multiobjective Optimization," *Evolutionary Computation*, Vol. 3, No. 1, 1995, pp. 1–16.

[13] Scott, C. J. and Spencer, D. B., "Optimal Reconfiguration of Satellites in Formation," *Journal of Spacecraft and Rockets*, Vol. 44, No. 1, Jan-Feb 2007, pp. 230–239.

[14] Scott, C. J. and Spencer, D. B., "Optimal Low-Thrust Reconfiguration of Satellites in Formation," *Advances in the Astronautical Sciences*, Vol. 120, No. I, 2005, pp. 3–21.

[15] Walker, J., "Continuous whole-earth coverage by circular orbit satellite patterns," Tech. Rep. 77044, Royal Aircraft Establishment, Farnborough, Hampshire, England, March 1977.

[16] Mortari, D., Wilkins, M. P., and Bruccoleri, C., "The Flower Constellations," *Journal of the Astronautical Sciences*, Vol. 52, No. 1 and 2, January–June 2004, pp. 107–127.

[17] Henderson, T., Mortari, D., Avendaño, M., and Junkins, J., "An Adaptive and Learning Approach to Sampling Optimization," *Proceedings of the 2009 Space Flight Mechanics Meeting Conference*, Savannah, GA, February 2009, pp. 1669–1686.

[18] Henderson, T. and Mortari, D., "A Learning Approach to Sampling Optimization Applied to a Global Trajectory Optimization Problem," *Proceedings of the AAS Astrodynamics Specialists Conference*, Pittsburgh, PA, August 2009, pp. 489–496.

[19] Henderson, T., Mortari, D., Avendaño, M., and Denton, R., "Admissible n-Impulse Orbit Transfer and Rendezvous Solved Using a Learning Optimization Algorithm," *Proceedings of the 2010 Space Flight Mechanics Meeting Conference*, San Diego, CA, February 2010, AAS Paper 10-252.

[20] Dutruel-Lecohier, G. and Mora, M. B., "ORION-A Constellation Mission Analysis Tool," *Mission Design and Implementation of Satellite Constellations; Proceedings of the International Workshop*, Toulouse, France, 1998, pp. 373–393.

[21] Draim, J., "Satellite Constellations: The Breakwell Memorial Lecture," *Proceedings of the 55th International Astronautical Congress*, Vancouver, BC, Canada, 2004, pp. 517–526.

[22] Walker, J., "Satellite Constellations," *International Conference on Maritime and Aeronautical Satellite Communication and Navigation*, London, England, March 1978, pp. 119–122.

[23] Walker, J., "Satellite Constellations," *Journal of the British Interplanetary Society*, Vol. 37, No. 12, December 1984, pp. 559–571.

[24] Draim, J., "A Common Period Four-Satellite Continuous Coverage Constellation," *AIAA/AAS Astrodynamics Specialists Conference*, Williamsburg, VA, August 1986, pp. 112–120.

[25] Draim, J., "A Six Satellite Continuous Global Double Coverage Constellation," *AIAA/AAS Astrodynamics Specialists Conference*, Kalispell, MN, August 1987, p. 1173.

[26] Avendaño, M. E., Davis, J. J., and Mortari, D., "The Lattice Theory of Flower Constellations," *Proceedings of the 2010 Space Flight Mechanics Meeting Conference*, San Diego, CA, February 2010, AAS Paper 10-172.

[27] Mortari, D. and M.P.Wilkins, "The Flower Constellation Set Theory Part I: Compatibility and Phasing," *IEEE Transactions on Aerospace and Electronic Systems*, Vol. 44, No. 3, 2008, pp. 953–963.

[28] Bruccoleri, C. and Mortari, D., "The Flower Constellations Visualization and Analysis Tool," *IEEE Aerospace Conference*, Big Sky, MT, 2005, pp. 601–606.

[29] Avendaño, M. and Mortari, D., "Rotating Symmetries in Space - The Flower Constellations," *Proceedings of the 2009 Space Flight Mechanics Meeting Conference*, Savannah, GA, February 2009, pp. 1315–1332.

[30] Knuth, D., *The Art of Computer Programming, Vol. 2*, Addison-Wesley, Reading, MA, 1997.

[31] Dufour, F., "Coverage Optimization of Elliptical Satellite Constellations with an Extended Satellite Triplet Method," *Proceedings of the 54th International Astronautical Congress*, Bremen, Germany, October 2003, pp. 181–189.

[32] Dufour, F., "Optimal Continuous Coverage of the Northern Hemisphere with Elliptical Satellite Constellations," *Proceedings of the 2004 Space Flight Mechanics Meeting Conference*, Maui, HI, February 2004, pp. 121–135.

[33] Draim, J., "Continuous Globel N-Tuple Coverage with (2N+2) Satellites," *Journal of Guidance, Control, and Dynamics*, Vol. 6, No. 1, Jan-Feb 1991, pp. 17–23.

[34] Speckman, L., Lang, T., and Boyce, W., "An Analysis of the Line of Sight Vector Between Two Satellites in Common Altitude Circular Orbits," *Proceedings of AIAA/AAS Astrodynamics Conference*, Portland, OR, August 1990, AIAA Paper 90-2988-CP.

[35] Piriz, R., Martin-Peiro, B., and Romay-Merino, M., "The Galileo Constellation Design: A Systematic Approach," *Proceedings of the 18th International Technical Meeting of the Satellite Division of the Institute of Navigation*, Long Beach, CA, September 2005, pp. 1296–1301.

[36] Colwell, P., *Solving Kepler's Equation over Three Centuries*, Willmann-Bell, Richmond, VA, 1993.

[37] Battin, R., *An Intro to Mathematics and Methods of Astrodynamics*, AIAA Education Series, Reston, VA, 1999.

[38] Vallado, D., *Fundamentals of Astrodynamics and Applications*, McGraw–Hill, New York, 2001.

[39] Nijenhuis, A., "Solving Kepler's Equation with High Efficiency and Accuracy," *Celestial Mechanics and Dynamical Astronomy*, Vol. 51, No. 4, December 1991, pp. 319–330.

[40] Markley, F., "Kepler Equation Solver," *Celestial Mechanics and Dynamical Astronomy*, Vol. 63, No. 1, March 1996, pp. 101–111.

[41] Fukushima, T., "A Method Solving Kepler's Equation without Transcendental Function Evaluations," *Celestial Mechanics and Dynamical Astronomy*, Vol. 66, No. 3, September 1997, pp. 309–319.

[42] Feinstein, S. and McLaughlin, C., "Dynamic Discretization Method for Solving Kepler's Equation," *Celestial Mechanics and Dynamical Astronomy*, Vol. 96, No. 1, September 2006, pp. 49–62.

[43] Odell, A. and Gooding, R., "Procedures for Solving Kepler's Equation," *Celestial Mechanics and Dynamical Astronomy*, Vol. 38, No. 4, April 1986, pp. 307–334.

[44] Taff, L. and Brennan, T., "On Solving Kepler's Equation," *Celestial Mechanics and Dynamical Astronomy*, Vol. 46, No. 2, June 1989, pp. 163–176.

[45] Broucke, R., "On Kepler's Equation and Strange Attractors," *Journal of Astronautical Sciences*, Vol. 28, No. 3, 1980, pp. 255–265.

[46] Mikkola, S., "A Cubic Approximation for Kepler's Equation," *Celestial Mechanics and Dynamical Astronomy*, Vol. 40, No. 3-4, September 1987, pp. 329–334.

[47] Schönhage, A. and Strassen, V., "Schnelle Multiplikation Großer Zahlen," *Computing*, Vol. 7, No. 3-4, 1971, pp. 281–292.

[48] Mortari, D., Davis, J., and Bruccoleri, C., "Fast Orbit Propagation Without Solving Kepler's Equation," *Proceedings of the 2009 Space Flight Mechanics Meeting Conference*, Savannah, GA, 2009, pp. 829–842.

[49] Pardalos, P. and Pitsoulis, L., *Nonlinear Assignment Problems: Algorithms and Applications*, Kluwer Academic Publishers, Boston, MA, 2000.

[50] Lawler, E., "The Quadratic Assignment Problem," *Management Science*, Vol. 9, No. 4, July 1963, pp. 586–599.

[51] Pferschy, U., "Solution Methods and Computational Investigations for the Linear Bottleneck Assignment Problem," *Computing*, Vol. 59, No. 3, 1997, pp. 237–258.

[52] Burkard, R., "Selected Topics on Assignment Problems," *Discrete Applied Mathematics*, Vol. 123, No. 1-3, 2002, pp. 257–302.

[53] Pentico, D., "Assignment Problems: A Golden Anniversary Survey," *European Journal of Operational Research*, Vol. 176, No. 2, 2007, pp. 774–793.

[54] Gooding, R., "A Procedure for the Solution of Lambert's Orbital Boundary-Value Problem," *Celestial Mechanics and Dynamical Astronomy*, Vol. 48, No. 2, June 1990, pp. 145–165.

[55] Gobetz, F. and Doll, J., "A Survey of Impulsive Trajectories," *AIAA Journal*, Vol. 7, No. 5, 1969, pp. 801–834.

[56] Edelbaum, T., "How Many Impulses?" *Astronautics and Aeronautics*, Vol. 5, No. 11, 1967, pp. 64–69.

[57] Prado, A. and Broucke, R., "The Minimum Delta-V Lambert's Problem," *Controle e Automação*, Vol. 7, No. 2, 1996, pp. 84–90.

[58] Altman, S. and Pistiner, J., "Analysis of the Orbital Transfer Problem in Three-Dimensional Space," *Proceedings of the AIAA Astrodynamics Conference*, New Haven, CT, 1963, pp. 627–654.

[59] Schulz, W. and Prado, A., "Optimal Space Maneuvers in Three Dimensions," *Journal of the Brazilian Society of Mechanical Sciences and Engineering*, Vol. 28, No. 4, 2006, pp. 375–377.

[60] Davis, J., Avendaño, M., and Mortari, D., "A Closed-Form Solution to the Minimum Δv_{tot}^2 Lambert's Problem," *Proceedings of the 2009 AAS Astrodynamics Specialists Conference*, Pittsburgh, PA, 2009, pp. 1037–1052.

[61] Eberhart, R. and Shi, Y., "Comparison Between Genetic Algorithms and Particle Swarm Optimization," *Evolutionary Programming VII*, San Diego, CA, March 1998, pp. 611–616.

[62] Kirkpatrick, S., "Optimization by Simulated Annealing: Quantitative Studies," *Journal of Statistical Physics*, Vol. 34, No. 5-6, 1984, pp. 975–986.

[63] von Neumann, J., "Various Techniques Used in Connection with Random Digits," *National Bureau of Standards Applied Math Series*, Vol. 12, 1951, pp. 36–38.

[64] Spratling, B. and Mortari, D., "Recursive Star Identification with the K-Vector ND," *Proceedings of the 2010 Space Flight Mechanics Meeting Conference*, San Diego, CA, February 2010, AAS Paper 10-206.

[65] Bentley, J., "Multidimensional Binary Search Trees Used for Associative Searching," *Communications of the ACM*, Vol. 18, No. 9, 1975, pp. 509–517.

[66] Mortari, D., Davis, J., and Denton, R., "Constrained n-impulse Periodic Close

Encounters," *Proceedings of the 2010 Space Flight Mechanics Meeting Conference*, San Diego, CA, February 2010, AAS Paper 10-261.

[67] de Berg, M., Cheong, O., van Kreveld, M., and Overmars, M., *Computational Geometry: Algorithms and Applications, 3rd Ed.*, Springer, New York, NY, 2008.

[68] "Iridium NEXT Satellite Constellation," http://www.iridium.com/About/IridiumNEXT.aspx [retrieved 4 May 2010].

[69] Park, K., Wilkins, M., and Mortari, D., "Uniformly Distributed Flower Constellation Design Study for Global Positioning System," *Proceedings of the 2004 Space Flight Mechanics Meeting Conference*, Maui, HI, 2004, pp. 3127–3140.

[70] Tonetti, S., "Optimization of Flower Constellations: Applications in Global Navigation System and Space Interferometry," *Proceedings of the 2009 AIAA Aerospace Sciences Meeting*, Orlando, FL, January 2009, AIAA Paper 2009-205.

[71] C. Bruccoleri, *Flower Constellation Optimization and Implementation*, Ph.D. thesis, Texas A&M University, College Station, TX, December 2007.

[72] Mozo-Garcia, A., Herraiz-Monseco, E., Martin-Peiro, A., and Romay-Merino, M., "Galileo Constellation Design," *GPS Solutions*, Vol. 4, No. 4, April 2001, pp. 9–15.

[73] Parkinson, B. and Jr., J. S., *Global Positioning System: Theory and Applications, Volume I*, American Institute of Aeronautics and Astronautics, Washington, DC, 1996.

[74] Parkinson, B. and Jr., J. S., *Global Positioning System: Theory and Applications, Volume II*, American Institute of Aeronautics and Astronautics, Washington, DC, 1996.

[75] "Flight ST 21 Launch Kit (GIOVE-B)," http://www.starsem.com/news/kits.htm [retrieved 4 May 2010], April 2008.

[76] Finkelstein, S. and Sanford, S., "Learning from Corporate Mistakes: The Rise and Fall of Iridium," *Organizational Dynamics*, Vol. 29, No. 2, 2000, pp. 138–148.

VITA

Jeremy John Davis graduated summa cum laude in 2005 from Virginia Tech with a B.S. in aerospace engineering and immediately began graduate work at Texas A&M University as a National Defense Science & Engineering Graduate (NDSEG) Fellow. In 2008, Jeremy was named a Bradley Fellow, and also received the AIAA Willy Z. Sadeh Graduate Student Award in Space Engineering and Space Sciences and a Texas Space Grant Consortium Fellowship. Jeremy completed his graduate work under the supervision of Dr. John L. Junkins and Dr. Daniele Mortari. His graduate research has focused on orbital mechanics, star tracker sensing systems, and spacecraft attitude control in addition to the constellation reconfiguration work of this dissertation. Jeremy has also played an integral role in the development of the Land, Air, and Space Robotics (LASR) Laboratory, and has been involved in robotics projects ranging from satellite proximity operations to autonomous quad-rotor flight systems. Upon graduation in August 2010 with a Ph.D. in Aerospace Engineering, he pursued a post doctoral appointment with the LASR Lab. Jeremy has also recently co-founded the Axiodyne Engineering Corporation, an engineering consulting and consumer robotics company. He can be reached at JeremyJohnDavis@gmail.com, or in care of John L. Junkins at the Aerospace Engineering Department of Texas A&M University, 77843-3141.